

# **DEVELOPMENT OF THE TIMING SYSTEM FOR THE BUNCH-TO-BUCKET TRANSFER BETWEEN THE FAIR ACCELERATORS**

Vom Fachbereich  
Institut für Angewandte Physik  
der Goethe-Universität, Frankfurt am Main  
zur Erlangung des akademischen Grades  
eines Doktor der Naturwissenschaften  
genehmigte Dissertation

Von  
**Jiaoni Bai**  
geboren am 9. November 1986 in China

*Referent : Dr.D.Ondreka and Dr.D.Beck  
Korreferent : Prof.Dr.O.Kester  
Tag der Einreichung :  
Tag der mündlichen Prüfung : March, 2017*

Darmstadt 2016

---

I would like to dedicate this dissertation to my dear parents,  
loving husband and good friends ...

# Acknowledgement

First and foremost, I would like to thank my professor Prof. Oliver Kester. I have been so lucky to be his Ph.D. student. He gave me the chance to study at Goethe Universität, Frankfurt am Main and work in GSI for this interesting Ph.D. topic. It has been an honor to be his Ph.D. student. I appreciate all his contributions of time, ideas and funding to make my Ph.D. experience productive and stimulating. I was deeply influenced by his enthusiasm for his research and his selfless support for his students. I was thankful for his support, that I participated many international conferences, schools and workshops. This experience enriched my life and broadened my horizons.

I wish to express my sincere gratitude to Dr. David Ondreka and Dr. Dietrich Beck for their supervision, valuable guidance and helpful suggestions throughout my Ph.D. study. I have been greatly lucky to have so good supervisors, who cared much about my work and who answered my doubts patiently. They were like a lighthouse in the ocean, which guides me in the right direction. They are not only my scientific supervisors, but also my mentor. They encouraged and motivated me during tough time of my Ph.D. They always told me “Don’t be frustrated and take it easy, everything will be fine”. Hence, I will keep a positive attitude and keep moving forward when I face with challenges, difficulties and temporary setbacks in the future.

I would like to acknowledge all colleagues in the timing group, CSCO department, GSI, Mathias Kreider, Stefan Rauch, Marcus Zweig, Alexander Hahn and former employee Dr. Wesley Terpstra, who provided me much technical support. I would like to extend my appreciation to department leader Dr. Ralph Baer, who gave much support for my Ph.D. topic. Thanks for their friendship and collaboration. I am especially grateful for the group member Cesar Prados, by whom I learned not only technical knowledge, but also how to work efficiently and how to become a good engineer. I would also like to thank Matthias Thieme, who provided me the devices for the test setup.

I am also thankful for the good cooperation with Thibault Ferrand, who studies at Technische Universität Darmstadt and works in PBRF department, GSI. Thanks for his valuable contribution of the development of the LLRF system for the B2B transfer system for FAIR. I would like to extend my sincerest thanks and appreciation to PBRF department leader Prof. Harald Klingbeil for his support. In addition, a special thanks is also extended to Dr. Dieter Lens and Stefan Schaefer for their technical support. Thanks for Dr. Bernhard Zipfel to give me support about BuTiS.

I wish to express my sincere gratitude to SBES department leader Dr. Markus Steck for his technical support of ESR and CRYRING, Dr. Blell Udo in PBHV department for the technical support of kicker and Dr. Michael Block in SHE-P department for the supply of two SRS function generators.

---

I must express my gratitude to GSI, who provides the Facility for Antiproton and Ion Research project for my experiment. And also HGS-HiRe, who provided the scholarship which allowed me to undertake this research.

Lastly, I would like to thank my family for all their love and encouragement. My parents always support me to pursuing my dreams. Most of all, my loving husband Zigao Li is so appreciated, who always encourages me to realize my dreams. Thank you.

Jiaoni Bai  
Darmstadt, September 2016

# Abstract

This dissertation contributes to the conceptual development, systematic investigation and timing system realization of the Bunch-to-Bucket (B2B) transfer system for FAIR, Facility for Antiproton and Ion Research at GSI Helmholtzzentrum für Schwerionenforschung GmbH.

The B2B transfer system for FAIR plays an important role for FAIR project, which will achieve various complex bunch to bucket transfer for FAIR accelerators in the future. It focuses first of all on the transfer from SIS18 to SIS100, but it will be firstly tested for the transfer from SIS18 to ESR and further to CRYRING. The system is developed based on the FAIR existing infrastructures, LLRF and FAIR control systems. It coordinates with the Machine Protection System (MPS), which protects SIS100/SIS300 from unacceptable failure or situation and indicates beam for the Beam Instrumentation (BI).

The B2B transfer system obtains the rf phase difference between two synchrotrons by means of a campus distributed reference signals with picosecond precision, which is synchronized with Bunchphase Timing System (BuTiS). The source synchrotron works as a “B2B transfer master” for the rf phase collection, data (e.g. synchronization window indicating the coarse time frame for the transfer, phase shift for the phase match between two rf systems, phase correction for the bucket label and so on) calculation, synchronization window redistribution and B2B transfer status check. The synchronization window is a coarse time frame for the transfer and the bucket label signal is used to indicate the fine transfer. All application cases of FAIR project are analyzed with this system and all transfers achieve the bunch-to-bucket center mismatch smaller than the tolerance.

Because the system focuses first of all on the transfer from SIS18 to SIS100, the beam dynamic of the  $U^{28+}$  B2B transfer from SIS18 to SIS100 is simulated for two synchronization methods, the phase shift and frequency beating method. In addition, the SIS18 extraction and SIS100 injection kickers are analyzed for different triggering strategies. The dissertation also explains the timing constraints of the system, the calculation of the synchronization window and presents the usage of the WR network for the B2B transfer system.

The test setup of the timing system of the B2B transfer system for FAIR is also presented in this dissertation.

# Kurzfassung

# Contents

<b>Abstract</b>	<b>v</b>
<b>Glossary</b>	<b>xiii</b>
<b>List of Abbreviations</b>	<b>xvi</b>
<b>List of Symbols</b>	<b>xix</b>
<b>1 Introduction</b>	<b>2</b>
1.1 Objectives, Contribution and Structure of the Dissertation . . . . .	5
<b>2 Theoretical background</b>	<b>7</b>
2.1 Energy match . . . . .	7
2.2 Loop freeze . . . . .	8
2.3 Phase difference between two RF systems . . . . .	8
2.4 RF synchronization . . . . .	8
2.4.1 Phase shift method . . . . .	10
2.4.2 Frequency beating method . . . . .	13
2.5 Bucket label . . . . .	14
2.6 Synchronization of the extraction and injection kicker . . . . .	14
2.7 Beam indication for the beam instrumentation . . . . .	15
<b>3 Technical basis for the B2B transfer system</b>	<b>16</b>
3.1 FAIR control system . . . . .	16
3.1.1 BuTiS . . . . .	16
3.1.2 GMT . . . . .	17
3.1.3 FESA . . . . .	17
3.1.4 SM . . . . .	18
3.2 LLRF system . . . . .	18
3.3 MPS system . . . . .	20
3.4 Comparison . . . . .	21
<b>4 Concept of the B2B transfer system for FAIR</b>	<b>22</b>
4.1 Basic procedure of the B2B transfer system for FAIR . . . . .	23
4.2 Realization of the basic B2B functionalities . . . . .	25
4.2.1 RF phase difference between two RF systems . . . . .	25
4.2.2 RF phase difference synchronous to the absolute timestamp .	27
4.2.3 RF synchronization . . . . .	28
4.2.4 Coarse synchronization . . . . .	29

## CONTENTS

---

4.2.5	Bucket label . . . . .	30
4.2.6	Fine synchronization of the extraction and injection kicker . .	31
4.2.7	Beam indication for the beam instrumentation . . . . .	32
4.2.8	WR network . . . . .	32
4.2.9	B2B transfer status check . . . . .	35
4.3	Data/Signal flow of the B2B transfer system . . . . .	35
<b>5</b>	<b>Application of the B2B transfer system for FAIR accelerators</b>	<b>37</b>
5.1	Circumference ratio is an ideal integer . . . . .	38
5.1.1	Harmonic ratio equals to the circumference ratio . . . . .	40
5.1.1.1	User case of the $U^{28+}$ B2B transfer from SIS18 to SIS100 . . . . .	40
5.1.2	Harmonic ratio does not equal to the circumference ratio . .	41
5.1.2.1	User case of the $H^+$ B2B transfer from SIS18 to SIS100	41
5.1.2.2	User case of the B2B transfer from ESR to CRYRING	42
5.2	Circumference ratio is not an ideal integer . . . . .	43
5.2.1	Circumference ratio is close to an ideal integer . . . . .	44
5.2.1.1	User case of h=4 B2B transfer from SIS18 to ESR .	45
5.2.1.2	User case of h=1 B2B transfer from SIS18 to ESR .	46
5.2.2	Circumference ratio is far away from an ideal integer . . . .	46
5.2.2.1	User case of $H^+$ B2B transfer from SIS100 to CR .	48
5.2.2.2	User case of RIB B2B transfer from SIS100 to CR .	48
5.2.2.3	User case of B2B transfer from CR to HESR . . . . .	49
5.2.2.4	User case of B2B transfer from SIS18 to ESR via FRS	50
5.3	Summary of the synchronization for different scenarios . . . . .	51
<b>6</b>	<b>Realization and systematic investigation of the B2B transfer system for FAIR</b>	<b>53</b>
6.1	Investigation of two synchronization methods for $U^{28+}$ B2B transfer from SIS18 to SIS100 from the beam dynamics viewpoint . . . . .	53
6.1.1	Phase shift method . . . . .	53
6.1.1.1	Longitudinal dynamic analysis for the simulation .	56
6.1.1.2	Transverse dynamics analysis for the simulation .	60
6.1.2	Frequency beating method . . . . .	60
6.1.2.1	Longitudinal dynamics analysis of the frequency beating for SIS18 . . . . .	61
6.2	GMT systematic investigation for the B2B transfer system . . . . .	61
6.2.1	Calculation of the synchronization window . . . . .	62
6.2.1.1	The best estimate of alignment and the probable range of alignment for the phase shift method . . . .	64
6.2.1.2	The best estimate of alignment and the probable range of alignment for the frequency beating method	66
6.2.1.3	Calculation the synchronization window and its accuracy . . . . .	68
6.2.2	Measurement of the WR network for the B2B transfer . . . .	69
6.2.2.1	WR network test setup . . . . .	71
6.2.2.2	Frame loss rate test result for B2B frames . . . . .	72
6.2.2.3	Latency and jitter test result for B2B frames . . . . .	73
6.2.2.4	Result and conclusion . . . . .	75

## CONTENTS

---

6.3	Kicker systematic investigation for the B2B transfer system . . . . .	76
6.3.1	SIS18 extraction kicker units . . . . .	77
6.3.2	SIS100 injection kicker units . . . . .	78
6.4	Test setup for the data collection, merging and redistribution of the B2B transfer system . . . . .	79
6.4.1	Test functional requirement . . . . .	79
6.4.2	Test setup . . . . .	80
6.4.3	The firmware of the B2B transfer system . . . . .	81
6.4.4	The time constraints of the B2B transfer system . . . . .	84
6.4.5	Test result . . . . .	87
<b>7</b>	<b>Conclusion and outlook</b>	<b>89</b>
<b>A</b>	<b>B2B timing frames</b>	<b>91</b>
<b>B</b>	<b>Parameters of B2B transfer for FAIR accelerator pairs</b>	<b>93</b>
B.1	Parameters for the B2B transfer from SIS18 to SIS100 . . . . .	93
B.2	Parameters for the B2B transfer from SIS18 to ESR . . . . .	95
B.3	Parameters for the B2B transfer from SIS18 to ESR via FRS . . . . .	97
B.4	Parameters for the B2B transfer from ESR to CRYRING . . . . .	99
B.5	Parameters for the B2B transfer from CR to HESR . . . . .	100
B.6	Parameters for the B2B transfer from SIS100 to CR . . . . .	101
<b>Bibliography</b>		<b>101</b>
<b>Publications</b>		<b>105</b>

# List of Figures

1.1	Bunch-to-bucket injection with phase and energy error. . . . .	4
1.2	Bunch-to-bucket injection with voltage error. . . . .	4
1.3	Structure of the dissertation. . . . .	5
2.1	The illustration of the phase shift method. . . . .	10
2.2	The illustration of the frequency beating method. . . . .	14
3.1	Local Cavity Synchronization . . . . .	19
3.2	Reference RF Signal Distribution . . . . .	20
4.1	The illustration of B2B transfer from SIS18 to SIS100. . . . .	22
4.2	The procedure for the B2B transfer within one acceleration cycle. . .	24
4.3	The topology of the B2B transfer system . . . . .	25
4.4	The realization of the phase difference between two synchrotrons . .	26
4.5	The synchronization of the rf phase difference to the timestamp . .	27
4.6	The normalized frequency and phase modulation profile and the ac- tual profiles . . . . .	29
4.7	The realization of the bucket label for the normal extraction and injection. . . . .	30
4.8	The realization of the bunch gap for the emergency extraction. . . .	31
4.9	Timing frames transfer for the B2B transfer . . . . .	34
6.1	Examples of RF frequency modulation. . . . .	55
6.2	Time derivation of four modulations . . . . .	55
6.3	The phase shift modulation of four cases . . . . .	56
6.4	Average radial excursions of four cases. . . . .	56
6.5	Relative momentum shift of four cases. . . . .	57
6.6	Changes in synchronous phase of four cases . . . . .	58
6.7	Ratio of bucket areas of a running bucket to the stationary bucket of four cases . . . . .	59
6.8	Adiabaticity parameter estimation of case (3) and (4) . . . . .	60
6.9	RF frequency derivation of the $U^{28+}$ rf ramp . . . . .	61
6.10	The illustration of the best estimate of alignment, the probable range of alignment and the synchronization window . . . . .	62
6.11	The illustration of symbols for the calculation . . . . .	63
6.12	Scenarios for the phase shift method . . . . .	65
6.13	Two scenarios for the frequency beating method . . . . .	67
6.14	The illustration of the synchronization window and its accuracy . .	68
6.15	The WR network test setup . . . . .	71

## **LIST OF FIGURES**

---

6.16	The frame loss rate for B2B Broadcast and B2B Unicast frames . . . . .	73
6.17	The average latency and jitter for B2B Broadcast frames . . . . .	73
6.18	The maximum latency and jitter for B2B Broadcast frames . . . . .	74
6.19	The average latency and jitter for B2B Unicast frames . . . . .	75
6.20	The maximum latency and jitter for B2B Unicast frames . . . . .	75
6.21	Three scenarios for the delay of SIS18 extraction kicker . . . . .	77
6.22	SIS100 injection kicker . . . . .	79
6.23	Schematic of the test setup . . . . .	80
6.24	The front and back view of the test setup . . . . .	81
6.25	Flow chart of the firmware for B2B source SCU. . . . .	82
6.26	Flow chart of the firmware for B2B target SCU. . . . .	83
6.27	The time constraints of the B2B transfer system. . . . .	86

# List of Tables

5.1	FAIR user cases of the B2B transfer . . . . .	38
5.2	Synchronization when the circumference ratio is an ideal integer . . . . .	39
5.3	Synchronization when the revolution frequency ratio is an ideal integer .	39
5.4	Synchronization of $U^{28+}$ B2B transfer from SIS18 to SIS100 . . . . .	40
5.5	Synchronization of $H^+$ B2B transfer from SIS18 to SIS100 . . . . .	42
5.6	Synchronization of B2B transfer from ESR to CRYRING . . . . .	43
5.7	Synchronization when circumference ratio is close to an ideal integer .	44
5.8	Synchronization of $h=4$ B2B transfer from SIS18 to ESR . . . . .	45
5.9	Synchronization of $h=1$ B2B transfer from SIS18 to ESR . . . . .	46
5.10	Synchronization when circumference ratio is far away from an ideal integer . . . . .	47
5.11	Synchronization of $H^+$ B2B transfer from SIS100 to CR . . . . .	48
5.12	Synchronization of RIB B2B transfer from SIS100 to CR . . . . .	49
5.13	Synchronization of B2B transfer from CR to HESR . . . . .	50
5.14	Synchronization of B2B transfer from SIS18 to ESR via FRS . . . . .	51
5.15	Summary of the synchronization . . . . .	52
6.1	The maximum average radial excursion of four cases . . . . .	57
6.2	The maximum relative momentum shift of four cases . . . . .	57
6.3	The minimum bucket area factor of four cases . . . . .	59
6.4	The B2B transfer requirements for the WR network . . . . .	71
6.5	The connection between Xena ports and WR switches . . . . .	72
6.6	The average latency and jitter of the B2B Broadcast frames . . . . .	74
6.7	The maximum latency and jitter of the B2B Broadcast frames . . . . .	74
6.8	The result of the WR network test for the B2B transfer . . . . .	76
6.9	The delay for firing two crates of SIS18 extraction kicker . . . . .	78
6.10	The delay for firing SIS00 injection kicker . . . . .	79
A.1	B2B timing frames . . . . .	92
B.1	Parameters for the B2B transfer from SIS18 to SIS100 . . . . .	94
B.2	Parameters for the B2B transfer from SIS18 to ESR . . . . .	96
B.3	Parameters for the B2B transfer from SIS18 to ESR via FRS . . . . .	98
B.4	Parameters for the B2B transfer from ESR to CRYRING . . . . .	99
B.5	Parameters for the B2B transfer from CR to HESR . . . . .	100
B.6	Parameters for the B2B transfer from from SIS100 to CR . . . . .	101

# Glossary

accuracy	Closeness of agreement between the observed start and the best estimate of the start of the synchronization window, which is the sum of the precision and trueness
B2B target SCU	Collection the predicted phase of the target synchrotron and transfer it to the source synchrotron
B2B source SCU	B2B master: data collection, calculation and distribution for the B2B transfer system
batch	SIS100 batch: Train of $4 \times 2 U^{28+}$ bunches injected into SIS100 in one SIS18 to SIS100 super cycle. Or train of $4 \times 1 H^+$ bunches injected into SIS100 in one SIS18 to SIS100 super cycle
best estimate of alignment	Fine time for the alignment of two RF Reference Signals
bucket	The RF system provides longitudinal focusing which constrains the particle motion in the longitudinal phase space to a confined region called the RF bucket
bucket pattern	Rules for the buckets to be filled
bunch	Collection of particles captured within one RF bucket
bunch gap	Area without any bunches in the bunch train that fits the time required for building up the nominal field of the kicker

## Glossary

---

Cavity DDS	Cavity DDS provides RF signal for cavities
circumference ratio	Ratio of the circumference of the injection/extraction orbit of the large synchrotron to that of the small synchrotron
error propagation	Uncertainties in the original measurements “propagate“ through calculations to cause uncertainties in the calculated final answers
frame loss rate	The ratio of the number of the lost frames to the number of the theoretic received frames of a tested port
Group DDS	DDS module that generates an Reference RF Signal for a group of cavities
jitter	The absolute value of the difference between the latency of two consecutive received frames belonging to the same stream from one Xena port to another Xena port
latency	The time interval between the time of Xena port receiving frame and the time of another Xena port sending frame
machine cycle	One complete operation cycle of a machine, i.e. injection, ramp up, flattop, ejection and ramp down
precision	Closeness of agreement between the actual start of the synchronization window of different SCUs
probable range of alignment	Range within which the fine alignment lies because of the propagation of the uncertainty
Reference RF Signal	Signal generated by the Group DDS and delivered to an individual RF cavity as a reference for the gap signal
revolution frequency ratio	Ratio of the revolution frequency of the small to that of the large synchrotrons

## Glossary

---

Synchronization Reference Signal	Shared reference signal whose frequency is a multiple of the BuTiS T0 100 kHz and whose zero-crossing is aligned with T0 edges
timing frame	A specified ethernet frame with 110 byte frame length, which contains one or more timing message
Trigger SCU	Production of the trigger signal for kicker electronics
trueness	Closeness of agreement between the average actual start of the synchronization window of different SCUs and the best estimation start of the synchronization window
tune	Number of particle trajectory oscillations during one revolution in the ring (transverse and longitudinal)
uncertainty	A non-negative parameter characterizing the dispersion of the values attributed to a measured quantity
virtual RF cavity	A virtual position around the ring, to which the Reference RF Signal corresponds

# List of Abbreviations

API	Application Programming Interface
B2B	Bunch to Bucket
BI	Beam Instrumentation
BPID	Beam Process ID
BuTiS	Bunchphase Timing System
CCS	Central Control System
CERN	European Organization for Nuclear Research
CM	Clock Master
CPU	Central Processing Unit
CR	Collector Ring
CSCO	Common Systems Control Systems
DDS	Direct Digital Synthesizer
DM	Data Master
DSP	Digital Signal Processor
ESR	Experimental Storage Ring
FAIR	Facility for Antiproton and Ion Research
FBAS	Fast Beam Abort System
FEC	Front End Controller
FESA	Front-End software Architecture
FID	Format ID

## List of Abbreviations

---

FPGA	Field Programmable Gate Array
FRS	Fragment Seperator
GCD	Greatest Common Divisor
GID	Group ID
GMT	General Machine Timing
GUI	Graphical User Interface
HESR	High Energy Storage Ring
IP	Internet Protocol
LLRF	Low-level RF
LSA	LHC Software Architecture
MM	Management Master
MPS	Machine Protection System
NESR	New Experimental Storage Ring
PAM	Phase Advance Measurement
PAP	Phase Advance Prediction
PBHV	Primary Beam High Voltage
PBRF	Primary Beam Radio Frequency
PC	Personal Computer
PCM	Phase Correction Module
PSM	Phase Shift Module
RESR	Recycled Experimental Storage Ring
RF	Radio Frequency
SBES	Experimentierspeicherring ESR
SCU	Scalable Control Unit

## **List of Abbreviations**

---

SHE-P	SHE-Physik
SIS100	Heavy Ion Synchrotron - SchwerIonen Synchrotron (100 Tm magnetic rigidity)
SIS18	Heavy Ion Synchrotron - SchwerIonen Synchrotron (18 Tm magnetic rigidity)
SM	Settings Management
SR	Signal Reproduction
TD	Trigger Decision
TM	Timing Master
TOF	Time Of Flight
TTL	Transistor–Transistor Logic
UNILAC	Universal Linear Accelerator
VLAN	Virtual Local Area Network
WR	White Rabbit

# List of Symbols

e	Charge of the particle
$\rho_0$	Bending radius of a particle immersed in a magnetic field $B$
$\beta$	Relative speed to the speed of light
$R(t)$	Orbit radius. $R_0$ the nominal value
$B(t)$	Magnetic field
$\alpha_p$	Momentum compaction factor
$p(t)$	Particle momentum
$f(t)$	Revolution frequency
$v(t)$	Velocity of particle
$\gamma(t)$	Relativistic factor, which measures the total particle energy, $E(t)$ , in units of the particle rest energy, $E_0$
$E(t)$	Total particle energy
$E_0$	Particle rest energy
$\gamma_t$	Transition energy
$\eta(t)$	Phase-slip factor
$F(t)$	Force
$V(t)$	RF accelerating voltage
$\omega_s(t)$	Small-amplitude synchrotron frequency
$\varepsilon$	Adiabaticity parameter

## List of Symbols

---

$t_{pattern}$	Time delay for a specified bucket pattern
$t_{TOF}$	Time-of-Flight between two synchrotrons
$t_{v\_ext}$	Time corresponds to the distance between the virtual RF cavity driving signals and the extraction position of the source synchrotron
$t_{v\_inj}$	Time corresponds to the distance between the virtual RF cavity driving signals and the injection position of the target synchrotron
$t_{ext}$	Extraction kicker delay
$t_{inj}$	Injection kicker delay
$t_{diff\_sync}$	Time difference between rf systems of two synchrotrons after the synchronization
$\Delta\varphi 1$	Phase difference between the Reference RF Signal and the Synchronization Reference Signal of the source synchrotron, measured by PAM module
$\Delta\varphi 2$	Phase difference between the Reference RF Signal and the Synchronization Reference Signal of the target synchrotron, measured by PAM module
$\psi 1$	Phase difference between the Reference RF Signal and the Synchronization Reference Signal of the source synchrotron at BuTiS T0 edges, predicted by PAP module
$\psi 2$	Phase difference between the Reference RF Signal and the Synchronization Reference Signal of the target synchrotron at BuTiS T0 edges, predicted by PAP module
$f_{normalized}$	Normalized rf frequency modulation profile, preloaded from SM
$f_{actual}$	Actual rf freqnecy modulation profile, calculated by PSM
$T_{sync\_win}$	Length of the synchronization window

## List of Symbols

---

$\Delta\theta$	Mismatch between the bunch and bucket center
$\Delta f$	Beating frequency
$t_{v\_emg}$	Time corresponds to the distance between the virtual RF cavity and the emergency extraction position of SIS100
$t_{emg}$	Extraction kicker delay of SIS100
$h^X$	X=l, Cavity harmonic of large synchrotron; X=s, Cavity harmonic of small synchrotron
$\alpha_b(\phi_s)$	Bucket area factor
$\phi_s$	Synchronous phase
$Q_x$	Horizontal chromaticity
$Q_y$	Vertical chromaticity
$\Delta Q_x$	Horizontal chromatic tune shift due to the rf frequency modulation
$\Delta Q_y$	Vertical chromatic tune shift due to the rf frequency modulation
$t_{best}$	Best estimate of alignment of zero crossing points of Reference RF Signals of source and target synchrotrons
$\delta t_{best}$	Uncertainty of the best estimate of alignment of zero crossing points of Reference RF Signals of source and target synchrotrons
$\psi_{h=1}^{SIS100}$	Predicted SIS100 h=1 rf phase at $t_\psi$
$h$	Harmonic number of the rf signal
$\psi_{h=1/5}^{SIS18}$	Predicted SIS18 h=1/5 rf phase at $t_\psi$
$t_\psi$	Time of the predicted phase
$\phi_{h=2}^{SIS18}$	RF phase at the cavity frequency h=2 of SIS18 at $t_\psi$

## List of Symbols

---

$\phi_{h=10}^{SIS100}$	RF phase at the cavity frequency h=10 of SIS100 at $t_\psi$
$\delta t_\psi$	Uncertainty of the predicted phase advance at time domain
$\delta\psi_{h=1}^{SIS100}$	Uncertainty of the predicted SIS100 rf phase at h=1
$\delta\psi_{h=1/5}^{SIS18}$	Uncertainty of the predicted SIS18 rf phase at h=1/5
$\delta\phi_{h=10}^{SIS100}$	Uncertainty of RF phase at the cavity frequency h=10 of SIS100
$\delta\phi_{h=2}^{SIS18}$	Uncertainty of RF phase at the cavity frequency h=2 of SIS18
$T_{phase\_shift}^{upper\_bound}$	Upper bound time of the phase shift process
$\delta T_{phase\_shift}^{upper\_bound}$	Uncertainty of the upper bound time of the phase shift process
$\Delta\phi_{adjustment}$	Phase adjustment of the frequency beating method, calculated by B2B source SCU
$\psi_{s\_alignment}$	RF phase of the cavity driving frequency at the start of the probable rang of alignment
$\Delta t_{win\_correct}$	Time correction for the start of the probable range of alignment $[t_{best}-\delta t_{best}, t_{best}+\delta t_{best}]$ to the best estimate of the start of the synchronization window
G	Bunch gap
L	Distance from the leftmost to the rightmost SIS18 extraction/SIS100 injection kicker unit
D	Sum distance of d and the 2nd crate
d	Distance between two extraction kicker crates of SIS18
c	Speed of the light
$t_{B2B}$	Start time of the B2B transfer

## List of Symbols

---

$\Delta t$	Beating time for the synchronization
$\Delta\phi_s(t)$	Change of the synchronous phase
$T_{rev}^X$	Period of the revolution period of machine X
$T_{rf}^X$	Period of the cavity frequency of machine X
$\Delta\phi_{shift}$	Phase shift to be achieved by the phase shift method
$\Delta f_{rf}(t)$	Rf frequency modulation for the phase shift method
$C^X$	X=l, Circumference of the injection/extraction orbit of large synchrotron; X=s, Circumference of the injection/extraction orbit of small synchrotron
$f_{rev}^X$	oder $f_{h=1}^X$ . X=l, Revolution frequency of large synchrotron; X=s, Revolution frequency of small synchrotron
$f_{rf}^X$	oder $f_{h=cavity\_harmonic}^X$ . X=l, Cavity frequency of large synchrotron; X=s, Cavity frequency of small synchrotron
$\kappa$	Integer, m and n are also integer
$\lambda$	Decimal
Y	Greatest common divisor
T	Period of rf frequency modulation for the phase shift method
$t_0$	Start time of the rf frequency modulation for the phase shift method

# Chapter 1

## Introduction

With regard to excellence, it is not enough to know,  
but we must try to have and use it.

- Aristotle (384 BC - 322 BC), *Nicomachean Ethics, ch. 9*

Research leading to the discovery of elementary particles and to ideas for the acceleration of such particles to high energy is dotted with particularly important milestones which from time to time set the directions for further experimental and theoretical research [1]. Due to the thirst for knowledge of human beings, the particle accelerator has big progress in the past 100 years. First of all, we look back at the history of the particle accelerator.

In 1927 Rolf Widerøe developed the first linear accelerator, which made use of an alternating current (AC) voltage and a series of drift tubes. As the particle gets faster and faster, the drift tubes need to be longer and longer. The linear accelerator needs to be very long for particles to be accelerated to high energies. In 1928, Ernest Lawrence of the University of California, inspired by the work of Widerøe, had the idea of utilizing a curved path for a particle accelerator. A magnetic field perpendicular to the plane of motion of an accelerated particle makes the particle taking a curved path. By studying the simple relationship between the forces acting on the particle, Lawrence realized that the increase in the radius of the path taken by the particle is compensated by the increased velocity of the particle if the magnetic field, the charge of the particle and the particles mass remain constant. With this in mind, he built what became known as a cyclotron. As the speed of the particle increases, the radius of the semi-circular motion of the particle increases until the particles are eventually focused out of the cyclotron as a high energy beam. The physical principles governing the Betatron were first described by Widerøe in a paper in 1928 and put into practice in 1940 by Donald Kerst. The development of the Betatron was driven by the demand for high energy X-rays and gamma rays for medical and research usage. The Betatron consists of a main ring, a doughnut shaped vacuum chamber, in which electrons, produced by an electron gun within the chamber, are accelerated. The chamber is set up between the two poles of an electromagnet driven by an AC current, which results in a constantly changing magnetic field. The basic principle of the Synchrotron is to maintain the accelerated particles at a constant orbital radius. This is achieved by synchronizing the magnetic field strength with the energy of the accelerated particles. So, as the particles are accelerated and gain energy, the magnetic field is increased, keeping the particles

## CHAPTER 1. INTRODUCTION

---

orbit constant. The first Synchrotron to be built was a modified Betatron and was completed by two English physicists, Frank Goward and D. Barnes [2].

Mankind has never stopped learning and practice about the particle accelerators. Nowadays, particle accelerators is playing an important role not only in research application (particle physics, nuclear physics, atomic physics, cosmology and astrophysics, chemistry and biology), but also in element analysis, power engineering, medicine for diagnostics and for therapy and industrial processing [3].

FAIR, Facility for Antiproton and Ion Research, is a new international accelerator facility under construction at GSI Helmholtz center for Heavy Ion Research GmbH (short: GSI)<sup>1</sup> [4, 5], which will use antiprotons and ions to perform research in many fields. It is aiming at providing high-energy beams with high intensities. Based on the existing GSI UNILAC and SIS18 serving as injectors, high intensity ion beams over the whole range of stable isotopes will be accelerated in the new heavy ion machine SIS100 to higher energies. The new FAIR accelerator complex with storage rings consists of SIS100, Collector Ring CR, accumulator/decelerator ring RESR and New Experimental Storage Ring NESR [6, 7]. An additional High Energy Storage Ring HESR serves experiments with high energy antiprotons and rare isotope beams. The bunch-to-bucket (B2B) transfer system for FAIR aims at supporting beam transfers between the following accelerators:

- The B2B transfer from SIS18 to SIS100
- The B2B<sup>2</sup> transfer from SIS18 to ESR
- The B2B transfer from ESR to CRYRING
- The B2B transfer from SIS100 to CR
- The B2B<sup>3</sup> transfer from CR to HESR and later to RESR

The system supports not only the simple transfer between two accelerators, but also various complex beam transfer for FAIR. It is capable to transfer different species beam from one machine cycle to another and parallel transfer beam through FAIR accelerators. It is able to transfer the beam between two synchrotrons via Fragment Separator (FRS)<sup>4</sup> or Super-Fragment Separator (Super FRS). The B2B transfer system focuses first of all on the transfer from SIS18 to SIS100, but it will be firstly tested for the transfer from SIS18 to ESR and further to CRYRING.

The bunches must be transferred from the buckets of an injecting machine into the middle of the buckets in the receiving machine, namely energy match and phase match. The red dots (1, 2, 3) on Fig. 1.1 show the trajectory followed by the center of the bunch after injection with a phase error (dot 1: correct momentum but displaced horizontally with respect to the bucket centre). The green dots (a, b, c) correspond to an injection with the correct phase but with an energy deviation [8].

The injection energy or phase error cause dipole oscillation, that the bunch profile does not change but the phase of the center of charge moves back and forth with respect to the stable phase.

---

<sup>1</sup>Plackstrasse 1, 64291 Darmstadt, www.gsi.de

<sup>2</sup>B2B system supports Bunch-to-Barrier bucket transfer as well

<sup>3</sup>Bunch-to-Barrier bucket

<sup>4</sup>An ion-optical device used to focus and separate products from the collision of relativistic ion beams with thin targets.

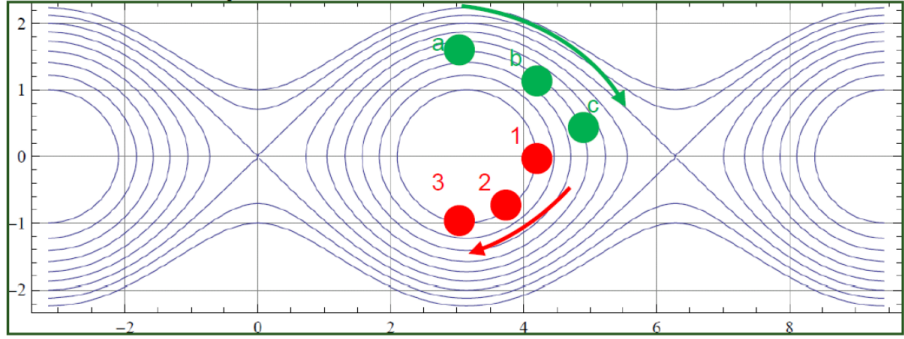


Figure 1.1: Bunch-to-bucket injection with phase and energy error.  
X-axis: Phase in radian. Y-axis: momentum, energy or frequency deviation from synchronism. The red dots (1, 2, 3) show the trajectory followed by the bunch center for an injection phase error. The green dots (a, b, c) correspond to an injection energy error [8].

Besides, the RF voltage must also match. Fig. 1.2 shows the capture of a bunch (marked in red) with perfect phase and energy matching.

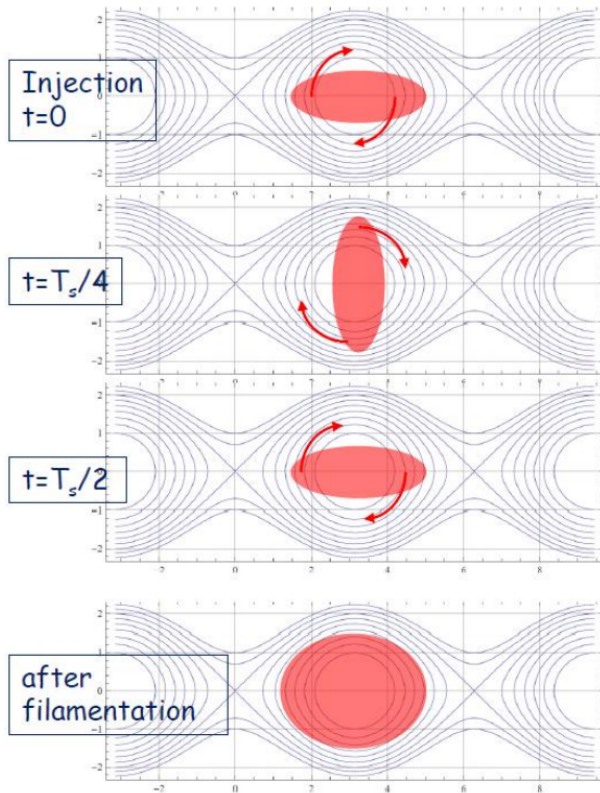


Figure 1.2: Bunch-to-bucket injection with voltage error.  
Injection of a bunch (dark red) in the exact center of the bucket but with phase space trajectories mismatched to the two dimensional phase-momentum bunch profile. The result is a quadrupole oscillation at twice the synchrotron frequency and, after filamentation, significant emittance increase [8].

The center of the bunch falls in the middle of the bucket. The bunch has a non-zero length and therefore occupies an area defined by the phase space trajectories in

## **1.1. Objectives, Contribution and Structure of the Dissertation**

---

the injector. But it is not matched to the phase space trajectories in the receiving machine (the voltage is too high). The particles of the bunch will follow these trajectories, resulting in the evolution shown on the figure: after one-quarter synchrotron period, the bunch length has been reduced (projection on the phase axis) and the momentum spread has been increased. We call this a quadrupole oscillation. It is a modulation of the bunch length (and momentum spread) at twice the synchrotron frequency. After filamentation the bunch emittance will be much increased and this must be avoided [8].

### **1.1 Objectives, Contribution and Structure of the Dissertation**

This dissertation contributes to the development of the B2B transfer system for FAIR from the timing system view of point. It concentrates on the introduction of the concept of the system and its application for FAIR accelerators. In addition, it explains the realization and systematic investigation of the B2B transfer system from the timing system perspective in details.

The dissertation is structured as follows and as depicted in Fig. 1.3.

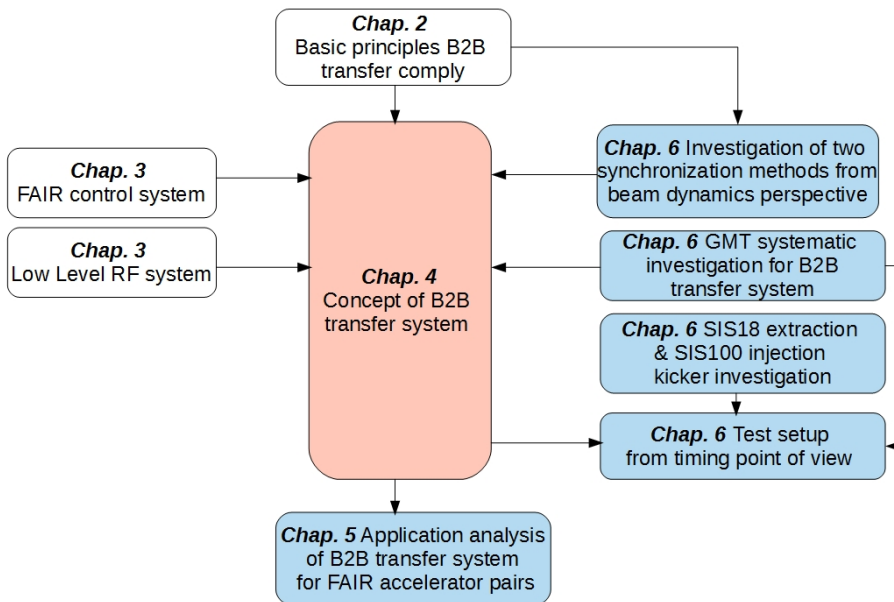


Figure 1.3: Structure of the dissertation.

Contributions are marked blue and red is team work; existing system or theory are not colored.

In Chap.2 the basic principles for the B2B transfer are reviewed. First of all, the energy match between the source and target synchrotrons is introduced. Secondly, two RF synchronization methods are discussed from the perspective of beam dynamics in order for the phase match. Once more, the bucket label and the extraction/injection kicker synchronization are discussed. At the end of this chapter, the beam indication for the beam instrumentation is mentioned.

## **1.1. Objectives, Contribution and Structure of the Dissertation**

---

Chap.3 is concerned with the existing FAIR technical basis for the development of the B2B transfer system and the uniqueness of the system. The system is realized based on the FAIR control system and Low-Level RF system, so these two systems are introduced. In addition, the uniqueness of the B2B transfer system for FAIR is discussed before the chapter ends.

In Chap.4, a brief overview on the basic procedure of the B2B transfer system is presented. The detailed realization of every basic principles mentioned in Chap.2 for B2B transfer system for FAIR is presented. In addition, the B2B transfer system is explained from the data/signal flow point of view.

The application of the B2B transfer system for FAIR accelerators are outlined in Chap.5. The applications are classified into two categories according to the feature of the circumference ratio. For each category, the corresponding FAIR applications are presented.

Chap.6 presents the realization of the systematic investigation for the system, mainly from the timing point of view. The calculation of the synchronization window is explained and the transfer of the B2B timing messages via the WR network is tested. In addition, for the B2B transfer from SIS18 to SIS100, two synchronization methods are analyzed from the beam dynamics point of view. The SIS18 extraction and SIS100 injection kicker are systematically investigated. Finally, the test setup is introduced and the test result is presented and analyzed.

# Chapter 2

## Theoretical background

Transferring bunches of particles from a synchrotron into specified buckets of another synchrotron has several underlying basic principles. The energy of the beam is same before and after the B2B transfer, so the energy of the source synchrotron must first of all match that of the target synchrotron. Principally speaking, every synchrotron has its independent RF system. Then the phase advance between the bunch and the bucket must be precisely controlled before the bunch is ejected. The process of achieving the detailed phase adjustment between two RF systems is termed "RF synchronization". For the correct bucket injection, the filled buckets and the bucket to be filled must be marked. The bunch fast extraction must happen exactly one "time of flight" before the required bucket of the target synchrotron passes the injection region. The injection kicker must kick when the bucket passes the injection region. In this chapter, all of the B2B basic principles will be explained.

### 2.1 Energy match

The bunch coordinates in the longitudinal phase plane of the source synchrotron, just before transfer, must be accurately controlled, according to the bucket to be filled [9]. The target synchrotron has to center the bucket on the desired orbit <sup>1</sup>, according to the energy of the bunch. This requirement guarantees the energy match between the bunch and bucket. The energy of a beam is determined by the 'magnetic rigidity', which is defined as the following:

$$B(t)\rho_0 = \frac{p(t)}{e} \quad (2.1)$$

where  $p(t)$  is the magnitude of the particle momentum,  $e$  is the charge of the particle,  $B(t)$  is magnetic field, and  $\rho_0$  is the bending radius of a particle immersed in a magnetic field  $B(t)$ . The ratio of  $p(t)$  to  $e$  describes the 'stiffness' of a beam, it can be considered as a measure of how much angular deflection results when a particle travels through a given magnetic field [10].

The bunch is transferred from the source to the target synchrotron with the same energy. So the beam has the same momentum and velocity for both synchrotrons. According to eq. 2.1, the magnetic rigidity of two synchrotrons must be matched:

$$B^{src}(t)\rho_0^{src} = \frac{p}{e} = B^{trg}(t)\rho_0^{trg} \quad (2.2)$$

---

<sup>1</sup>Design orbit or injection orbit

## 2.4. RF synchronization

---

Where the superscript of the symbol denotes the synchrotron, “src“ represents the source synchrotron and “trg“ the target synchrotron.

Besides, the rf frequency of two synchrotrons must meet the following relation [9].

$$C^{src} \frac{f_{rf}^{src}(t)}{h^{src}} = \beta c = C^{trg} \frac{f_{rf}^{trg}(t)}{h^{trg}} \quad (2.3)$$

where  $C$  is the circumference of the synchrotron,  $h$  the harmonic number of the rf signal and  $f_{rf}$  denotes the cavity rf frequency,  $\beta$  the fraction of the particle velocity to the lightspeed.

## 2.2 Loop freeze

During the B2B transfer process, feedback loops for the deviations correction of the particles from reference states (e.g. position and velocity) must switch off or freeze. E.g. Beam phase feedback loop [11] and bunch-by-bunch longitudinal rf feedback loop [12].

## 2.3 Phase difference between two RF systems

For the RF synchronization between two synchrotrons, the prerequisite is to know the phase difference between two independent RF systems.

## 2.4 RF synchronization

There are usually two methods available for the synchronization process. The synchronization is achieved by an azimuthal positioning of the bunch in the source synchrotron or the bucket in the target synchrotron. This is so-called ”phase shift method“. When two rf frequencies are slightly different, they are beating, perceived as periodic variations in phase difference, whose rate is the difference between the two frequencies. The synchronization is automatically achieved. This is so-called ”frequency beating method“. Both methods provide a time frame for the B2B transfer, within which a bunch could be transferred into a bucket with the bunch-to-bucket center mismatch smaller than the upper bound. The time frame is called ”synchronization window“.

For both methods, the accompanying beam dynamics must be taken into consideration. The momentum of particle is given by

$$p(t) = e\rho_0 \left[ \frac{R(t)}{R_0} \right]^{1/\alpha_p} B(t) \quad (2.4)$$

where  $R_0$  is its nominal value,  $R(t)$  the orbit radius,  $B(t)$  the magnetic field and  $\alpha_p$ , the momentum compaction factor. From eq. 2.4, the first-order total differential of  $p(t)$  is given as

$$dp(t) = \frac{e\rho_0}{\alpha_p(R_0)^{1/\alpha_p}} B(t) R(t)^{1/\alpha_p - 1} dR(t) + e\rho_0 \left[ \frac{R(t)}{R_0} \right]^{1/\alpha_p} B(t) dB(t) \quad (2.5)$$

## 2.4. RF synchronization

---

Dividing both sides of eq. 2.5 by  $p(t)$ , we obtain

$$\frac{dp(t)}{p(t)} = \gamma_t^2 \frac{dR(t)}{R(t)} + \frac{dB(t)}{B(t)} \quad (2.6)$$

Now, for circular accelerators, the following general relation holds

$$f(t) = \frac{v(t)}{2\pi R(t)} \quad (2.7)$$

where  $f(t)$  is the revolution frequency and  $v(t)$  the velocity. The total differential of  $f(t)$  is given by

$$df(t) = \frac{1}{2\pi} \left[ \frac{dv(t)}{R(t)} - \frac{v(t)}{R^2(t)} dR(t) \right] \quad (2.8)$$

Dividing both sides of eq. 2.8 by  $f(t)$  yields

$$\frac{df(t)}{f(t)} = \frac{dv(t)}{v(t)} - \frac{dR(t)}{R(t)} \quad (2.9)$$

The fractional change in  $v(t)$  is related to the fractional change in  $p(t)$ :

$$\frac{dp(t)}{p(t)} = \gamma^2(t) \frac{dv(t)}{v(t)} \quad (2.10)$$

where  $\gamma(t)$  is the relativistic factor, which measures the total particle energy,  $E(t)$ , in units of the particle rest energy,  $E_0$ . Solving  $dv(t)/v(t)$  from eq. 2.10 and substituting it into eq. 2.9 yields

$$\frac{df(t)}{f(t)} = \gamma^2(t) \frac{dp(t)}{p(t)} - \frac{dR(t)}{R(t)} \quad (2.11)$$

Replacing  $dp(t)/p(t)$  in eq. 2.11 with eq. 2.6, we have

$$\frac{df(t)}{f(t)} = \gamma^2(t) \frac{dB(t)}{B(t)} + \left[ \frac{\gamma_t^2}{\gamma^2(t)} - 1 \right] \frac{dR(t)}{R(t)} \quad (2.12)$$

where  $\gamma_t$  is the transition gamma, which is related to  $\alpha_p$  as  $\gamma_t = 1/\sqrt{\alpha_p}$ . In the same way, solving  $dR(t)/R(t)$  from eq. 2.6 and substituting it into eq. 2.11, we obtain

$$\frac{df(t)}{f(t)} = \left( \frac{1}{\gamma^2(t)} - \frac{1}{\gamma_t^2} \right) \frac{dp(t)}{p(t)} + \frac{1}{\gamma_t^2} \frac{dB(t)}{B(t)} \quad (2.13)$$

where  $\eta(t)$  is the phase-slip factor defined as

$$\eta(t) = \frac{1}{\gamma^2(t)} - \frac{1}{\gamma_t^2} = \alpha_p - \frac{1}{\gamma_t^2} \quad (2.14)$$

Of the four variables,  $f(t)$ ,  $B(t)$ ,  $p(t)$  and  $R(t)$ , only two are independent. This leads to four very useful differential relations, eq. 2.6, eq. 2.11, eq. 2.12 and eq. 2.13 [13, 14].

## 2.4. RF synchronization

---

### 2.4.1 Phase shift method

Based on the phase difference on Sec. 2.3, the rf system of the source or target or both synchrotrons are modulated away from their nominal value for a period of time and then modulated back so that the phase shift created by the frequency modulation could compensate for the expected phase difference. After the phase shift, the bunches of the source synchrotron are synchronized with random buckets of the target synchrotron. The phase shift process must be performed adiabatically for the longitudinal emittance to be preserved.

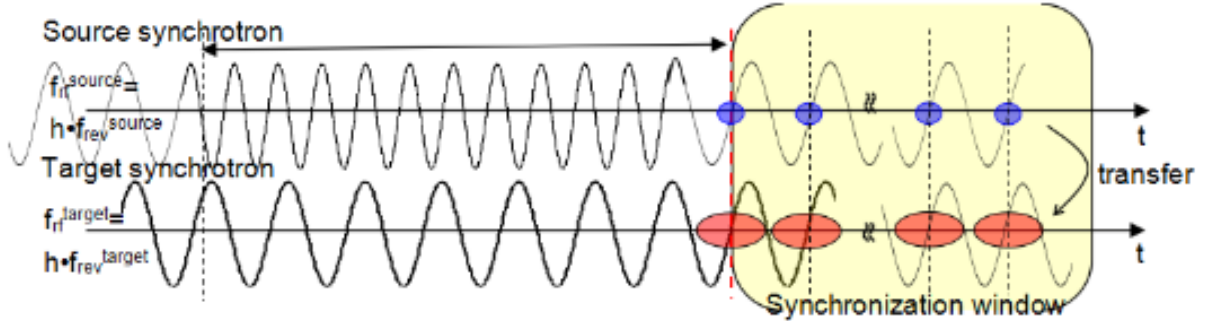


Figure 2.1: The illustration of the phase shift method.

Fig. 1 illustrates the phase shift method. The top and bottom RF signals are respectively from the source and target synchrotrons. For the phase shift method two RF signals are of the same frequency. The blue dots show the position of the bunches of the source synchrotron, the red dots correspond to the bucket positions of the target synchrotron. The time-of-flight between the bunch and bucket is compensated here. The red dashed line shows the end of the phase shift process and the beginning of the synchronization window, drawn in yellow. After the phase shift, bunches match with the random buckets.

A particular case of the B2B synchronization occurs, when the target synchrotron is empty, i.e. it did not capture any bunch yet, the phase shift can be done for the target synchrotron without adiabatical consideration (e.g. Phase jump is possible).

Now we analyze the rf frequency modulation of the phase shift from the beam dynamics viewpoint.

- Radial excursion and momentum shift due to rf frequency modulation

For the phase shift method, the magnetic field is not affected by the frequency modulation, so  $\Delta B = 0$ . By substituting  $\Delta B = 0$  into eq. 2.12 and eq. 2.13, we could get respectively the accompanying radial excursion and momentum shift by the frequency modulation.

$$\frac{\Delta f}{f} = \left( \frac{\gamma_t^2}{\gamma^2} - 1 \right) \frac{\Delta R}{R} \quad (2.15)$$

and

$$\frac{\Delta f}{f} = \left( \frac{1}{\gamma^2} - \frac{1}{\gamma_t^2} \right) \frac{\Delta p}{p} \quad (2.16)$$

## 2.4. RF synchronization

---

- Transverse dynamics analysis

The momentum spread  $\Delta p/p \neq 0$  during the phase shift process causes chromaticity drift  $\Delta Q$ .  $Q$  is the chromaticity of the machine [15].

$$\Delta Q = Q \frac{\Delta p}{p} \quad (2.17)$$

- Shift of synchronous phase

The synchronous phase deviates from  $0^\circ$  during the frequency modulation. From the expression of the particle momentum,  $p(t)$ , given in eq. 2.4, the time derivative of  $p(t)$  can be written as

$$\frac{dp(t)}{dt} = \frac{e\rho_0 B(t)}{\alpha_p R_0^{1/\alpha_p}} R(t)^{1/\alpha_p - 1} \frac{dR(t)}{dt} + e\rho_0 \left(\frac{R(t)}{R_0}\right)^{1/\alpha_p} \frac{dB(t)}{dt} \quad (2.18)$$

Now, the relationship between the rate of change in momentum of a particle,  $dp(t)/dt$ , and the force applied on it,  $F(t)$ , is governed by Newton's second law:

$$\frac{dp(t)}{dt} = F(t) \quad (2.19)$$

$F(t)$  is given by the product of the accelerating electric field,  $E(t)$ , and the charge of particle,  $e$ . Substituting  $dp(t)/dt$  given in eq. 2.18 and  $F(t) = eE(t)$  into eq. 2.19, we have

$$\frac{e\rho_0 B(t)}{\alpha_p R_0^{1/\alpha_p}} R(t)^{1/\alpha_p - 1} \frac{dR(t)}{dt} + e\rho_0 \left(\frac{R(t)}{R_0}\right)^{1/\alpha_p} \frac{dB(t)}{dt} = eE(t) \quad (2.20)$$

From this equation, we obtain the expression of energy gain in one turn,

$$2\pi R_0 \left[ \frac{e\rho_0 B(t)}{\alpha_p R_0^{1/\alpha_p}} R(t)^{1/\alpha_p - 1} \frac{dR(t)}{dt} + e\rho_0 \left(\frac{R(t)}{R_0}\right)^{1/\alpha_p} \frac{dB(t)}{dt} \right] = eV(t) \sin[\phi_{s0}(t) + \Delta\phi_s(t)] \quad (2.21)$$

where  $V(t)$  is the RF accelerating voltage per turn;  $\phi_{s0}$ , the synchronous phase in the operation with no frequency modulation; and  $\Delta\phi_s(t)$ , the change in the synchronous phase originating from the rf frequency modulation.

The magnetic field is not affected by the frequency change, we can assume  $dB(t)/dt = 0$ . Before the synchronization, it is a stationary bucket with the synchronous phase  $0^\circ$ . Then, eq. 2.21 reduce to

$$2\pi R_0 \left[ \frac{e\rho_0 B(t)}{\alpha_p R_0^{1/\alpha_p}} R(t)^{1/\alpha_p - 1} \frac{dR(t)}{dt} \right] = eV(t) \sin[\Delta\phi_s(t)] \quad (2.22)$$

Solving  $\Delta\phi_s(t)$  from eq. 2.22, we have

$$\Delta\phi_s(t) = \sin^{-1} \left[ \frac{2\pi\rho_0 B(t)}{\alpha_p V} \left( \frac{R(t)}{R_0} \right)^{1/\alpha_p - 1} \frac{dR(t)}{dt} \right] \quad (2.23)$$

From eq. 2.23, we know that  $\Delta\phi_s(t)$  is only determined by  $dR(t)/dt$  during the frequency modulation.

## 2.4. RF synchronization

---

- Bucket area factor

At the flattop, the bucket is a stationary bucket with  $\phi_{s0}(t) = 0$ . During the frequency modulation process, the bucket becomes a running bucket with  $\Delta\phi_s(t) \neq 0$ . The ratio of bucket areas of a running bucket to a stationary bucket is bucket area factor  $\alpha(\Delta\phi_s)$ . The bucket area factor could be estimated by [16].

$$\alpha_b(\Delta\phi_s) \approx (1 - \sin(\Delta\phi_s))(1 + \sin(\Delta\phi_s)) \quad (2.24)$$

- Adiabaticity analysis

$\omega_s(t)$  is the small-amplitude synchrotron frequency given by

$$\omega_s(t) = \left[ -\frac{\eta(t)h\omega_{rev}^2(t)eV(t)\cos\phi_s(t)}{2\pi\beta^2(t)E(t)} \right]^{1/2} \quad (2.25)$$

A process is called “adiabatic” when the RF parameters are changed slowly enough for the longitudinal emittance to be preserved. The condition that the parameters are slowly varying can be expressed by

$$\varepsilon = \frac{1}{\omega_s^2(t)} \left| \frac{d\omega_s(t)}{dt} \right| \ll 1 \quad (2.26)$$

Compared with  $\phi_s(t)$ , all of the other variables change very slowly.  $\phi_s(t) = \phi_{s0}(t) + \Delta\phi_s(t)$ . From eq. (2.26) and eq. (2.25), we can write the adiabaticity parameter  $\varepsilon$ , as follows [13]:

$$\varepsilon \approx \frac{1}{2\omega_{s0}(t)} \left| \tan\phi_s(t) \frac{d\phi_s(t)}{dt} \right| \quad (2.27)$$

- Constraints on the RF frequency modulation

From eq. 2.27, we can clearly see that  $\phi_s(t)$  and  $d\phi_s(t)/dt$  play deterministic roles for the adiabaticity when the frequency is modulated. Now let us deduce how the rf frequency modulation affects  $\phi_s(t)$  and  $d\phi_s(t)/dt$ . From eq. (2.15), we could get the following equation.

$$\frac{dR(t)}{dt} \left( \frac{\gamma_t^2}{\gamma^2} - 1 \right) f_0 = \frac{df(t)}{dt} R_0 \quad (2.28)$$

Substituting eq. 2.28 into eq. 2.22, we get

$$V \sin\phi_s = \frac{2\pi R_0 \rho B}{f_0 \left( \frac{1}{\gamma}^2 - \frac{1}{\gamma_t}^2 \right)} \left[ \frac{R(t)}{R_0} \right]^{\left( \frac{1}{\alpha_p} - 1 \right)} \frac{df(t)}{dt} \quad (2.29)$$

Because  $(R(t) - R_0)/R_0$  is about  $10^{-4}$ ,  $[1 + \frac{\Delta R}{R_0}]^{\left( \frac{1}{\alpha_p} - 1 \right)} \approx 1$ . We can get the relation between  $df(t)/dt$  and  $\phi_s$  from eq. 2.29.

$$V \sin\phi_s = \frac{2\pi R_0 \rho B}{f_0 \left( \frac{1}{\gamma}^2 - \frac{1}{\gamma_t}^2 \right)} \frac{df(t)}{dt} \quad (2.30)$$

## 2.4. RF synchronization

---

From eq. 2.24, we know that the bucket area factor is determined by the synchronous phase change  $\Delta\phi_s$ . Based on eq. 2.30, we know the synchronous phase  $\Delta\phi_s$  is determined by  $df(t)/dt$ , so  $df(t)/dt$  is important for the bucket size.

In order to get the relation between  $d\phi_s(t)/dt$  and the frequency modulation, we get the time derivative of eq. 2.30

$$V \cos\phi_s \frac{d\phi_s}{dt} = \frac{2\pi R_0 \rho B}{f_0 \left( \frac{1}{\gamma}^2 - \frac{1}{\gamma_t}^2 \right)} \frac{df(t)/dt}{dt} \quad (2.31)$$

Based on the adiabaticity eq. (2.27),  $d\phi_s(t)/dt$  must be existing and small enough. So  $\frac{df(t)/dt}{dt}$  must be existing and small enough. It means that  $df(t)/dt$  and  $\phi_s(t)$  must be continuous. In a word, there are three constraints for the rf frequency modulation.

- The  $df(t)/dt$  of the rf frequency modulation must be small enough to guarantee the bucket size.
- The  $df(t)/dt$  of the rf frequency modulation must be continuous to guarantee the continuous synchronous phase.
- The  $df(t)/dt/dt$  of the rf frequency modulation must be small enough to guarantee the change of the synchronous phase slow enough for the beam to follow.

### 2.4.2 Frequency beating method

The frequency beating method uses the effect of two RF signals of slightly different frequencies, perceived as periodic variations in phase difference whose rate is the difference between the two frequencies. The RF frequency of the source or the target or both synchrotrons is detuned long before the ejection, then the difference between the phase of the bunch and bucket is measured. Based on the measured phase, the synchronization is realized when the phase difference of the two RF frequencies corresponds to the ideal phase difference ( $\Delta\theta = 0^\circ$ ). The  $\Delta\theta$  is the mismatch between the bunch center and the corresponding bucket center. Because of the slightly different RF frequencies, a mismatch between the bunch and bucket centers exists. In principle, the B2B transfer requirement for FAIR allows a bunch to bucket center mismatch of  $1^\circ$ , which brings a symmetric time frame with respect to the time of the ideal phase difference, resulting in the maximum synchronization window for the frequency beating method, drawn in yellow, see Fig. 2.2. The red dashed line shows the time for the expected phase difference.

The RF frequency is detuned at the end of the ramp. During the rf frequency detune process, the magnetic field and radius excursion react and the momentum is not affected for the energy match.

- Longitudinal dynamics analysis

Because the momentum is not affected by the frequency change, namely  $\Delta p = 0$ , the general relation between the radial excursion and RF frequency change eq. 2.11 reduces to eq. 2.32 and the general relation between the magnetic field change and RF frequency change eq. 2.6 reduces to eq. 2.33.

## 2.6. Synchronization of the extraction and injection kicker

---

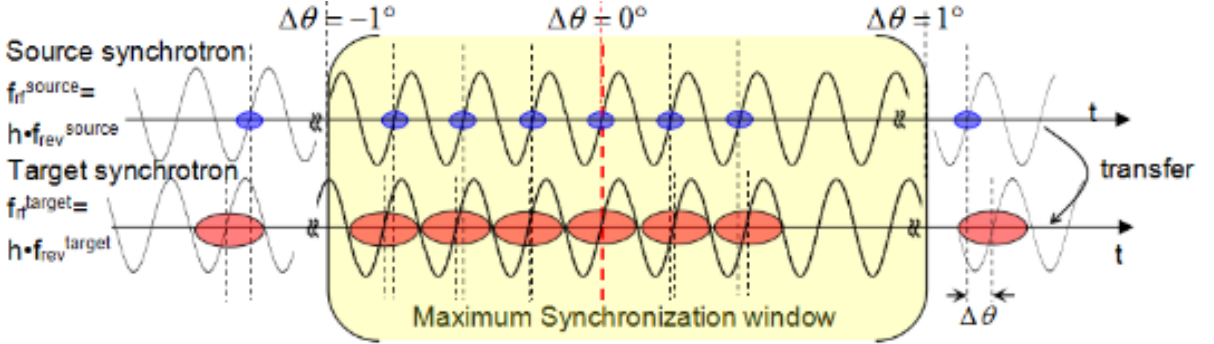


Figure 2.2: The illustration of the frequency beating method.

$$\frac{\Delta f}{f} = -\frac{\Delta R}{R} \quad (2.32)$$

$$\frac{\Delta f}{f} = \frac{1}{\gamma_t^2} \times \frac{\Delta B}{B} \quad (2.33)$$

## 2.5 Bucket label

After the synchronization, the bunch is synchronized to an arbitrary RF bucket. For the proper injection, we must know which buckets are already filled and which buckets should be filled by next injection cycle. The fast extraction can only proceed when the required bucket comes.

## 2.6 Synchronization of the extraction and injection kicker

For the proper B2B transfer, the extraction and injection kickers must be synchronized with the beam. The kicker time consists of the rise time, flat-top and fall time [17].

- Extraction kicker

Here we discuss that all bunches are extracted by one time extraction kick. The flattop is at least with the length of the bunches to be injected. The fall time is not constrained. If there is no empty RF bucket of the ring, the rise time of the extraction kicker must be shorter than the bunch gap. If there is at least one empty RF bucket, the rise of the magnetic field could be achieved within the gap of the empty RF buckets.

- Injectin kicker

For multi-batch injection, the rise time of the injection kicker must be shorter than the bunch gap. The flat-top is determined by the length of the bunches to be injected. If all buckets must be filled, the fall time must be shorter than

## **2.7. Beam indication for the beam instrumentation**

---

the bunch gap. If at least one bucket is kept empty, the fall of the magnetic field could be achieved within the gap of the empty RF buckets. If the ring needs only one time injection, the rise time is not constrained. The flat-top determined by the length of the bunches to be injected. The fall time must be shorter than the bunch gap or the gap of the empty RF buckets.

## **2.7 Beam indication for the beam instrumentation**

In order to observe the beams and measure related parameters for accelerators and transfer lines [18], the beam instrumentation (BI) equipments must be synchronized and triggered within the beam schedule. For the B2B transfer, the data acquisition for the beam instrumentation equipments should be triggered before the bunch is extracted. They should not be triggered too early because of the limitation of sampling time. So a pre-trigger is necessary, which indicates that the bunch will be extracted/injected soon.

# Chapter 3

## Technical basis for the B2B transfer system

For the FAIR accelerator complex, synchronization of the B2B transfer will be realized by the FAIR control system and the Low-Level RF (LLRF) system. For the synchronization of LLRF system, the General Machine Timing (GMT) system is complemented and linked to the Bunchphase Timing System (BuTiS). Machine Protection System (MPS) protects SIS100 and subsequent accelerators or experiments from damage. Hence, the B2B transfer system for FAIR coordinates with the MPS system.

### 3.1 FAIR control system

The FAIR control system takes advantage of collaborations with CERN in using proven framework solutions like Front-End System Architecture (FESA) [19], LHC Software Architecture (LSA), White Rabbit (WR), etc [20]. It consists of the equipment layer, middle layer and application layer. The equipment layer consists of equipment interfaces, GMT and software representations of the equipment FESA. The middle layer provides service functionality both to the equipment layer and the application layer through the IP control system network. LSA is used for the Settings Management (SM). The application layer combines the applications for operators as GUI applications or command line tools. The application layer and the middle layer only request what the FAIR accelerator complex should do and transmit set values to the equipment layer. The actual beam production is controlled by the GMT. The GMT system is synchronized to BuTiS. The SM supplies the schedule for the GMT by LSA [20, 21].

#### 3.1.1 BuTiS

Bunch Phase Timing System (BuTiS) serves as a campus-wide clocks distribution system with subnanosecond resolution and stability over distances of several hundred meters while maintaining 100ps per km timing stability [22]. Two BuTiS reference clocks T0 10 MHz and C2 200 MHz and a trigger identification pulse at 100 kHz are generated centrally in the BuTiS center. A star-shaped optical fiber distribution network transfers these signals to BuTiS receivers all over the FAIR campus. A BuTiS receiver and a local reference synthesizer are installed in each supply room

### **3.1. FAIR control system**

---

to produce the BuTiS reference clocks, which are in phase. For this purpose, a measurement setup in the BuTiS center continuously measures the optical signal transmission delay between the BuTiS center and the different BuTiS receivers. This measurement information is used to shift the phases of the signals generated in each local reference synthesizer for the delay compensation. The main task of BuTiS is the supply of the reference clock signals for Reference RF Signal in each rf supply rooms. [22, 23]

#### **3.1.2 GMT**

The GMT is contained in the equipment layer. The main tasks of the GMT system are time synchronization of more than 2000 Front-End Controllers (FEC) with nanosecond accuracy, distribution of timing messages and subsequent generation of real-time actions by the nodes of the timing system [21]. The GMT consists of the Timing Master (TM), the White Rabbit (WR) timing network and integrates nodes. The timing master's interface to the upper layers, e.g. online schedule monitor, is modeled as a FESA device. The timing master is a logical device, containing the data master (DM), the clock master (CM) and the management master (MM). The data master receives a schedule for the operation of the FAIR accelerator complex from the Settings Management and provides the real-time scheduler by broadcasting timing messages to the WR timing network, which will be received and executed by the corresponding node at the designated time. The clock master is a dedicated White Rabbit switch. It is the topmost switch layer of the WR timing network and provides the grandmaster clock and timestamps which are distributed to all other nodes in the timing network. The clock master derives its clock from the BuTiS clocks and timestamps distributed are phase locked to BuTiS clocks. The GMT could deliver BuTiS T0 and C2 clocks to any nodes and nodes are capable to timestamp clock edges. All active components including receiver nodes and switches are registered to the MM. The MM monitor and manage the active components of the GMT system [24].

The DM sends timing messages<sup>1</sup> to nodes, which contains Event ID, Format ID, Group ID, Event No, Sequence ID, Beam Process ID, parameter, timestamp and so on [25]. A timing message is sent across the WR network, so it must be contained in the ethernet frame. An ethernet frame including one timing message has a length of 110 byte, which is called the timing frame in this dissertation.

#### **3.1.3 FESA**

The FESA<sup>2</sup> is a framework used to fully integrate the large amount of front-end equipments into the accelerator control system. FESA was developed by CERN and has already been implemented into the CERN control system. Now it is developed further in collaboration with GSI for the FAIR project. FESA develops FESA classes, the equipment-type specific front-end software [19]. For a specific type of equipments, a FESA class implementation accesses to the control interface of the equipments. The FESA class models the equipment as device, so the FESA output is called device class. One device class can instantiate several devices and thus

---

<sup>1</sup><https://www-acc.gsi.de/wiki/Timing/TimingSystemEvent>

<sup>2</sup><https://www-acc.gsi.de/wiki/FESA/WhatIsFESA>

### 3.2. LLRF system

---

generally handles several independent pieces of equipments. FESA provides JAVA based graphical user interfaces (GUI) to design, deploy, instantiate and test the device classes. For the FAIR project the necessary interaction with the timing nodes is realized in a lab-specific timing library of the FESA framework. The FEC use FESA to implement generic and equipment specific functions in form of the device classes. Interaction with the equipment is synchronized with the GMT system.

For time multiplexed operation of the accelerators, the FESA framework supports defining multiplexed properties. Before an accelerator schedule is started, the setting properties of FESA classes are pre-supplied by LSA from SM for all scheduled beams with specific settings accordingly. At runtime, FESA's real time software actions are triggered by timing message, the actual beam specific data is then selected based on information carried by the timing message and send to the equipment.

#### 3.1.4 SM

The SM is based on a physics model for accelerator optics, parameter space and overall relations between parameters and between accelerators, which is located in the middle layer of the control system. It supports off-line generation of synchrotron settings, sending these settings to all involved devices, and programming the schedule of the timing system [20]. The SM uses the LSA framework. A standardized API allows accessing data in a common way as basis for generic client applications for all accelerators. Using the LSA-API, trim-applications can coherently modify synchrotron settings [20]. E.g. the service generates timing constraints (e.g. ramp curve) as well as the equipment's data settings (e.g. field) for all devices derived from physics parameters (e.g. beam energy). For FAIR the framework is extended to model the overall schedule of all accelerators. Beams are described as Beam Production Chains to allow a description from beam source to beam target for settings organization and data correlation.

## 3.2 LLRF system

The FAIR low-level rf (LLRF) system will be used in the existing synchrotrons SIS18 and ESR, as well as in the FAIR synchrotrons SIS100 and SIS300 and in CR, NESR, and accumulator ring (RESR). It supports fast ramp rates and large frequency span for the acceleration of a variety of ion species, It supports different RF manipulations, including operation at different harmonic numbers, barrier bucket generation and bunch compression [26].

RF cavities are driven by one of Reference RF Signals, which are supplied in every supply room . Fig. 3.1 shows the local cavity synchronization system, which synchronizes the local Cavity Direct Digital Synthesizer (DDS) unit to the Reference RF Signal. The cavity gets the RF signal from a local Cavity DDS unit, which receives RF Frequency Ramps from the Central Control System (CCS). A Digital Signal Processor (DSP)-System measures the phase difference between the Reference RF Signal and the gap voltage of the cavity. In the DSP system, a closed-loop control algorithm is implemented, which generates frequency corrections for the local Cavity DDS unit. This process is called local synchronization loop, which ensures that the phase of the gap voltage follows the phase of the Reference RF signal [26].

### 3.2. LLRF system

---

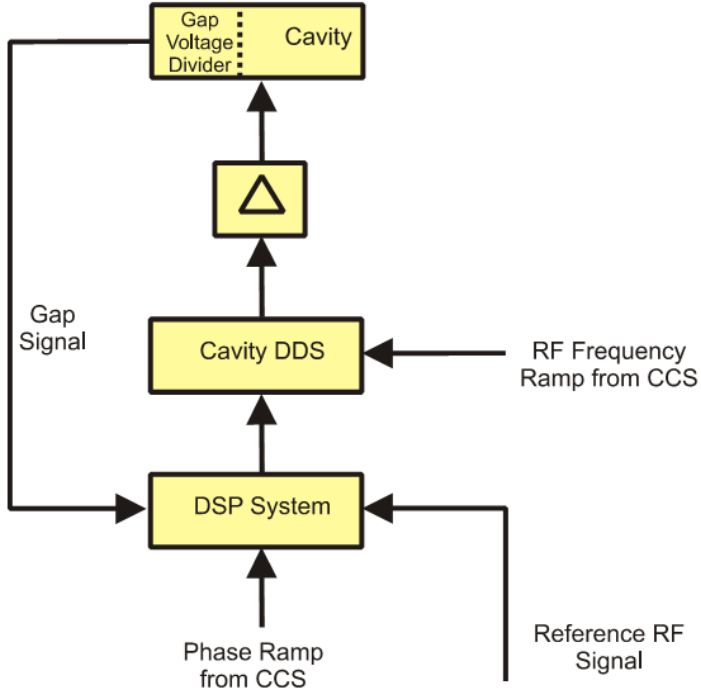


Figure 3.1: Local Cavity Synchronization  
[26]

In order to damp longitudinal rigid dipole oscillations, the beam phase feedback loop is used. The phase difference between the beam signal and the Reference RF Signal is fed back via an FIR filter. The beam signal is obtained by a fast current transformer or a beam position monitor. The filter output serves as a frequency change in the cavities resulting in a phase shift of the gap voltage [8].

The bunch-by-bunch longitudinal rf feedback loop generates a correction voltage in dedicated feedback cavities for a specified bunch [12].

Each supply room has a Reference RF Signal distribution shown in Fig. 3.2. The virtual RF cavity is a virtual position around the ring, to which the Reference RF Signal corresponds. The Reference RF Signals in different supply rooms are synchronized by the BuTiS. BuTiS 200MHz and 100kHz clock signals are received by BuTiS receivers in different supply rooms in phase. In Fig. 3.2, a number of Group DDS units are located in each supply room, which are synchronized to BuTiS local reference. The Group DDS signals can be routed to the different cavity systems by a Switch Matrix. All cavities in a synchrotron could be providing with the same Group DDS signal. The cavities at different harmonic numbers could be realized by using Group DDS signals with different harmonic numbers. The Group DDS concept allows to synchronize a variety of cavities in a very flexible way [26].

All the cavities of SIS18 are driven from one supply room. The SIS100 cavities will be gathered in three acceleration sections, each of them is driven by a dedicated supply room.

### 3.3. MPS system

---

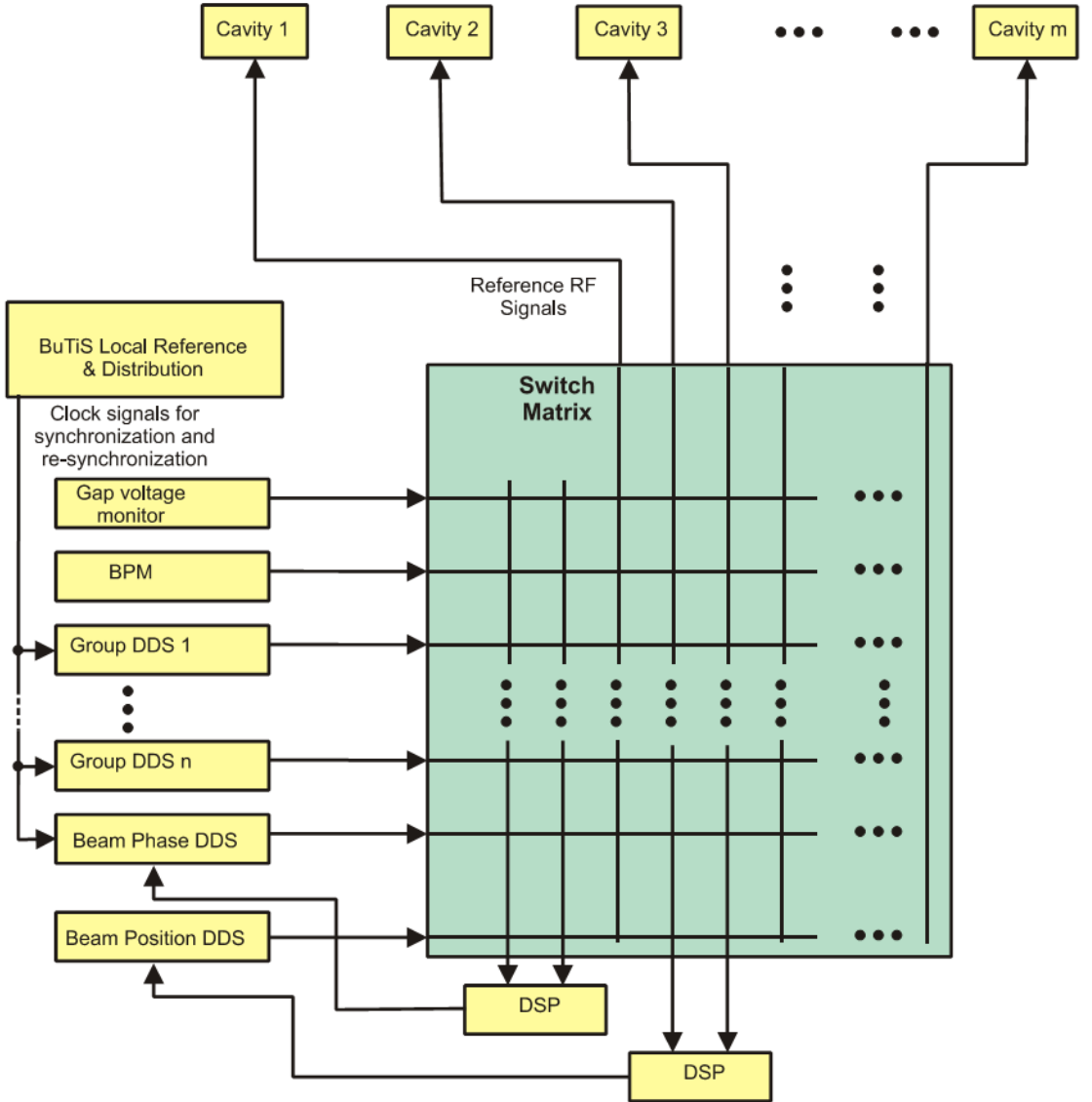


Figure 3.2: Reference RF Signal Distribution  
[26]

### 3.3 MPS system

The Fast Beam Abort System (FBAS) protects SIS100 and subsequent accelerators or experiments from damage by mislead beams, uncontrolled radioactive contamination and so on. Thereby, the individual equipment is assumed self-protecting, which could trigger accelerator safety critical actions, such as an emergency beam dump, a shutdown of magnets or a beam injection inhibit. In case of relevant equipment failures or other inappropriate equipment states, a MPS signal stems from this equipment. MPS propagates these signals by a proprietary net and combines them with the machine state or operator interventions. These signals must be processed to ensure the timeliness of the triggered actions. The entering of a safe equipment state is subordinate to a FBAS action [27].

## 3.4 Comparison

Based on the FAIR existing infrastructures, the B2B transfer system for FAIR is unique from other existing B2B transfer systems ([13, 28]). The uniqueness is the phase difference between two rf systems of the source and target synchrotrons are achieved based on the campus distributed reference signals with picosecond precision, which are in phase and have same frequency. The campus distributed reference signals are synchronized with BuTiS T0 clock. They are named Synchronization Reference Signal in this document. The phase difference between the Synchronization Reference Signal and the rf signal of the rf system is measured locally and transferred from one synchrotron to another via the WR network. The existing B2B transfer system for CERN measures the phase difference between two synchrotrons by the direct cable transfer of the rf signal of one synchrotron to another synchrotron [28]. The phase measurement between two rf systems of the B2B transfer system for FAIR is more stable and precise, which is less influenced by the external environment, e.g. temperature influence on the direct cable connection. It does not constraint by the distance between two synchrotrons.

Besides, the B2B transfer system for FAIR is more flexible, which supports various complex beam transfer for FAIR. It is capable to transfer different species beam from one machine cycle to another. It is capable to parallel transfer beam through FAIR accelerators. It is capable to transfer the beam between two synchrotrons via FRS or Super FRS.

It coordinates with the MPS system, which protects SIS100/SIS300 from unacceptable failure or situation. E.g. beam position is out of tolerance, rf cavity failure and so on. If the inhibit signal from MPS is off, the B2B transfer extraction and injection kickers will be fired. If the inhibit signal is on, the injection and extraction kickers will be blocked for firing. When the emergency signal from MPS is indicated, the beam is capable to be kicked to the beam dump at any time during the B2B transfer process.

# Chapter 4

## Concept of the B2B transfer system for FAIR

For the proper B2B transfer, the position of the bunch and bucket and the firing of the extraction and injection kicker must be precisely controlled. Before we explain the functional modules of the B2B transfer system, some basic concepts and their symbols are introduced.

- Bucket pattern  $t_{pattern}$ .
- Time-Of-Flight (TOF) between two synchrotrons  $t_{TOF}$ .
- Time-Of-Flight between the virtual RF cavity and the extraction/injection kicker,  $t_{v\_ext}$  and  $t_{v\_inj}$ .
- Extraction and injection kicker delays,  $t_{ext}$  and  $t_{inj}$ .

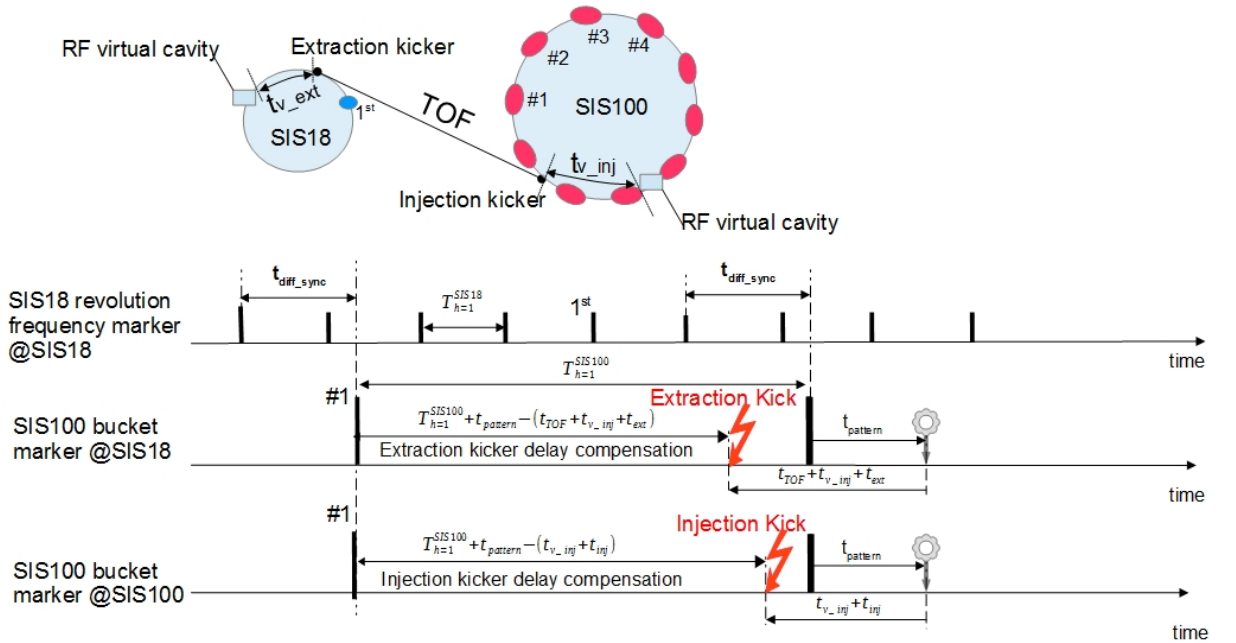


Figure 4.1: The illustration of B2B transfer from SIS18 to SIS100.

## 4.1. Basic procedure of the B2B transfer system for FAIR

---

Fig. 4.1 illustrates B2B transfer from SIS18 to SIS100. The SIS18 and SIS100 revolution frequency marker indicate the time when the first bunch or the first bucket pass by the RF virtual cavity (black bars named 1<sup>st</sup> and #1). The extraction and injection kicker firing (red lighting bolts) are time delay on the first bars of the SIS100 revolution frequency marker at SIS18 and SIS100, which are called extraction and injection kicker delay compensation. The mentioned four instances of time are related to the second bars of the SIS100 revolution frequency marker.  $T_{rev}^X$  represents the revolution period of the synchrotron X, e.g.  $T_{rev}^{SIS18}$ .  $T_{rf}^X$  represents the period of the cavity frequency of synchrotron X, e.g.  $T_{rf}^{SIS18}$ . After the RF synchronization, the time difference between the SIS18 and SIS100 revolution frequency markers is represented by  $t_{diff\_sync}$ , e.g.  $t_{diff\_sync} = t_{v\_ext} + t_{TOF} + t_{v\_inj}$  for  $U^{28+}$  and  $H^+$  odd bucket injection,  $t_{diff\_sync} = t_{v\_ext} + t_{TOF} + t_{v\_inj} - T_{rf}^{100}$  for  $H^+$  even bucket injection, more details about the user case from SIS18 to SIS100, please see Sec.5.1.1 and 5.1.2.

- Extraction kick

In order to inject into the proper buckets, the extraction kicker delay compensation for the first bar of the SIS100 revolution frequency marker is  $T_{rev}^{SIS100} + t_{pattern}$ , see gray gear at the SIS100 revolution frequency marker at SIS18. For example, when two  $U^{28+}$  bunches of SIS18 are to be injected into the bucket #3 and #4 of SIS100,  $t_{pattern} = 1 \times T_{rev}^{SIS18}$ . The extraction kicker must be fired  $t_{v\_inj} + t_{TOF} + t_{ext}$  earlier as the bucket passes the virtual RF cavity, so the extraction kicker delay compensation is  $T_{rev}^{SIS100} + t_{pattern} - (t_{TOF} + t_{v\_inj} + t_{ext})$ , see red lighting bolt at the SIS100 revolution frequency marker at SIS18.

- Injection kick

With the consideration of the bucket pattern, the injection kicker delay compensation for the first bar of the SIS100 revolution frequency marker is  $T_{rev}^{SIS100} + t_{pattern}$ , see gray gear at the SIS100 revolution frequency marker at SIS100. The injection kicker must be fired  $t_{v\_inj} + t_{inj}$  time earlier as the bucket passes the virtual RF cavity, so the injection kicker delay compensation is  $T_{rev}^{SIS100} + t_{pattern} - (t_{v\_inj} + t_{inj})$ , see red lighting bolt at the SIS100 revolution frequency marker at SIS100.

In order to realize the B2B transfer above, the standard procedure is defined and described in Sec. 4.1. We specify how the basic B2B principles mentioned in Chap.2 are realized for FAIR in Sec. 4.2. In Sec. 4.3, the data flow of the B2B transfer system is described.

## 4.1 Basic procedure of the B2B transfer system for FAIR

Fig. 4.2 illustrates the basic procedure of the B2B transfer with two different synchronization scenarios. The top part shows the chronological steps with the frequency beating method, while the bottom part shows the steps with the phase shift method. The emergency kickers can be triggered at any time during the acceleration cycle by the MPS. The purple region shows the valid time for the emergency kicker. The yellow region shows the synchronization window.

#### 4.1. Basic procedure of the B2B transfer system for FAIR

---

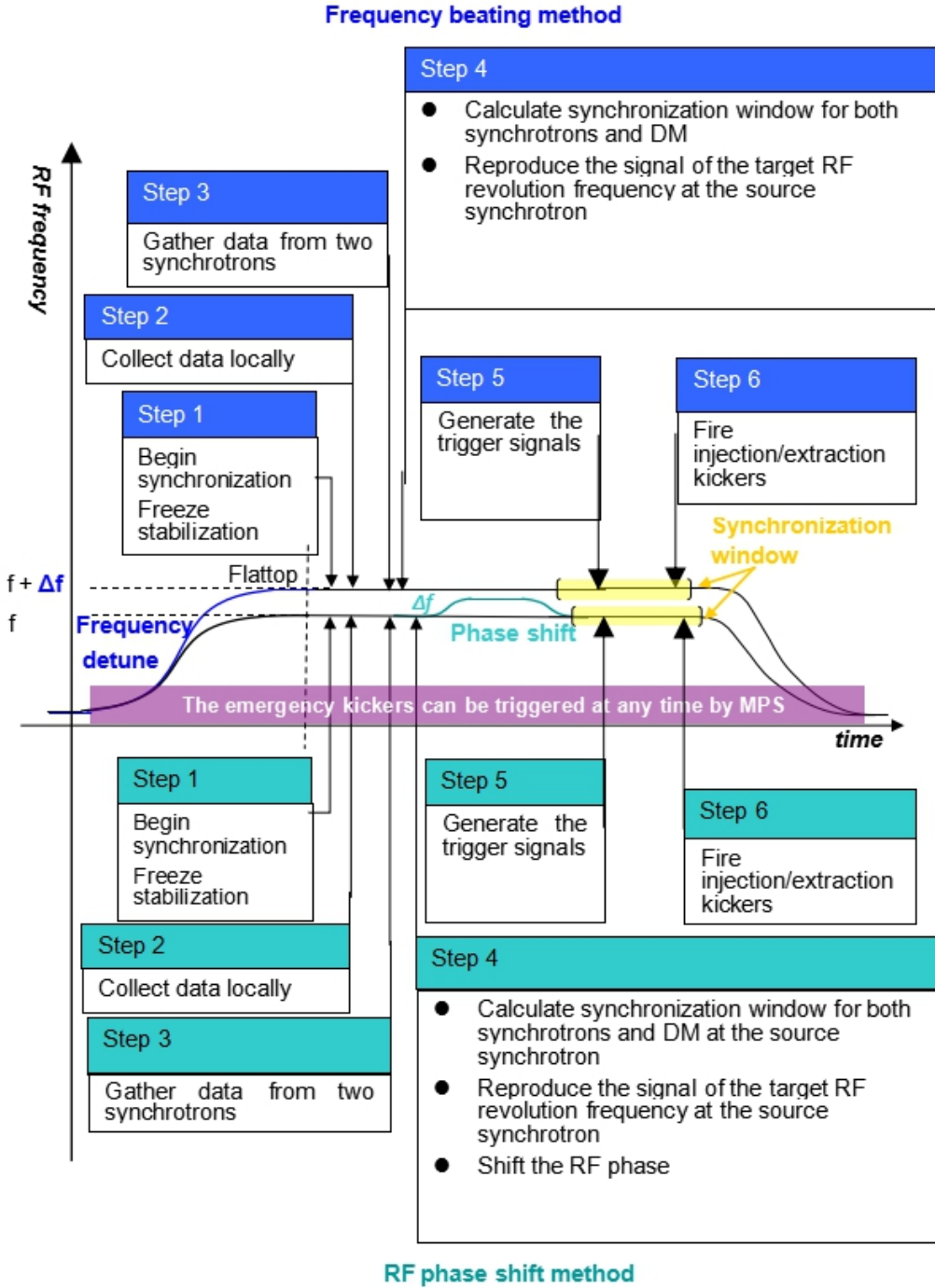


Figure 4.2: The procedure for the B2B transfer within one acceleration cycle. The procedure for the B2B transfer within one acceleration cycle. Shown are the frequency beating method (blue, top) and the phase shift method (green, bottom).

The B2B transfer process basically needs to follow six steps [29]:

1. The DM announces the B2B transfer and freezes the feedback loop (e.g. beam phase feedback loop), when required.
2. The two synchrotrons measure the rf phase locally.

## 4.2. Realization of the basic B2B functionalities

3. The source synchrotron gathers the measured rf phase from the target synchrotron.
4. The source synchrotron calculates the synchronization window with the kicker delay and sends it to both synchrotrons and to the DM. Besides, it reproduces the bucket label signal at the source synchrotron. For the phase shift method, the source synchrotron generally achieves the phase shift. But when the target synchrotron is empty, the phase shift is achieved by the method of the phase jump at the target synchrotron for simplicity's sake.
5. The trigger signal is generated for the kickers with the delay compensation.
6. The kicker electronics fire the kickers.

## 4.2 Realization of the basic B2B functionalities

In this section, how the basic B2B functionalities are realized based on the FAIR control system and LLRF system is introduced. Fig. 4.3 shows the topology of the B2B transfer system [29, 30].

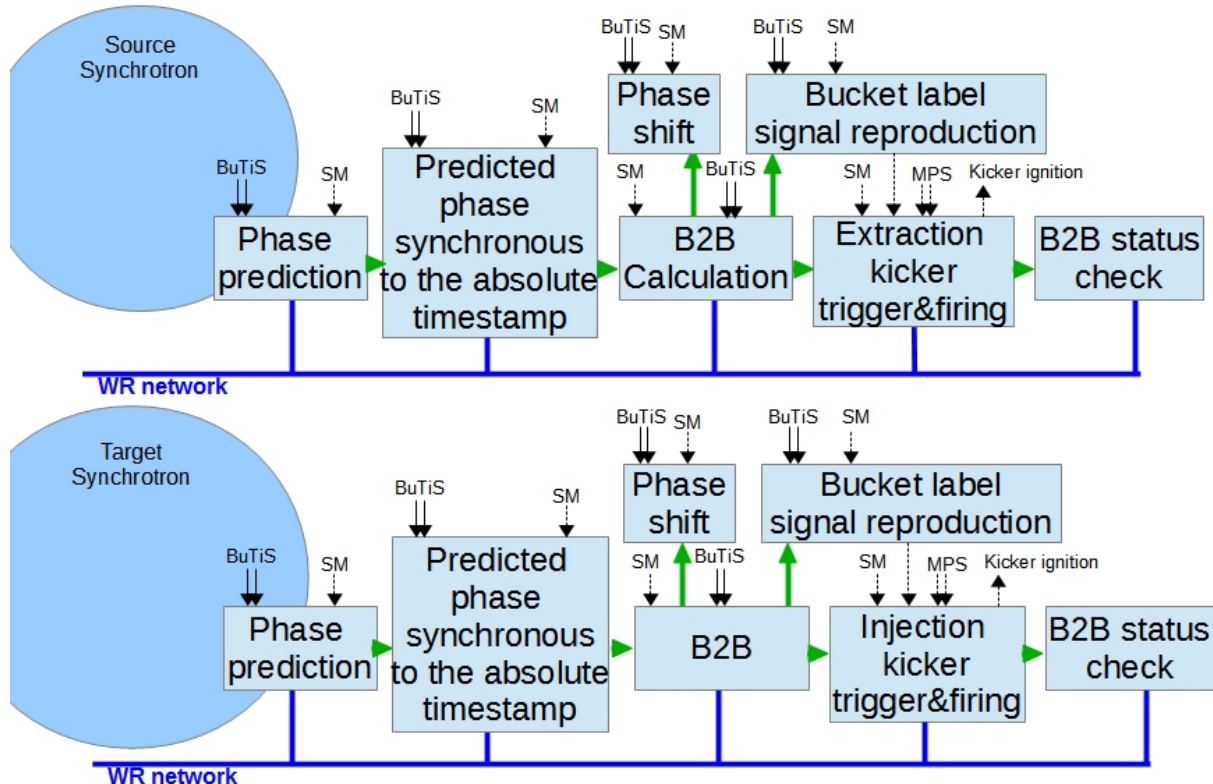


Figure 4.3: The topology of the B2B transfer system

### 4.2.1 RF phase difference between two RF systems

In order to get the phase difference between two RF systems, we make use of a shared reference signal at both source and target synchrotrons, which is called the

## 4.2. Realization of the basic B2B functionalities

---

Synchronization Reference Signal. It is with the fixed frequency and always in the same phase at two synchrotrons. It is a sine wave, whose frequency is a multiple of the BuTiS T0 100 kHz and whose zero-crossing is aligned with T0 edges in order to ensure the synchronization of the Synchronization Reference Signal in different synchrotrons [31, 32].

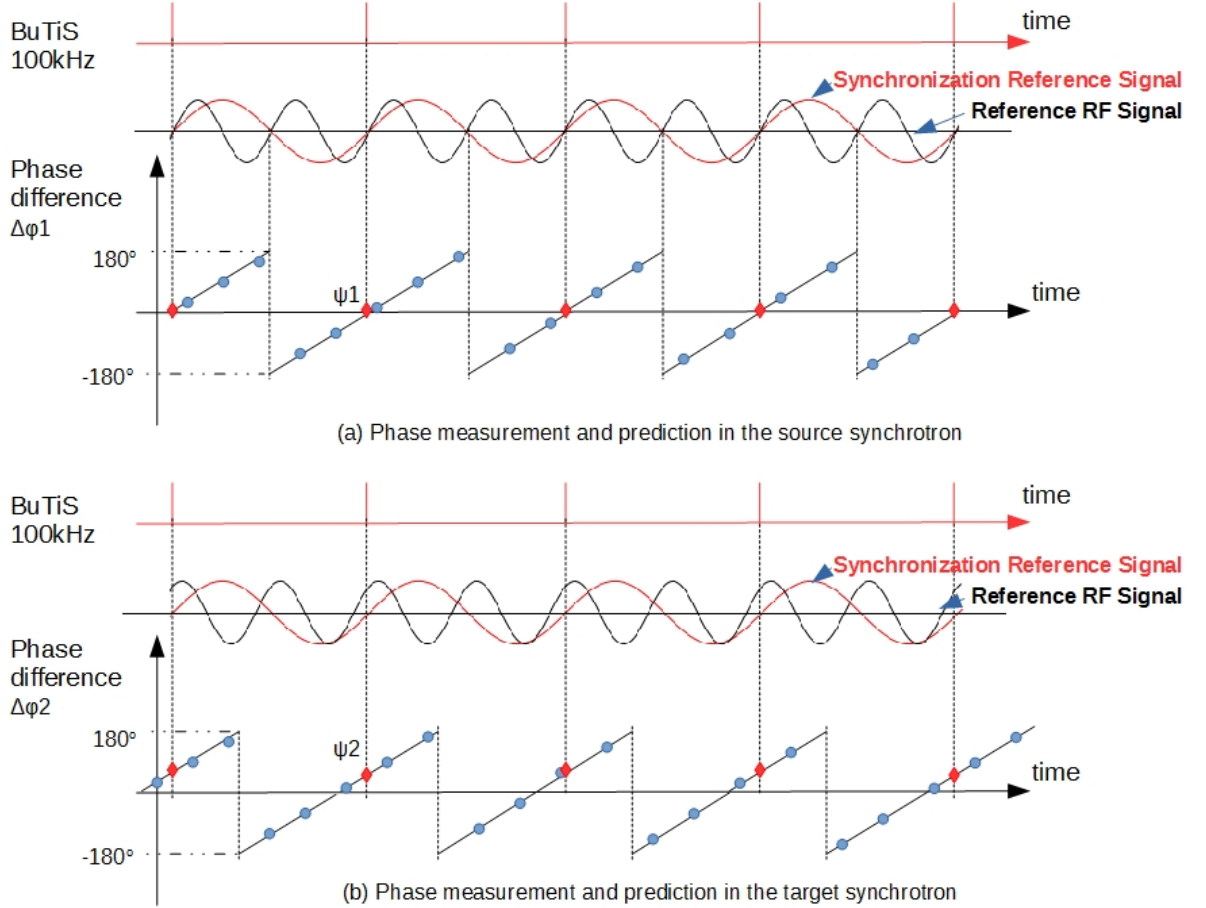


Figure 4.4: The realization of the phase difference between two synchrotrons

Fig. 4.4 shows the realization of the phase difference measurement between two RF systems. Fig. 4.4 (a) and (b) illustrate the phase measurement and prediction in the source and target synchrotrons. The red sine waves in Fig. 4.4 (a) and (b) represents the Synchronization Reference Signals (e.g 100 kHz) in two synchrotrons and the black waves the Reference RF signals (e.g. 200 kHz) from the Group DDS. The phase difference  $\Delta\varphi_1$  between the Reference RF Signal and the Synchronization Reference Signal is measured by the Phase Advance Measurement (PAM) Module at the source synchrotrons and  $\Delta\varphi_2$  at the target synchrotron. The phase measurement is performed synchronously to an internal clock, which is represented by the blue dots. Based on a series of the phase difference measurements, the phase difference at any T0 edge  $\psi_1$  and  $\psi_2$  could be predicted in every synchrotron by the Phase Advance Prediction (PAP) Module, which is represented by the red diamonds in Fig. 4.4. For more details about the implementation and realization of the PAP and PAM modules, please see “Development of the LLRF system for a deterministic Bunch-to-Bucket transfer for FAIR“. Because the phase prediction is synchronized

## 4.2. Realization of the basic B2B functionalities

---

with T0 clocks and the Synchronization Reference Signal's phase is  $0^\circ$  at T0 edges,  $\psi_1$  and  $\psi_2$  are the phase of the Reference RF Signals. In order to get the phase difference between two rf systems,  $\psi_1 - \psi_2$ , the phase of the target synchrotron is transferred by the B2B target SCU (Scalable Control Unit) [21, 33] to the B2B source SCU at the source synchrotron via the WR network. The B2B source and target SCUs are installed in the source and target synchrotrons locally. The transfer of the phase is achieved by the timing frame TGM\_PHASE\_TIME, please see Appendix A.

### 4.2.2 RF phase difference synchronous to the absolute timestamp

Both B2B source and target SCUs could get the timestamp of every BuTiS T0 edge. Fig. 4.5 illustrates the synchronization of the rf phase difference to the timestamp. When B2B source SCU and B2B target SCU receive the timing frame CMD\_START\_B2B from DM at a T0 edge, they need maximum 1  $\mu$ s to inform the PAP modules to start the phase prediction respectively. The PAP modules use e.g. 500  $\mu$ s for the prediction and updates the predicted phase value every T0 edge. After 500  $\mu$ s, the B2B source and target SCUs need another maximum 1  $\mu$ s to get the predicted phase (represented as the red diamond in Fig. 4.5) from the PAP modules and they also get the BuTiS T0 edge timestamp which corresponds to the predicted phase. Then the rf phase difference between two rf systems and the corresponding timestamp are known.

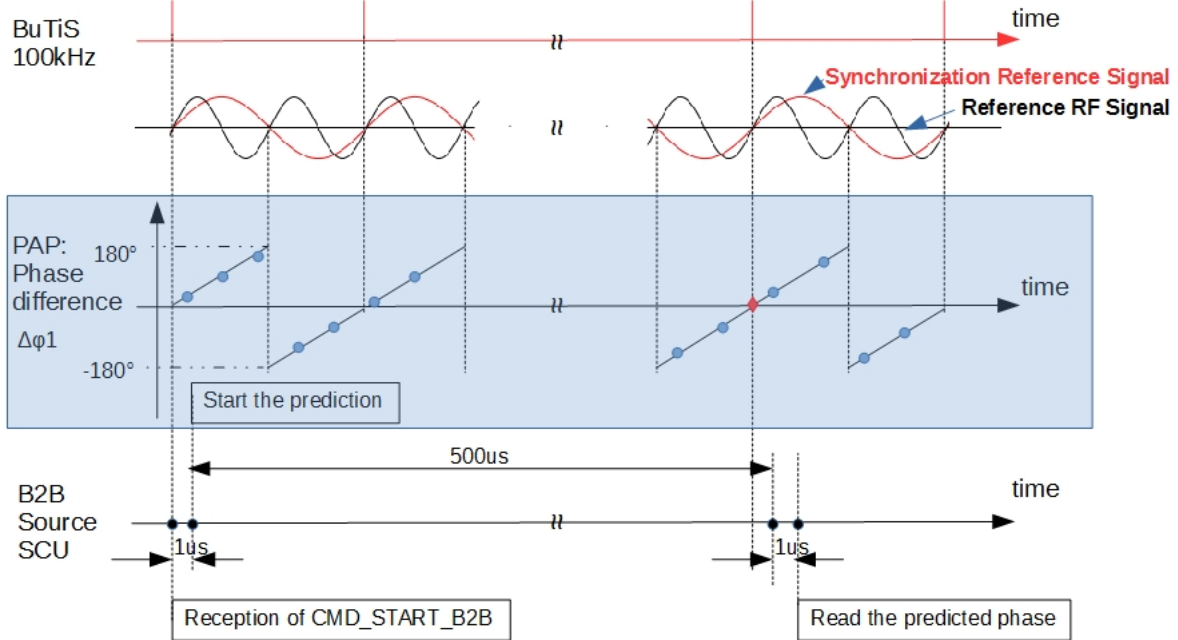


Figure 4.5: The synchronization of the rf phase difference to the timestamp

### 4.2.3 RF synchronization

The B2B transfer system for FAIR is available for both the phase shift and frequency beating methods, see Sec. 2.4.

- RF synchronization with the phase shift method

Eq. 4.1 gives the relation between the required phase shift  $\Delta\phi_{shift}$  and the frequency modulation.

$$\Delta\phi_{shift} = 2\pi \int_{t_0}^{t_0+T} \Delta f_{rf}(t) dt \quad (4.1)$$

The required phase shift is determined by the frequency offset  $\Delta f_{rf}(t)$  and the duration of the frequency modulation T. The phase shift must be executed adiabatically in order to guarantee the bucket size and continuous synchronous phase, see Sec. 2.4 at page 13. We introduce a phase shift of up to  $\pm 180^\circ$  of the phase shift for FAIR. A normalized frequency modulation profile  $f_{normalized}$  for  $180^\circ$  can be precalculated, which guarantees the adiabaticity. The actual frequency modulation profile  $f_{actual}$  is decided by the normalized frequency modulation profile and the required phase shift, see eq. 4.2. The required phase shift,  $\Delta\phi_{shift}$ , is calculated by the B2B source SCU.

$$\frac{\Delta\phi_{shift}}{180^\circ} = \frac{f_{actual}}{f_{normalized}} \quad (4.2)$$

Fig. 4.6 shows an example of a normalized and several actual frequency modulation profiles and the corresponding phase shift profile. The magenta profile is the normalized profile  $f_{normalized}$  with the phase shift of  $180^\circ$ . The blue one is  $1/2f_{normalized}$  with the phase shift of  $90^\circ$  and the green one is  $1/3f_{normalized}$  with  $60^\circ$ .

The B2B source SCU sends the required phase shift to the Phase Shift Module (PSM), which controls the phase shift of the Reference RF Signal of Group DDS by means of either frequency (Fig. 4.6 (a)) or phase (Fig. 4.6 (b)) modulation. The Reference RF Signal is routed to the different cavity systems by a Switch Matrix to realize the phase shift of all cavities on the synchrotron. For more details about the implementation and realization of the PSM modules, please see “Development of the LLRF system for a deterministic Bunch-to-Bucket transfer for FAIR“.

A particular case of the B2B synchronization occurs, when the target synchrotron is empty, i.e. it does not capture any bunch yet, the phase shift can be done for the target synchrotron without adiabatical consideration (e.g. Phase jump is possible). In this case, the B2B source SCU sends the timing frame TGM\_PHASE\_JUMP to the B2B target SCU, which contains the required phase jump. After the B2B target SCU receives the timing frame, it sends the value to the PSM for the phase jump of the Group DDS of the target synchrotron.

- RF synchronization with the frequency beating method

The ratio of the circumference between many pair of machines in FAIR is not a perfect integer, e.g. SIS18 and ESR (injection orbit), SIS100 and CR, CR and

## 4.2. Realization of the basic B2B functionalities

---

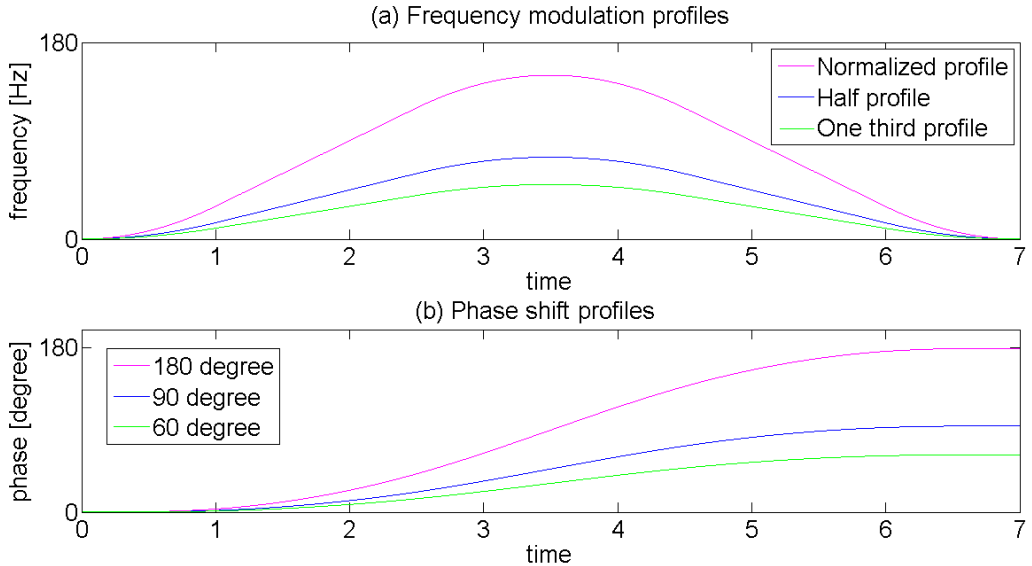


Figure 4.6: The normalized frequency and phase modulation profile and the actual profiles

HESR. so the frequencies of two synchrotrons begin beating automatically. For the pairs with the perfect integer ratio of the circumference, e.g. SIS18 and SIS100, the rf frequency of the source synchrotron is detuned by modifying the magnetic field and radial excursion to get the frequency beating. For more details about the synchronization with the frequency beating method, please see Chap. 5.

### 4.2.4 Coarse synchronization

The coarse synchronization is achieved by the synchronization window with a certain length. Within this window, the bunch is injected into the bucket with the center mismatch smaller than the upper bound<sup>1</sup>. The length of the synchronization window  $T_{sync\_win}$  is two times the period of the reproduced signal for the bucket label, see Sec. 4.2.5. For the phase shift method, the mismatch between the bunch and bucket center within the synchronization window is almost  $0^\circ$ . For the frequency beating method, the maximum bunch-to-bucket center mismatch  $\Delta\theta$  with the synchronization window is calculated by

$$\frac{T_{sync\_win}}{1/\Delta f} = \frac{\Delta\theta}{360^\circ} \quad (4.3)$$

where  $\Delta f$  is the beating frequency. The B2B source SCU is capable of receiving the values (kicker delay for extraction kicker of the source synchrotron, kicker delay for injection kicker of the target synchrotron,  $t_{TOF}$ , rf frequencies of the source and target synchrotrons, the upper bound time for the phase shift of the source synchrotron) from the SM by FESA classes via the accelerator network. The B2B

---

<sup>1</sup>B2B transfer from SIS18 to SIS100: upper bound of the bunch-to-bucket center mismatch is  $1^\circ$

## 4.2. Realization of the basic B2B functionalities

---

source SCU calculates the synchronization window, taking kicker delays into consideration and transfers the timestamp of the start of the synchronization window, TGM\_SYNCH\_WIN, to the DM and the source and target Trigger SCUs via the WR network. The Trigger SCUs are used to produce the kicker trigger signal. The TGM\_SYNCH\_WIN could also be used for the triggering of the bunch rotation of both machines (e.g. SIS100 and CR) with a specified advance.

### 4.2.5 Bucket label

The B2B transfer system for FAIR needs the bucket label not only at the rf flattop, but also during the whole acceleration cycle. The former is used for the normal extraction and injection and the latter is used for the emergency kick of SIS100.

- Bucket label for the normal extraction and injection

For the bucket label for the normal extraction and injection, three steps are necessary. Fig. 4.7 shows these three steps for the reproduction of the bucket label. Here we use B2B trasfer from SIS18 to SIS100 as an example.

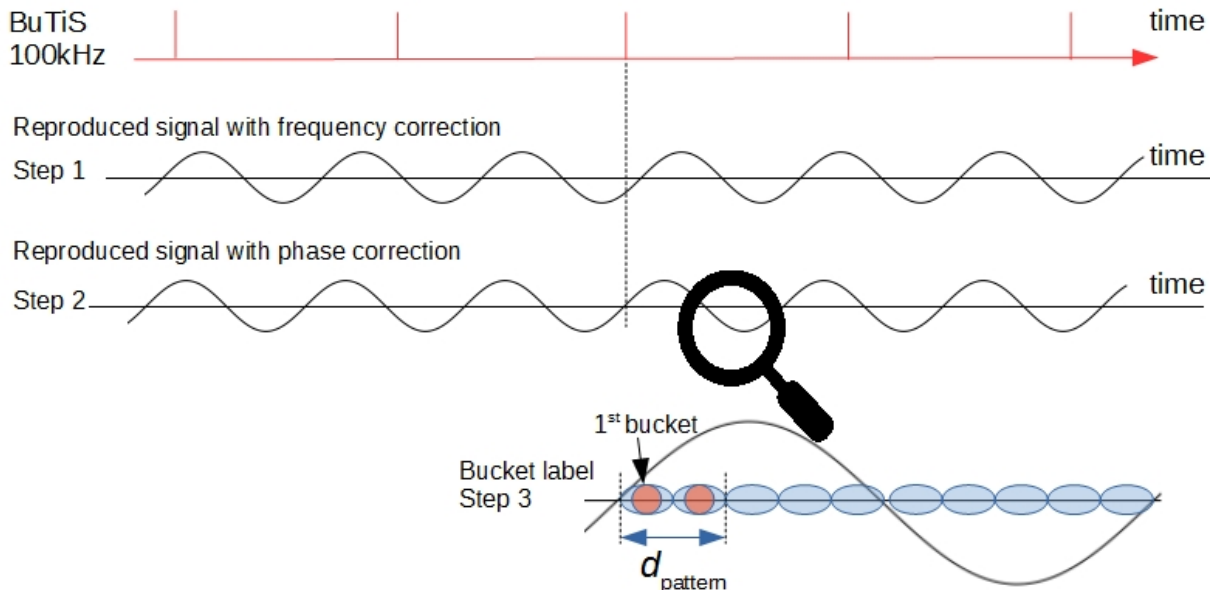


Figure 4.7: The realization of the bucket label for the normal extraction and injection.

- Step 1. Frequency correction

A signal with the same frequency as the Reference RF Signal at the flattop of the target synchrotron (e.g. RF revolution frequency of SIS100) is produced by the Signal Reproduction (SR) module, which is called the reproduced signal. For the B2B transfer system for FAIR, the zero-crossing of the reproduced signal always indicates the start of the 1st bucket.

## 4.2. Realization of the basic B2B functionalities

---

- Step 2. Phase correction

For the phase synchronization with the bucket, the bucket label signal must do phase correction at a specified T0 edge. The phase correction value is calculated by the B2B source SCU and transferred by the timing frame TGM\_PHASE\_CORRECTION to the Trigger SCU. Then the Trigger SCU gives the phase correction value to the SR module.

- Step 3. Bucket label

The SM manages the bucket pattern with the parameter of  $d_{pattern}$  on the reproduced signal. In Fig. 4.7, the 3rd and 4th buckets will be filled with  $d_{pattern} = 1 \times T_{rev}^{SIS18}$ . The bucket pattern is considered in the kicker delay compensation.

- Bunch gap label for the emergency extraction

Only for SIS100 emergency procedure, the bunch gap label is important during the whole acceleration cycle. There are two steps for the realization of the bunch gap label, see Fig. 4.8.

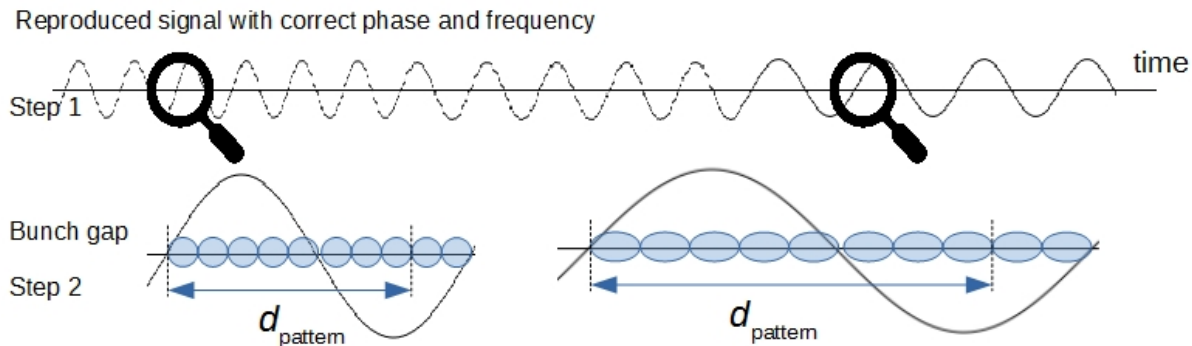


Figure 4.8: The realization of the bunch gap for the emergency extraction.

- Step 1. The reproduced signal is directly distributed from the switch matrix, which synchronizes with the Reference RF Signal in frequency and phase.

- Step 2. Bunch gap label

The SM informs the bunch gap with the parameter of  $d_{pattern}$  on the reproduced signal during the whole acceleration cycle. In Fig. 4.8, the 9th and 10th buckets services as the bunch gap. The  $d_{pattern} = 4 \times T_{rev}^{SIS18}$  is with variable value, which is considered in the kicker delay compensation and applied to the reproduced signal on T0 edges.

### 4.2.6 Fine synchronization of the extraction and injection kicker

For the normal B2B extraction/injection, the synchronization window is a gating signal, which is received by the source and target Trigger SCUs from the WR network by TGM\_SYNCH\_WIN. Within this window, the first reproduced signal will

## 4.2. Realization of the basic B2B functionalities

---

be selected by the Trigger Decision (TD) module . The extraction and injection kicker are synchronized with the bunch and bucket by the extraction and injection kicker delay compensation. If the inhibit signal of MPS is off, the kicker delay compensation must be considered for the kicker synchronization. The extraction kicker will be triggered by the extraction kick delay compensation,  $T_{rev}^{SIS100} + T_{rev}^{SIS18} - (t_{TOF} + t_{v,inj} + t_{ext})$  and the injection kicker will be triggered by the injection kick delay compensation,  $T_{rev}^{SIS100} + T_{rev}^{SIS18} - (t_{v,inj} + t_{inj})$ , see Fig. 4.1. Both extraction and injection kick delay compensation values are preloaded from the SM to the Trigger SCU and the Trigger SCU gives these values to the TD module. The kicker delay compensation is applied to the first selected reproduced signal by TD module. If the inhibit signal is on, the normal injection and extraction trigger signals will be blocked.

For the SIS100 emergency kick, the extraction delay compensation is calculated by  $T_{rev}^{SIS100} + t_{pattern} - (t_{v,emg} + t_{emg})$ , where  $t_{v,emg}$  is the time delay between the virtual RF cavity and the emergency extraction position and  $t_{emg}$  the emergency kicker delay. The emergency extraction delay compensation values are preloaded from the SM to the Trigger SCU and the Trigger SCU gives these values to the TD module. The kicker delay compensation is applied to the selected reproduced signal by TD module. Only when the emergency signal is valid, the emergency kicker will be triggered by the TD module.

### 4.2.7 Beam indication for the beam instrumentation

Two timing frames will be send from the B2B source SCU to the DM. DM sends them further to the FECs for BI.

- Timing frame *TGM\_SYNCH\_WIN*

This time frame indicates the start of the synchronization window for the beam instrumentation.

- Timing frame *TGM\_B2B\_STATUS*

The time frame *TGM\_B2B\_STATUS* indicates the status of the B2B transfer system and the actual beam injection time.

### 4.2.8 WR network

The B2B transfer involves a certain amount of frames within the WR network [34]. More details about the B2B frames, please see Appendix A. The name of the timing frames from the DM is beginning with *CMD\_*, the name of other telegrams is beginning with *TGM\_*. The B2B related frames make use of the format of the timing frame. The Format ID (FID) of the timing frame is used to indicate the B2B transfer, the Group ID (GID) the source and target machines and the Beam Process ID (BPID) the B2B process steps for the B2B related SCUs.

A Virtual Local Area Network (VLAN) is a group of FECs in the WR network that is logically segmented by function or application, without regard to the physical locations of the FECs.

All FECs in the WR network are assigned to the DM VLAN, within which the DM forwards broadcast timing telegrams downwards to all FECs. The telegrams

## **4.2. Realization of the basic B2B functionalities**

---

sent from the source B2B SCU upwards to the DM are unicast packets within this VLAN. E.g. TGM\_SYNCH\_WIN and TGM\_B2B\_STATUS.

## 4.2. Realization of the basic B2B functionalities

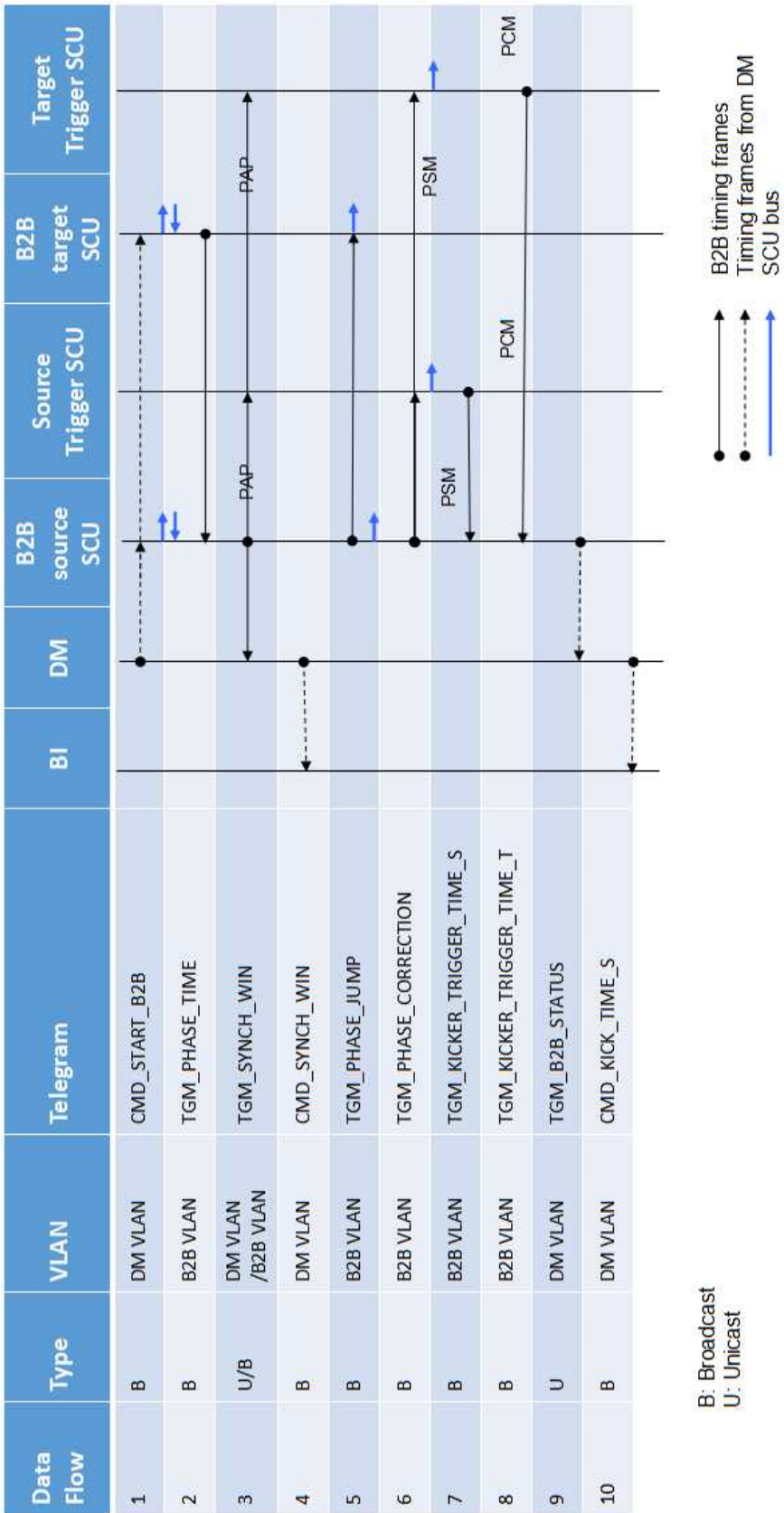


Figure 4.9: Timing frames transfer for the B2B transfer

### **4.3. Data/Signal flow of the B2B transfer system**

---

Besides, the SCUs for the B2B transfer are assigned to the B2B VLAN. The specified VLAN for the B2B transfer could reduce the traffic of the WR network [30]. All B2B related telegrams TGM\_ except TGM\_SYNCH\_WIN and TGM\_B2B\_STATUS are broadcasted in the B2B VLAN. The broadcast packet is much safer, because it does not need to know the Internet Protocol address (IP address) of B2B related SCUs. Besides, it increases the flexibility of the system that all SCUs for the B2B transfer could have changeable IP addresses. Fig. 4.9 shows the types of the B2B timing frames, their VLANs and the frames transfers among B2B related SCUs.

#### **4.2.9 B2B transfer status check**

The B2B source SCU shall receive the trigger time of the extraction kicker and actual beam extraction time, TGM\_KICKER\_TRIGGER\_TIME\_S, from the source Trigger SCU via the WR network and also the trigger time of the injection kicker and actual beam injection time, TGM\_KICKER\_TRIGGER\_TIME\_T, from the target Trigger SCU via the WR network. The Trigger SCU is responsible for the trigger of the kicker electronics. The B2B source SCU is capable of examining the status of the B2B transfer system and transferring the status and the actual beam injection time (TGM\_B2B\_STATUS) to the DM. If all components of the B2B transfer system work correctly and the B2B transfer process is accomplished, the status bit is ‘0’. Otherwise it is ‘1’. For this purpose, it shall do simple checking based on the extraction/injection trigger time and the actual beam extraction/injection time. E.g. Source trigger time < actual beam extraction time.

## **4.3 Data/Signal flow of the B2B transfer system**

In this section, the procedure for the B2B transfer is explained from the viewpoint of the data/signal flow, which follows the basic six steps in Fig. 4.2. Before the synchronization, the feedback loop, e.g. beam phase feedback loop and bunch-to-bunch feedback loop, should be frozen.

1. The DM sends the timing frame CMD\_START\_B2B for the B2B transfer.
2. The B2B source and target SCUs send the timing frame tag to the PAP module. They read the predicted phase advance and the time slope from the PAP module after a fixed delay.
3. The B2B target SCU sends the predicted phase advance and the time slope (TGM\_PHASE\_TIME) to the B2B source SCU via the WR network.
4. The B2B source SCU calculates the synchronization window and transfers the timestamp of the start of the window (TGM\_SYNCH\_WIN) to the DM, as well as the Trigger SCUs of both machines. The B2B source SCU calculates the phase correction value and transfers it to all Trigger SCUs via the WR network. Then the Trigger SCUs transfer the phase correction value to its Phase Correction Module (PCM). The PCM triggers the phase correction of the SR module. Only for the phase shift method, the B2B source SCU calculates the required shifted phase and transfers it to the PSM. Then the PSM transfers the phase or frequency modulation profile to the Group DDS.

#### **4.3. Data/Signal flow of the B2B transfer system**

---

5. When the source and target Trigger SCUs receive the telegram (TGM\_SYNCH\_WIN), they produce the synchronization window pulse for the TD module. With the help of the bucket label signal, inhibit signal and emergency extraction signal, the TD module will produce the extraction and injection trigger signals for the kicker electronics. The source Trigger SCU gets the timestamp of the extraction trigger signal and the target Trigger SCU the timestamp of the injection trigger signal.
6. The extraction and injection kickers are fired. After that, the source Trigger SCU gets the actual beam extraction time and transfers it together with the timestamp of the extraction trigger signal (TGM\_KICKER\_TRIGGER\_TIME\_S) to the source B2B SCU via the WR network. The target Kicker SCU gets the timestamp of actual beam injection time and transfers it together with the timestamp of the injection trigger signal (TGM\_KICKER\_TRIGGER\_TIME\_T) to the source B2B SCU via the WR network.

The regular extraction and injection kickers are not fired, when one of the following situation happens.

- The calculation (synchronization window, the phase correction and phase shift value) is not correct.
- The telegrams are not received within a specified timeout interval.
- The inhibit signal from the MPS is on and the emergency extraction signal from the MPS is valid.

Besides of the basic six steps, the B2B source SCU transfers the B2B status together with the timestamp of the beam injection (TGM\_B2B\_STATUS) to the DM via the WR network.

# Chapter 5

## Application of the B2B transfer system for FAIR accelerators

Due to the ratio of the circumference of the injection/extraction orbit, there are several user cases of the B2B transfer for FAIR.

- The circumference ratio between the large and small synchrotron is an ideal integer.
  - $U^{28+}$  B2B transfer from SIS18 to SIS100
  - $H^+$  B2B transfer from SIS18 to SIS100
  - B2B transfer from ESR to CRYRING
- The circumference ratio between the large and small synchrotron is close to an ideal integer.
  - $h=4$  B2B transfer from SIS18 to ESR
  - $h=1$  B2B transfer from SIS18 to ESR
- The circumference ratio between the large and small synchrotron is far away from an ideal integer.
  - B2B transfer from CR to HESR

Besides, FAIR has many user cases of B2B transfers that the extraction and injection beam have different energy because of the targets installed between two synchrotrons (e.g. Pbar, FRS). In this situation, the beam revolution frequency ratio between the small and large synchrotrons is equivalent to the circumference ratio between the large and small synchrotrons .

- The revolution frequency ratio between the small and large synchrotron is far away from an ideal integer.
  - $H^+$  B2B transfer from SIS100 to CR via Pbar
  - RIB B2B transfer from SIS100 to CR via Super FRS
  - B2B transfer from SIS18 to ESR via FRS

### 5.1. Circumference ratio is an ideal integer

---

In this document, the circumference of the injection/extraction orbit of the synchrotron is denoted by  $C^X$ , the revolution frequency and rf cavity frequency by  $f_{rev}^X$  and  $f_{rf}^X$ , the beating frequency by  $\Delta f$  and the harmonic number by  $h^X$ . The superscript X could be either “l” or “s” denoting the large or small synchrotron.  $\kappa$  is used to represent integers and  $\lambda$  the decimal numbers.

Tab. 5.1 lists all FAIR user cases of the B2B transfer.

Table 5.1: FAIR user cases of the B2B transfer

Circumference ratio	$C^l/C^s$	$\frac{f_{rev}^s}{f_{rev}^l}$	User case of FAIR accelerators
$C^l/C^s = \kappa$ Integer	5		$U^{28+}$ B2B transfer from SIS18 to SIS100
	5		$H^+$ B2B transfer from SIS18 to SIS100
	5		B2B transfer from ESR to CRYRING
$C^l/C^s = \iota + \lambda$ or $frev^s/frev^l = \iota + \lambda$ close to integer ( $\iota$ is integer)	2-0.003		$h=4$ B2B transfer from SIS18 to ESR
	2-0.003		$h=1$ B2B transfer from SIS18 to ESR
$C^l/C^s = \iota + \lambda$ or $frev^s/frev^l = \iota + \lambda$ far away from integer ( $\iota$ is expressed by $\frac{m}{n}$ )		4.9-0.0004	$H^+$ B2B transfer from SIS100 to CR
		4.9-0.0004	RIB B2B transfer from SIS100 to CR
	2.6-0.003		B2B transfer from CR to HESR
		1.8+0.048	B2B transfer from SIS18 to ESR via FRS

## 5.1 Circumference ratio is an ideal integer

If the ratio of the circumference of the injection/extraction orbit of the large synchrotron to that of the small synchrotron is an ideal integer, we have the following relation.

$$\frac{C^l}{C^s} = \kappa \quad (5.1)$$

From the circumference ratio, the revolution frequency ratio of two synchrotrons can be calculated.

$$\frac{f_{rev}^l}{f_{rev}^s} = \frac{1}{\kappa} \quad (5.2)$$

Based on eq. 5.2 and harmonic number, the  $f_{rf}^X$  is calculated by eq. 5.3 and eq. 5.4

$$f_{rf}^s = h^s \times f_{rev}^s = h^s \times \kappa \times f_{rev}^l \quad (5.3)$$

## 5.1. Circumference ratio is an ideal integer

---

$$f_{rf}^l = h^l \times f_{rev}^l \quad (5.4)$$

Diving eq. 5.4 by eq. 5.3, we get

$$\frac{f_{rf}^l}{f_{rf}^s} = \frac{h^l}{h^s \times \kappa} \quad (5.5)$$

$Y$  is defined as the GCD (Greatest Common Divisor) of  $h^l$  and  $h^s \times \kappa$ .

Tab. 5.2 shows the formulas for the frequency of the bucket label signal, two slightly different frequencies for beating, the length of the synchronization window and the bunch and bucket center mismatch in this scenario.

Table 5.2: Synchronization when the circumference ratio is an ideal integer (the period of the beating frequency is longer than the revolution period)

	Large synchrotron is target synchrotron	Small synchrotron is target synchrotron
Bucket label	$\frac{f_{rf}^l}{h^l/Y}$	$\frac{f_{rf}^s}{(h^s \times \kappa)/Y}$
Different frequencies	$\frac{f_{rf}^l}{h^l/Y}$ and $\frac{f_{rf}^s}{(h^s \times \kappa)/Y} + \Delta f$ or $\frac{f_{rf}^l}{h^l/Y} + \Delta f$ and $\frac{f_{rf}^s}{(h^s \times \kappa)/Y}$	
Synchronization window	$2 \times (h^l/Y) \times T_{rf}^l$	$2 \times [(h^s \times \kappa)/Y] \times T_{rf}^s$
Center mismatch	$\pm \frac{1}{2} \times \frac{2 \times (h^l/Y) \times T_{rf}^l}{1/\Delta f} \times 360^\circ$	$\pm \frac{1}{2} \times \frac{2 \times [(h^s \times \kappa)/Y] \times T_{rf}^s}{1/\Delta f} \times 360^\circ$

The formulas in Tab. 5.2 is based on the assumption that  $\frac{f_{rf}^l}{h^l/Y} < f_{rev}^l$ , namely the frequency for beating is smaller than the revolution frequency, so the period of the frequency for beating is long enough to indicate all buckets in one revolution period. If  $\frac{f_{rf}^l}{h^l/Y} \geq f_{rev}^l$ , the period of the frequency for beating is shorter than the revolution period, which could not be used for the bucket indication. So does for the small synchrotron. In this case, we have the formulas in Tab. 5.3.

Table 5.3: Synchronization when the revolution frequency ratio is an ideal integer (the period of the beating frequency is shorter than the revolution period)

	Large synchrotron is target synchrotron	Small synchrotron is target synchrotron
Bucket label	$f_{rev}^l$	$f_{rev}^s$
Different frequencies	$\frac{f_{rf}^l}{h^l/Y}$ and $\frac{f_{rf}^s}{(h^s \times \kappa)/Y} + \Delta f$ or $\frac{f_{rf}^l}{h^l/Y} + \Delta f$ and $\frac{f_{rf}^s}{(h^s \times \kappa)/Y}$	
Synchronization window	$2 \times T_{rev}^l$	$2 \times T_{rev}^s$
Center mismatch	$\pm \frac{1}{2} \times \frac{2 \times T_{rev}^l}{1/\Delta f} \times 360^\circ$	$\pm \frac{1}{2} \times \frac{2 \times T_{rev}^s}{1/\Delta f} \times 360^\circ$

## 5.1. Circumference ratio is an ideal integer

---

### 5.1.1 Harmonic ratio equals to the circumference ratio

When the ratio of the harmonic number of the large synchrotron to that of the small synchrotron equals to the circumference ratio, we have the following relation.

$$\frac{h^l}{h^s} = \frac{C^l}{C^s} = \kappa \quad (5.6)$$

So the GCD of  $h^l$  and  $h^s \times \kappa$  is  $h^l = h^s \times \kappa$ , namely  $Y = h^l = h^s \times \kappa$ .

Substituting eq. 5.6 into eq. 5.5, the following relation is deduced.

$$\frac{f_{rf}^l}{f_{rf}^s} = 1 \quad (5.7)$$

In this scenario, the rf cavity frequencies of two synchrotrons are same. For the RF synchronization, both phase shift and frequency beating methods are applicable for the small or large synchrotrons. There is no difference of the implementation of two methods either on the large or small synchrotron, because they implement their species dependent rf frequency modulation profiles for a same required phase shift and same frequency dutune for the frequency beating method. Only when the target synchrotron is empty, the phase will be shifted for the target synchrotron by the phase jump. With the phase shift method, the phase advance between two synchrotrons is a constant, so the synchronization window is ideally infinitely long, within which two synchrotrons remain perfect synchronized. Bunches can be transferred at any time within the window.

There exists  $\frac{f_{rf}^l}{h^l/Y} >= f_{rev}^l = \frac{f_{rf}^l}{h^l}$ , so the formulas in Tab. 5.3 is applicable.

#### 5.1.1.1 User case of the $U^{28+}$ B2B transfer from SIS18 to SIS100

The user case of the  $U^{28+}$  B2B transfer from SIS18 to SIS100 belongs to this scenario. Four batches of  $U^{28+}$  at 200 MeV/u are injected into continuous eight out of ten buckets of SIS100. Each batch consists of two bunches [35, 36]. The large synchrotron is SIS100 and the small one SIS18.  $\kappa = 5$ ,  $h^{SIS100} = 10$  and  $h^{SIS18} = 2$ , so it complies with eq. 5.6. Substituting  $h^X$ ,  $\kappa$ ,  $f_{rf}^X$ ,  $f_{rev}^X$  and  $Y$  into formulas in Tab. 5.3, the synchronization of  $U^{28+}$  B2B transfer from SIS18 to SIS100 is obtained, see Tab. 5.4. Here we assume that SIS18 is detuned with 200 Hz for the frequency beating method.

Table 5.4: Synchronization of  $U^{28+}$  B2B transfer from SIS18 to SIS100

	Large synchrotron (SIS100) is target synchrotron
Bucket label	$f_{rev}^{SIS100}$
Different frequencies	$f_{rf}^{SIS18} + 200\text{Hz}$ and $f_{rf}^{SIS100}$
Synchronization window	$2 \times T_{rev}^{SIS100} = 12.718\text{us}$
Center mismatch	$\pm \frac{1}{2} \times \frac{2 \times T_{rev}^{SIS100}}{1/200} \times 360^\circ = \pm 0.50^\circ$

## 5.1. Circumference ratio is an ideal integer

---

After the synchronization, the phase difference between the SIS18 and SIS100 revolution frequency markers equals to the sum of  $t_{v\_inj}$ ,  $t_{v\_ext}$  and  $t_{TOF}$ . The SIS100 revolution frequency marker works for the bucket label. When the 1st and 2nd buckets are to be filled,  $t_{pattern}=0$ . When the 3rd and 4th buckets,  $t_{pattern}=T_{rev}^{SIS18}$ . When the 5th and 6th buckets,  $t_{pattern}=2 \times T_{rev}^{SIS18}$ . When the 7th and 8th buckets,  $t_{pattern}=3 \times T_{rev}^{SIS18}$ . Detailed parameters of  $U^{28+}$  B2B transfer from SIS18 to SIS100, please see Appendix B.1.

### 5.1.2 Harmonic ratio does not equal to the circumference ratio

When the ratio of the harmonic number of the large synchrotron to that of the small synchrotron does not equal to the circumference ratio, we have the following relation.

$$\frac{h^l}{h^s} \neq \frac{C^l}{C^s} = \kappa \quad (5.8)$$

In this scenario, the rf cavity frequency of one synchrotron is integer times of that of the other synchrotron for FAIR accelerators. Both phase shift and frequency beating methods are applicable for the RF synchronization. There is no difference of the implementation of the phase shift method either on the large or small synchrotron, because they implement their species dependent rf frequency modulation profiles for a same required phase shift. Only when the target synchrotron is empty, the phase jump is applied to the target synchrotron. With the phase shift method, we have an infinite synchronization window.

For the frequency beating method, from eq. 5.5, we get

$$\frac{f_{rf}^l}{h^l} = \frac{f_{rf}^s}{h^s \times \kappa} \quad (5.9)$$

If we detune  $\Delta f$  for  $\frac{f_{rf}^l}{h^l}$  of the large synchrotron, the rf cavity frequency  $f_{rf}^l$  must detune  $\Delta f \times h^l$ . If we detune  $\Delta f$  for  $\frac{f_{rf}^s}{h^s \times \kappa}$  of the small synchrotron, the rf cavity frequency  $f_{rf}^s$  must detune  $\Delta f \times (h^s \times \kappa)$ . According to the relation between  $h^l$  and  $h^s \times \kappa$ , we have the following two cases.

- $h^l > h^s \times \kappa \rightarrow \Delta f \times h^l > \Delta f \times (h^s \times \kappa)$

The frequency detune for the rf cavity frequency of the small synchrotron is smaller than that of the large synchrotron, so the frequency detune is preferred for the small synchrotron.

- $h^l < h^s \times \kappa \rightarrow \Delta f \times h^l < \Delta f \times (h^s \times \kappa)$

The frequency detune for the rf cavity frequency of the large synchrotron is smaller than that of the small synchrotron, so the frequency detune is preferred for the large synchrotron.

#### 5.1.2.1 User case of the $H^+$ B2B transfer from SIS18 to SIS100

Four batches of  $H^+$  at 4 GeV/u are injected into continuous four out of ten buckets of SIS100. Each batch consists of one bunch [35, 36]. The large synchrotron is

### 5.1. Circumference ratio is an ideal integer

---

SIS100 and the small one SIS18.  $\kappa = 5$ ,  $h^{SIS100} = 10$  and  $h^{SIS18} = 1$ . Substituting these values into eq. 5.5, we get

$$\frac{f_{rf}^{SIS100}}{f_{rf}^{SIS18}} = \frac{h^{SIS100}}{h^{SIS18} \times \kappa} = \frac{10}{1 \times 5} = \frac{2}{1} \quad (5.10)$$

For the frequency beating method, the frequency detune is preferred for SIS18 because of  $h^{SIS100} > h^{SIS18} \times \kappa$ . The GCD of  $h^{SIS100} = 10$  and  $h^{SIS18} \times \kappa = 1 \times 5$  is 5. There exists  $\frac{f_{rf}^l}{h^l/Y} = \frac{f_{rf}^{SIS100}}{10/5} \geq f_{rev}^l = \frac{f_{rf}^{SIS100}}{10}$ . Substituting  $h^X$ ,  $\kappa$ ,  $f_{rf}^X$ ,  $f_{rev}^X$  and Y into formulas in Tab. 5.3, the synchronization of  $H^+$  B2B transfer from SIS18 to SIS100 is obtained, see Tab. 5.5. Here we assume that SIS18 is detuned with 200 Hz for the frequency beating method.

Table 5.5: Synchronization of  $H^+$  B2B transfer from SIS18 to SIS100

	Large synchrotron (SIS100) is target synchrotron
Bucket label	$f_{rev}^{SIS100}$
Different frequencies	$\frac{f_{rf}^{SIS100}}{2}$ and $f_{rf}^{SIS18} + \Delta f$
Synchronization window	$2 \times T_{rev}^{SIS100} = 7.356 \text{ us}$
Center mismatch	$\pm \frac{1}{2} \times \frac{2 \times T_{rev}^{SIS100}}{1/200} \times 360^\circ = \pm 0.31^\circ$

In order to inject into the odd and even number buckets, there are two scenarios of the phase difference between the SIS18 and SIS100 revolution frequency markers after the synchronization.

- Injection into the odd number buckets

The phase difference between the SIS18 and SIS100 revolution frequency markers equals to  $t_{v\_ext} + t_{v\_inj} + t_{TOF}$ . When the 1st bucket is to be filled,  $t_{pattern}=0$ . When the 3rd bucket is to be filled,  $t_{pattern}=2 \times T_{rev}^{SIS18}$ .

- Injection into the even number buckets

The phase difference between the SIS18 and SIS100 revolution frequency markers equals to  $t_{v\_ext} + t_{v\_inj} + t_{TOF} - T_{rf}^{SIS100}$ . When the 2nd bucket is to be filled,  $t_{pattern}=1 \times T_{rev}^{SIS18}$ . When the 4th bucket is to be filled,  $t_{pattern}=3 \times T_{rev}^{SIS18}$ .

The SIS100 revolution frequency marker works for the bucket label. Detailed parameters of the  $H^+$  B2B transfer from SIS18 to SIS100, please see Appendix B.1.

#### 5.1.2.2 User case of the B2B transfer from ESR to CRYRING

Only one bunch is injected into one bucket of CRYRING [37, 38]. The large synchrotron is SIS18 and the small one is CRYRING.  $\kappa = 2$ ,  $h^{ESR} = 1$  and  $h^{CRYRING} = 1$ , substituting into eq. 5.5.

$$\frac{f_{rf}^{ESR}}{f_{rf}^{CRYRING}} = \frac{h^{ESR}}{h^{CRYRING} \times \kappa} = \frac{1}{1 \times 2} = \frac{1}{2} \quad (5.11)$$

## 5.2. Circumference ratio is not an ideal integer

---

For the RF synchronization, the phase jump for CRYRING is preferred, because CRYRING is empty before the injection. The 1/2 CRYRING revolution frequency marker works for the bucket label. The phase difference between the ESR and 1/2 CRYRING revolution frequency markers equals to  $t_{v,ext} + t_{v,inj} + t_{TOF}$  after the synchronization. For the frequency beating method, the frequency detune is preferred for ESR because of  $h^{ESR} < h^{CRYRING} \times \kappa$ . Here we assume 200 Hz frequency detune for 30 MeV/u proton of ESR. The GCD of  $h^{ESR} = 1$  and  $h^{CRYRING} \times \kappa = 1 \times 2$  is 1, namely Y=1.

There exists  $\frac{f_{rf}^s}{(h^s \times \kappa)/Y} = \frac{f_{rf}^{CRYRING}}{(1 \times 2)/1} < f_{rev}^s = \frac{f_{rf}^{CRYRING}}{1}$ , so Substituting  $h^X$ ,  $\kappa$ ,  $f_{rf}^X$ ,  $f_{rev}^X$  and Y into formulas in Tab. 5.2, the synchronization of the B2B transfer from ESR to CRYRING is obtained, see Tab. B.4.

Table 5.6: Synchronization of B2B transfer from ESR to CRYRING

	Small synchrotron (CRYRING) is target synchrotron
Bucket label	$1/2 f_{rf}^{CRYRING}$
Different frequencies	$f_{rf}^{ESR} + 200\text{Hz}$ and $\frac{f_{rf}^{CRYRING}}{2}$
Synchronization window	$2 \times (2 \times T_{rf}^{CRYRING}) = 5.488\text{ us}$
Center mismatch	$\pm \frac{1}{2} \times \frac{2 \times 2 \times T_{rf}^{CRYRING}}{1/200} \times 360^\circ = \pm 0.20^\circ$

Detailed parameters of the B2B transfer from ESR to CRYRING, please see Appendix B.4.

## 5.2 Circumference ratio is not an ideal integer

If the ratio of the circumference of the injection/extraction orbit of the large synchrotron to that of the small synchrotron is not an ideal integer,  $\kappa$  could be expressed as  $\iota + \lambda$  and we have the following relation.

$$\frac{C^l}{C^s} = \iota + \lambda \quad (5.12)$$

From the circumference ratio, the revolution frequency ratio of two synchrotrons can be calculated.

$$\frac{f_{rev}^l}{f_{rev}^s} = \frac{1}{\iota + \lambda} \quad (5.13)$$

Based on eq. 5.13 and harmonic number, the  $f_{rf}^X$  are calculated by eq. 5.14 and eq. 5.15

$$f_{rf}^s = h^s \times f_{rev}^s = h^s \times (\iota + \lambda) \times f_{rev}^l \quad (5.14)$$

$$f_{rf}^l = h^l \times f_{rev}^l \quad (5.15)$$

We could get the relation between  $f_{rf}^s$  and  $f_{rf}^l$  by dividing eq. 5.15 by eq. 5.14.

$$\frac{f_{rf}^l}{f_{rf}^s} = \frac{h^l}{h^s \times (\iota + \lambda)} = \frac{h^l}{h^s \times \iota + h^s \times \lambda} \quad (5.16)$$

## 5.2. Circumference ratio is not an ideal integer

---

In this scenario, two rf cavity frequencies begin beating automatically. So the frequency beating method is preferred. The synchronization window depends on the beating frequency. The beating frequency corresponding to this mismatch must not be too large in order to guarantee a long enough synchronization window, but also not too small to satisfy the constraint of the maximum synchronization time.

### 5.2.1 Circumference ratio is close to an ideal integer

When the circumference ratio of the large synchrotron to that of the small synchrotron is very close to an ideal integer,  $\iota$  in eq. 5.12 is an integer and  $\lambda$  has the order of magnitude  $10^{-2}$ .

In eq. 5.16,  $h^s \times \lambda$  is much smaller than  $h^s \times \iota$  and  $h^l$ , so the frequency beating method is preferred.  $Y$  is the GCD of  $h^l$  and  $h^s \times \iota$ .

Besides, it is also grouped to this scenario, that the revolution frequency ratio between the small and large synchrotrons is close to an ideal integer when the beam passes some target (e.g. FRS, Pbar) between two synchrotrons. The ratio between the revolution frequencies can be expressed as

$$\frac{f_{rev}^s}{f_{rev}^l} = \iota + \lambda \quad (5.17)$$

The realtion between two cavity rf frequencies is same as eq. 5.16.

Tab. 5.7 shows the formulas for the frequency of the bucket label signal, two slightly different frequencies for beating, the length of the synchronization window and the bunch and bucket center mismatch in this scenario.

Table 5.7: Synchronization when circumference ratio is close to an ideal integer

	Large synchrotron is target synchrotron	Small synchrotron is target synchrotron
Bucket label	$\frac{f_{rf}^l}{h^l/Y}$	$\frac{f_{rf}^s}{(h^s \times \iota)/Y}$
Different frequencies	$\frac{f_{rf}^l}{h^l/Y}$ and $\frac{f_{rf}^s}{(h^s \times \iota)/Y}$	
Beating frequencies	$\Delta f = \frac{f_{rf}^l}{h^l/Y} - \frac{f_{rf}^s}{(h^s \times \iota)/Y}$	
Synchronization window	$2 \times [h^l/Y] \times T_{rf}^l$	$2 \times [(h^s \times \iota)/Y] \times T_{rf}^s$
Center mismatch	$\pm \frac{1}{2} \times \frac{2 \times (h^l/Y) \times T_{rf}^l}{1/\Delta f} \times 360^\circ$	$\pm \frac{1}{2} \times \frac{2 \times [(h^s \times \iota)/Y] \times T_{rf}^s}{1/\Delta f} \times 360^\circ$

In fact, two slightly different frequencies could be fraction (between 1/Y and 1) times of the  $\frac{f_{rf}^l}{h^l/Y}$  and  $\frac{f_{rf}^s}{(h^s \times \iota)/Y}$ . The bucket label frequency and the beating frequency are proportional to the slightly difference frequencies by the coefficient of the fraction and the length of the synchronization window is inversely proportional to the slightly difference frequencies by the coefficient of the reciprocal for the fraction. The bunch to bucket center mismatch is proportional to the synchronization window and the beating frequency, whose coefficient product is 1, so the mismatch is determined by  $\frac{f_{rf}^l}{h^l/Y}$  and  $\frac{f_{rf}^s}{(h^s \times \iota)/Y}$ .

## 5.2. Circumference ratio is not an ideal integer

---

### 5.2.1.1 User case of h=4 B2B transfer from SIS18 to ESR

Continuous two of four bunches are injected into one bucket of the injection orbit of ESR [39]. The beam is accumulated in ESR. The large synchrotron is SIS18 and the small one is ESR.  $h^{SIS18} = 4$  and  $h^{ESR} = 1$ . Substituting the circumference of SIS18 and ESR into eq. 5.12, we get

$$\frac{C^l}{C^s} = \iota + \lambda = 2 - 0.003 \quad (5.18)$$

Substituting  $h^{SIS18}$ ,  $h^{ESR}$ ,  $\iota$  and  $\lambda$  into eq. 5.16, we get

$$\frac{f_{rf}^{SIS18}}{f_{rf}^{ESR}} = \frac{h^{SIS18}}{h^{ESR} \times (\iota + \lambda)} = \frac{4}{1 \times (2 - 0.003)} \quad (5.19)$$

The GCD of  $h^{SIS18} = 4$  and  $h^{ESR} \times \iota = 1 \times 2 = 2$  is 2, namely Y=2. Substituting  $h^X$ ,  $\iota$ ,  $\lambda$ ,  $f_{rf}^X$  and Y into formulas in Tab. 5.7, the synchronization of h=4 B2B transfer from SIS18 to ESR is obtained, see Tab. 5.8. Here we use 30 MeV/u heavy ion as an example.

Table 5.8: Synchronization of h=4 B2B transfer from SIS18 to ESR

	Small synchrotron (ESR) is target synchrotron
Bucket label	$\frac{1}{2/2} f_{rf}^{ESR}$
Different frequencies	$\frac{f_{rf}^{SIS18}}{4/2} = 686.600 \text{ kHz}$ and $\frac{f_{rf}^{ESR}}{2/2} = 685.652 \text{ kHz}$
Beating frequencies	948 Hz
Synchronization window	$2 \times (2/2) \times T_{rf}^{ESR} = 2.917 \text{ us}$
Center mismatch	$\pm \frac{1}{2} \times \frac{2 \times (2/2) \times T_{rf}^{ESR}}{1/948} \times 360^\circ = \pm 0.51^\circ$

Detailed parameters of the  $h = 4$  B2B transfer from SIS18 to ESR, please see Appendix B.2.

In the real operation, ESR uses different methods, e.g. barrier bucket or unstable fixed point, to accumulate beam instead of normal bucket [39]. Presently two general schemes of the particle accumulation are possible: moving or fixed barrier RF bucket [40]. In the scheme with moving barrier RF bucket, the bunch is injected in the longitudinal gap prepared by two barrier pulses. The injected beam becomes coasting after switching off the barrier voltages and merges with the previously stacked beam. The barrier voltages are switched on and moved away from each other to prepare the empty space for the next beam injection. In the fixed barrier bucket scheme, one prepares a stationary voltage distribution consisting of two barrier pulses of opposite sign. The resulting stretched rf potential separates the longitudinal phase space into a stable and an unstable region. After injection onto the unstable region (potential maximum), the particles circulate along all phases and cooling application leads to their capture in the stable region of the phase space

## 5.2. Circumference ratio is not an ideal integer

---

(potential well). After some time of the beam cooling the unstable region is free for a next injection without losing of the stored beam. With the barrier bucket, the bunch should be injected into the longitudinal gap or the unstable region of the barrier bucket.

After the synchronization, the phase difference between the 1/2 SIS18 and ESR cavity rf frequency markers depends on the accumulation method.

### 5.2.1.2 User case of h=1 B2B transfer from SIS18 to ESR

One bunch is injected into one bucket of the injection orbit of ESR. The beam is accumulated in ESR. The large synchrotron is SIS18 and the small one is ESR.  $h^{SIS18} = 1$  and  $h^{ESR} = 1$ . Substituting the circumference of SIS18 and ESR into eq. 5.12, we get

$$\frac{C^l}{C^s} = \iota + \lambda = 2 - 0.003 \quad (5.20)$$

Substituting  $h^{SIS18}$ ,  $h^{ESR}$ ,  $\iota$  and  $\lambda$  into eq. 5.16, we get

$$\frac{f_{rf}^{SIS18}}{f_{rf}^{ESR}} = \frac{h^l}{h^s \times (\iota + \lambda)} = \frac{1}{1 \times (2 - 0.003)} \quad (5.21)$$

The GCD of  $h^{SIS18} = 1$  and  $h^{ESR} \times \iota = 1 \times 2 = 2$  is 1, namely Y=1. Substituting  $h^X$ ,  $\iota$ ,  $\lambda$ ,  $f_{rf}^X$  and Y into formulas in Tab. 5.7, the synchronization of h=1 B2B transfer from SIS18 to ESR is obtained, see Tab. 5.9. Here we use 400 MeV/u proton as an example.

Table 5.9: Synchronization of h=1 B2B transfer from SIS18 to ESR

	Small synchrotron (ESR) is target synchrotron
Bucket label	$1/2f_{rf}^{ESR}$
Different frequencies	$\frac{f_{rf}^{SIS18}}{1} = 989.756 \text{ kHz}$ and $\frac{f_{rf}^{ESR}}{2} = 988.388 \text{ kHz}$
Beating frequencies	1368 Hz
Synchronization window	$2 \times 2 \times T_{rf}^{ESR} = 2.034 \text{ us}$
Center mismatch	$\pm \frac{1}{2} \times \frac{2 \times 2 \times T_{rf}^{ESR}}{1/1368} \times 360^\circ = \pm 0.50^\circ$

Detailed parameters of the  $h = 1$  B2B transfer from SIS18 to ESR, please see Appendix B.2. After the synchronization, the phase difference between the SIS18 and 1/2 ESR cavity rf frequency markers depends on the accumulation method.

### 5.2.2 Circumference ratio is far away from an ideal integer

When the circumference ratio of the large synchrotron to that of the small synchrotron is far away from an ideal integer,  $\iota$  in eq. 5.12 could be denoted by  $\frac{m}{n}$  ( $m$  and  $n$  are integers) and eq. 5.12 could be expressed as

## 5.2. Circumference ratio is not an ideal integer

---

$$\frac{C^l}{C^s} = \frac{m}{n} + \lambda \quad (5.22)$$

Substituting  $\lambda$  by  $\frac{m}{n}$  into eq. 5.16, we could get the relation between  $f_{rf}^s$  and  $f_{rf}^l$ .

$$\frac{f_{rf}^l}{f_{rf}^s} = \frac{h^l \times n}{h^s \times m + h^s \times \lambda \times n} \quad (5.23)$$

$Y$  is the GCD of  $h^l \times n$  and  $h^s \times m$ .

Besides, it is also grouped to this scenario, that the revolution frequency ratio between the small and large synchrotrons is far away from an ideal interger when the beam passes some target (e.g. FRS, Pbar) between two synchrotrons. The revolution frequency ratio can be expressed as

$$\frac{f_{rev}^s}{f_{rev}^l} = \frac{m}{n} + \lambda \quad (5.24)$$

The relation between two rf cavity frequencies is same as eq. 5.23.

Tab. 5.10 shows the formulas for the frequency of the bucket label signal, two slightly different frequencies for beating, the length of the synchronization window and the bunch and bucket center mismatch in this scenario.

Table 5.10: Synchronization when circumference ratio is far away from an ideal integer

	Large synchrotron is target synchrotron	Small synchrotron is target synchrotron
Bucket label	$\frac{f_{rf}^l}{(h^l \times n)/Y}$	$\frac{f_{rf}^s}{(h^s \times m)/Y}$
Different frequencies	$\frac{f_{rf}^l}{(h^l \times n)/Y}$ and $\frac{f_{rf}^s}{(h^s \times m)/Y}$	
Beating frequencies	$\Delta f = \frac{f_{rf}^l}{(h^l \times n)/Y} - \frac{f_{rf}^s}{(h^s \times m)/Y}$	
Synchronization window	$2 \times [(h^l \times n)/Y] \times T_{rf}^l$	$2 \times [(h^s \times m)/Y] \times T_{rf}^s$
Center mismatch	$\pm \frac{1}{2} \times \frac{2 \times [(h^l \times n)/Y] \times T_{rf}^l}{1/\Delta f} \times 360^\circ$	$\pm \frac{1}{2} \times \frac{2 \times [(h^s \times m)/Y] \times T_{rf}^s}{1/\Delta f} \times 360^\circ$

There are various combination of  $\frac{m}{n}$  and  $\lambda$ ,  $\lambda$  determines the beating speed. The smaller, the more precise bunch to bucket injection.  $(h^l \times n)/Y$  and  $(h^s \times m)/Y$  determines the two slightly different frequencies. The bigger  $(h^l \times n)/Y$  and  $(h^s \times m)/Y$ , the smaller two slightly different frequencies, which has higher requirement for LLRF system. So we have to find a balance between the bunch to bucket center mismatch and the low frequencies for beating.

Two slightly different frequencies could be fraction (between  $1/Y$  and 1) times of the  $\frac{f_{rf}^l}{(h^l \times n)/Y}$  and  $\frac{f_{rf}^s}{(h^s \times m)/Y}$ . The bucket label frequency and the beating frequency are proportional to the slightly difference frequencies by the coefficient of the fraction and the length of the synchronization window is inversely proportional to the slightly

## 5.2. Circumference ratio is not an ideal integer

---

difference frequencies by the coefficient of the reciprocal for the fraction. The bunch to bucket center mismatch is proportional to the synchronization window and the beating frequency, whose coefficient product is 1, so the mismatch is determined by  $\frac{f_{rf}^l}{(h^l \times n)/Y}$  and  $\frac{f_{rf}^s}{(h^s \times m)/Y}$ .

### 5.2.2.1 User case of $H^+$ B2B transfer from SIS100 to CR

Only one out of five bunches of proton is extracted from SIS100 and goes to Pbar, then antiproton is produced and injected into one bucket of CR [39]. The large synchrotron is SIS100 and the small one is CR,  $h^{SIS100} = 5$  and  $h^{CR} = 1$ . Here we take an example, that the proton energy before the Pbar is 28.8 GeV/u and the antiproton energy after the Pbar is 3 GeV/u. Substituting the extraction and injection revolution frequencies into eq. 5.24, we get

$$\frac{f_{rev}^{CR}}{f_{rev}^{SIS100}} = 4.9 - 0.0004 = \frac{m}{n} + \lambda = \frac{49}{10} - 0.0004 \quad (5.25)$$

Substituting  $h^{SIS100}$ ,  $h^{CR}$ , m, n and  $\lambda$  into eq. 5.23, we get

$$\frac{f_{rf}^{SIS100}}{f_{rf}^{CR}} = \frac{h^{SIS100} \times n}{h^{CR} \times m + h^{CR} \times \lambda \times n} = \frac{5 \times 10}{1 \times 49 - 1 \times 0.0004 \times 10} \quad (5.26)$$

The GCD of  $h^{SIS100} \times n = 5 \times 10 = 50$  and  $h^{CR} \times m = 1 \times 49 = 49$  is 1, namely Y=1. Substituting  $h^X$ , m, n,  $\lambda$ ,  $f_{rf}^X$  and Y into formulas in Tab. 5.10, the synchronization of proton B2B transfer from SIS100 to CR is obtained, see Tab. 5.11.

Table 5.11: Synchronization of  $H^+$  B2B transfer from SIS100 to CR

	Small synchrotron (CR) is target synchrotron
Bucket label	$1/49 f_{rf}^{CR}$
Different frequencies	$\frac{f_{rf}^{SIS100}}{50} = 26.658 \text{ kHz}$ and $\frac{f_{rf}^{CR}}{49} = 26.873 \text{ kHz}$
Beating frequencies	215 Hz
Synchronization window	$2 \times 49 \times T_{rf}^{CR} = 74.382 \text{ us}$
Center mismatch	$\pm \frac{1}{2} \times \frac{2 \times 49 \times T_{rf}^{CR}}{1/215} \times 360^\circ = \pm 2.88^\circ$

The CR is empty before the injection, so the phase jump is preferred for CR. Detailed parameters of the  $H^+$  B2B transfer from SIS100 to CR, please see Appendix B.6.

### 5.2.2.2 User case of RIB B2B transfer from SIS100 to CR

Only one out of two bunches is extracted from SIS100 and goes to Super FRS, then RIB is produced and injected into one bucket of CR. The large synchrotron is SIS100 and the small one is CR.  $h^{SIS100} = 2$  and  $h^{CR} = 1$ . Here we take an example, that

## 5.2. Circumference ratio is not an ideal integer

---

the energy of the heavy ion beam before the Super FRS is 1.5 GeV/u and the RIB energy after the Super FRS is 740 MeV/u. Substituting the extraction and injection revolution frequencies into eq. 5.24, we get

$$\frac{f_{rev}^{CR}}{f_{rev}^{SIS100}} = 4.4 - 0.005 = \frac{m}{n} + \lambda = \frac{22}{5} - 0.01 \quad (5.27)$$

Substituting  $h^{SIS100}$ ,  $h^{CR}$ , m, n and  $\lambda$  into eq. 5.23, we get

$$\frac{f_{rf}^{SIS100}}{f_{rf}^{CR}} = \frac{h^{SIS100} \times n}{h^{CR} \times m + h^{CR} \times \lambda \times n} = \frac{2 \times 5}{1 \times 22 - 1 \times 0.01 \times 5} \quad (5.28)$$

The GCD of  $h^{SIS100} \times n = 2 \times 5 = 10$  and  $h^{CR} \times m = 1 \times 22 = 22$  is 2, namely Y=2. Substituting  $h^l$ ,  $h^s$ , m, n,  $\lambda$ ,  $f_{rf}^X$  and Y into formulas in Tab. 5.10, the synchronization of RIB B2B transfer from SIS100 to CR is obtained, see Tab. 5.12.

Table 5.12: Synchronization of RIB B2B transfer from SIS100 to CR

	Small synchrotron (CR) is target synchrotron
Bucket label	$\frac{1}{22/2} f_{rf}^{CR}$
Different frequencies	$\frac{f_{rf}^{SIS100}}{10/2} = 102.326 \text{ kHz}$ and $\frac{f_{rf}^{CR}}{22/2} = 102.218 \text{ kHz}$
Beating frequencies	108 Hz
Synchronization window	$2 \times (22/2) \times T_{rf}^{CR} = 19.558 \text{ us}$
Center mismatch	$\pm \frac{1}{2} \times \frac{2 \times 22 \times T_{rev}^{CR}}{1/54} \times 360^\circ = \pm 0.39^\circ$

The CR is empty before the injection, so the phase jump is preferred for CR. Detailed parameters of RIB B2B transfer from SIS100 to CR, please see Appendix B.6.

### 5.2.2.3 User case of B2B transfer from CR to HESR

One bunch of CR is injected into one bucket of HESR. The beam is accumulated in HESR [41]. The large synchrotron is HESR and the small one is CR.  $h^{HESR} = 1$  and  $h^{CR} = 1$ . Substituting the circumference of HESR and CR to eq. 5.22, we have

$$\frac{C^{HESR}}{C^{CR}} = 2.6 - 0.003 = \frac{m}{n} + \lambda = \frac{13}{5} - 0.003 \quad (5.29)$$

Substituting  $h^{HESR}$ ,  $h^{CR}$ , m, n and  $\lambda$  into eq. 5.23, we get Eq. 5.23 is expressed as

$$\frac{f_{rf}^{HESR}}{f_{rf}^{CR}} = \frac{h^{HESR} \times n}{h^{CR} \times m + h^{ESR} \times \lambda \times n} = \frac{1 \times 5}{1 \times 13 - 1 \times 0.003 \times 5} \quad (5.30)$$

The GCD of  $h^{HESR} \times n = 1 \times 5 = 5$  and  $h^{CR} \times m = 1 \times 13 = 13$  is 1, namely Y=1. Substituting  $h^X$ , m, n,  $\lambda$ ,  $f_{rf}^X$  and Y into formulas in Tab. 5.10, the synchronization

## 5.2. Circumference ratio is not an ideal integer

---

of B2B transfer from CR to HESR is obtained. Tab. 5.13 shows two operations for antiproton and RIB.

Table 5.13: Synchronization of B2B transfer from CR to HESR

	Larger synchrotron (HESR) is target synchrotron
Bucket label	$1/5 f_{rf}^{HESR}$
	3 GeV/u antiproton
Different frequencies	$\frac{f_{rf}^{CR}}{13} = 101.290 \text{ kHz}$ and $\frac{f_{rf}^{HESR}}{5} = 101.426 \text{ kHz}$
Beating frequencies	136 Hz
Synchronization window	$2 \times 5 \times T_{rf}^{HESR} = 19.719 \text{ us}$
Center mismatch	$\pm \frac{1}{2} \times \frac{2 \times 5 \times T_{rev}^{CR}}{1/136} \times 360^\circ = \pm 0.48^\circ$
	740 MeV/u RIB
Different frequencies	$\frac{f_{rf}^{CR}}{13} = 86.493 \text{ kHz}$ and $\frac{f_{rf}^{HESR}}{5} = 86.608 \text{ kHz}$
Beating frequencies	113 Hz
Synchronization window	$2 \times 5 \times T_{rf}^{HESR} = 23.090 \text{ us}$
Center mismatch	$\pm \frac{1}{2} \times \frac{2 \times 5 \times T_{rev}^{CR}}{1/113} \times 360^\circ = \pm 0.47^\circ$

After the synchronization, the phase difference between the 1/13 CR and 1/5 HESR revolution frequency markers depends on the accumulation method. Detailed parameter about the B2B transfer from CR to HESR, please see Appendix B.5.

### 5.2.2.4 User case of B2B transfer from SIS18 to ESR via FRS

Only one bunch is extracted from SIS18 and goes to FRS, then RIB is produced and injected into one bucket of ESR. The large synchrotron is SIS18 and the small one is ESR.  $h^{SIS18} = 1$  and  $h^{ESR} = 1$ . Here we take an applied case as an example, that the energy of the heavy ion beam before the FRS is 550 MeV/u and the RIB energy after the FRS is 400 MeV/u. Substituting the extraction and injection revolution frequencies into eq. 5.24, we get

$$\frac{f_{rev}^{ESR}}{f_{rev}^{SIS18}} = 1.8 + 0.048 = \frac{m}{n} + \lambda = \frac{9}{5} + 0.048 \quad (5.31)$$

Substituting  $h^{SIS18}$ ,  $h^{ESR}$ , m, n and  $\lambda$  into eq. 5.23, we get

$$\frac{f_{rf}^{SIS18}}{f_{rf}^{ESR}} = \frac{h^{SIS18} \times n}{h^s \times m + h^{ESR} \times \lambda \times n} = \frac{1 \times 5}{1 \times 9 + 1 \times 0.048 \times 5} \quad (5.32)$$

### 5.3. Summary of the synchronization for different scenarios

---

Table 5.14: Synchronization of B2B transfer from SIS18 to ESR via FRS

	Small synchrotron (ESR) is target synchrotron
Bucket label	$1/9 f_{rf}^{ESR}$
Different frequencies	$\frac{f_{rf}^{SIS18}}{5/1} = 215.393 \text{ kHz}$ and $\frac{f_{rf}^{ESR}}{9/1} = 219.642 \text{ kHz}$
Beating frequencies	4.249 kHz
Synchronization window	$2 \times 9 \times T_{rf}^{ESR} = 9.106 \text{ us}$
Center mismatch	$\pm \frac{1}{2} \times \frac{2 \times 9 \times T_{rev}^{ESR}}{1/4249} \times 360^\circ = \pm 6.92^\circ$

The GCD of  $h^{SIS18} \times n = 1 \times 5 = 5$  and  $h^s \times m = 1 \times 9 = 9$  is 1, namely Y=1. Substituting  $h^X$ , m, n,  $\lambda$ ,  $f_{rf}^X$  and Y into formulas in Tab. 5.10, the synchronization of B2B transfer from SIS18 to ESR via FRS is obtained, see Tab. 5.14.

More parameters about the B2B transfer from SIS18 to ESR via FRS, please see Appendix B.3. For the detailed realization and implementation of two slightly different frequencies, please see “Development of the LLRF system for a deterministic Bunch-to-Bucket transfer for FAIR“.

## 5.3 Summary of the synchronization for different scenarios

In this section, all the synchronization methods are summarized in Tab. 5.15.

### 5.3. Summary of the synchronization for different scenarios

Table 5.15: Summary of the synchronization

Circumference ratio	RF cavity frequency ratio $f_{rf}^l/f_{rf}^s$	Bucket label <sup>1</sup> (large or small is target synchrotron)	Frequency beating Two slightly different frequencies	Frequency beating Bunch-Bucket center mismatch (large or small is target synchrotron)
$C^l/C^s = \kappa$ Integer	$\frac{h^l}{h^s \times \kappa}$ $\frac{f_{rf}^l}{h^l/Y} \text{ or } \frac{f_{rf}^s}{(h^s \times \kappa)/Y}$ $Y = GCD(h^l, h^s \times \kappa)$	$\frac{f_{rf}^l}{h^l/Y} \text{ and } \frac{f_{rf}^s}{(h^s \times \kappa)/Y} + \Delta f$ or $\frac{f_{rf}^l}{h^l/Y} + \Delta f \text{ and } \frac{f_{rf}^s}{(h^s \times \kappa)/Y}$	$\pm \frac{1}{2} \times \frac{2 \times (h^l/Y) \times T_{rf}^l}{1/\Delta f} \times 360^\circ$ or $\pm \frac{1}{2} \times \frac{2 \times [(h^s \times \kappa)/Y] \times T_{rf}^s}{1/\Delta f} \times 360^\circ$	
$C^l/C^s = \iota + \lambda$ or $frev^s/frev^l = \iota + \lambda$ close to integer ( $\iota$ is integer)	$\frac{h^l}{h^{s \times (\iota + \lambda)}}$ $\frac{f_{rf}^l}{h^l/Y} \text{ or } \frac{f_{rf}^s}{(h^s \times \iota)/Y}$ $Y = GCD(h^l, h^s \times \iota)$	$\frac{f_{rf}^l}{h^l/Y} \text{ and } \frac{f_{rf}^s}{(h^s \times \iota)/Y}$	$\pm \frac{1}{2} \times \frac{2 \times (h^l/Y) \times T_{rf}^l}{1/\Delta f} \times 360^\circ$ or $\pm \frac{1}{2} \times \frac{2 \times [(h^s \times \iota)/Y] \times T_{rf}^s}{1/\Delta f} \times 360^\circ$	
$C^l/C^s = \iota + \lambda$ or $frev^s/frev^l = \iota + \lambda$ far away from integer ( $\iota$ is expressed by $\frac{m}{n}$ )	$\frac{h^l}{h^{s \times (m/n+\lambda)}}^2$ $\frac{f_{rf}^l}{(h^l \times n)/Y} \text{ or } \frac{f_{rf}^s}{(h^s \times m)/Y}$ $Y = GCD(h^l \times n, h^s \times m)$	$\frac{f_{rf}^l}{(h^l \times n)/Y} \text{ and } \frac{f_{rf}^s}{(h^s \times m)/Y}$	$\pm \frac{1}{2} \times \frac{2 \times [(h^l \times n)/Y] \times T_{rf}^l}{1/\Delta f} \times 360^\circ$ or $\pm \frac{1}{2} \times \frac{2 \times [(h^s \times m)/Y] \times T_{rf}^s}{1/\Delta f} \times 360^\circ$	
The phase shift could be implemented either for the large or small synchrotron. When the target synchrotron is empty, the phase jump is implemented for the target synchrotron.				

<sup>1</sup>Here we assume that the frequency for beating is smaller than the revolution frequency

$$2 \frac{f_{rf}^l}{f_{rf}s} = \frac{h^l f_{rev}^l}{h^s f_{rev}} = \frac{h^l C^s}{h^s C_l} = \frac{h^l}{h^s(m/n+\lambda)} = \frac{h^l \times n}{h^s \times m + h^s \times \lambda \times n}$$

# Chapter 6

## Realization and systematic investigation of the B2B transfer system for FAIR

This chapter concentrates on the realization and systematic investigation of the B2B transfer system. In Sec. 6.1, both the phase shift and frequency beating synchronization methods are analyzed from the beam dynamic viewpoint. The WR network is investigated for the B2B transfer and the calculation of the synchronization window are presented in Sec. 6.2. The B2B transfer system for FAIR focuses first of all on SIS18 to SIS100 transfer, so the trigger possibility of the SIS18 extraction and SIS100 injection kicker is systematically investigated in Sec. 6.3. Besides, the test setup from the timing aspect is built in Sec. 6.4.

### 6.1 Investigation of two synchronization methods for $U^{28+}$ B2B transfer from SIS18 to SIS100 from the beam dynamics viewpoint

This section analyzes the phase shift and frequency beating methods from the beam-dynamics viewpoint for the synchronization of SIS18 with SIS100. In this chapter, the circumference of SIS18 and SIS100 are denoted by  $C^{SIS18}$  and  $C^{SIS100}$ , the revolution frequency by  $f_{h=1}^{SIS18}$  and  $f_{h=1}^{SIS100}$  and the rf frequency by  $f_{h=2}^{SIS18}$  and  $f_{h=10}^{SIS100}$ . Since SIS18 and SIS100 harmonic number are 2 and 10, the relationship between the revolution and rf frequencies are  $f_{h=2}^{SIS18} = 2f_{h=1}^{SIS18}$  and  $f_{h=10}^{SIS100} = 10f_{h=1}^{SIS100}$ . Since  $C^{SIS100}$  is five times as long as  $C^{SIS18}$ , we could get the relation  $f_{h=1}^{SIS18} = 5f_{h=1}^{SIS100}$  and  $f_{h=10}^{SIS100} = f_{h=2}^{SIS18}$ .

#### 6.1.1 Phase shift method

To achieve a required phase shift, the RF frequency is modulated away from the nominal value for a period of time and modulated back [13]. Let  $\Delta\phi_{shift}$  be the phase shift to be achieved and  $\Delta f_{rf}(t)$  the RF frequency variation to accomplish it; then,

$$\Delta\phi_{shift} = 2\pi \int_{t_0}^{t_0+T} \Delta f_{rf}(t) dt \quad (6.1)$$

## 6.1. Investigation of two synchronization methods for $U^{28+}$ B2B transfer from SIS18 to SIS100 from the beam dynamics viewpoint

---

where  $T$  is the period of frequency modulation and  $t_0$  is the time at which the modulation begins. To make the frequency modulation effective, the stabilization system, beam-phase feedback loop, must be frozen before the modulation begins.

The following four examples of frequency modulation are analyzed. Case (1) trapezoid modulation, Case (2) triangular modulation, Case (3) sinusoidal modulation and Case (4) parabolic modulation. Here I assume the phase shift must be achieved within 7ms. These frequency modulations are shown in Fig. 6.1. All the four modulations give the same phase shift,  $\Delta\phi_{shift} = \pi$ , which is proved by substituting each form of  $\Delta f_{rf}(t)$  into eq. 6.1 and performing integration.

Case (1)

$$\Delta f_{rf}(t) = \begin{cases} 50\text{Hz}/ms \times (t - t_0) & t_0 + 0 < t \leq t_0 + 2\text{ms} \\ 100\text{Hz} & t_0 + 2 < t \leq t_0 + 5\text{ms} \\ 100\text{Hz} - 50\text{Hz}/ms \times (t - t_0) & t_0 + 5\text{ms} < t \leq t_0 + 7\text{ms} \end{cases} \quad (6.2)$$

Case (2)

$$\Delta f_{rf}(t) = \begin{cases} \frac{10^3}{7 \times 3.5} \text{Hz}/ms \times (t - t_0) & t_0 + 0 < t \leq t_0 + 3.5\text{ms} \\ \frac{10^3}{7} \text{Hz} - \frac{10^3}{7 \times 3.5} \text{Hz}/ms \times (t - t_0 - 3.5\text{ms}) & t_0 + 3.5\text{ms} < t \leq t_0 + 7\text{ms} \end{cases} \quad (6.3)$$

Case (3)

$$\Delta f_{rf}(t) = \frac{10^3}{14} \text{Hz} \times \left(1 - \cos\left(\frac{2\pi}{7} \text{rad}/ms \times (t - t_0)\right)\right) \quad t_0 + 0 < t \leq t_0 + 7\text{ms} \quad (6.4)$$

Case (4)

$$\Delta f_{rf}(t) = \frac{20}{21} \times \begin{cases} 30\text{Hz}/ms^2 \times (t - t_0)^2 & t_0 + 0 < t \leq t_0 + 1\text{ms} \\ 30\text{Hz} + 60\text{Hz}/ms \times (t - t_0 - 1\text{ms}) & t_0 + 1\text{ms} < t \leq t_0 + 2.5\text{ms} \\ 30\text{Hz}/ms^2 \times [5\text{ms}^2 - (t - t_0 - 3.5\text{ms})^2] & t_0 + 2.5\text{ms} < t \leq t_0 + 4.5\text{ms} \\ 30\text{Hz} + 60\text{Hz}/ms \times [6\text{ms} - (t - t_0)] & t_0 + 4.5\text{ms} < t \leq t_0 + 6\text{ms} \\ 30\text{Hz}/ms^2 \times [7\text{ms}^2 - (t - t_0)]^2 & t_0 + 6\text{ms} < t \leq t_0 + 7\text{ms} \end{cases} \quad (6.5)$$

## 6.1. Investigation of two synchronization methods for $U^{28+}$ B2B transfer from SIS18 to SIS100 from the beam dynamics viewpoint

---

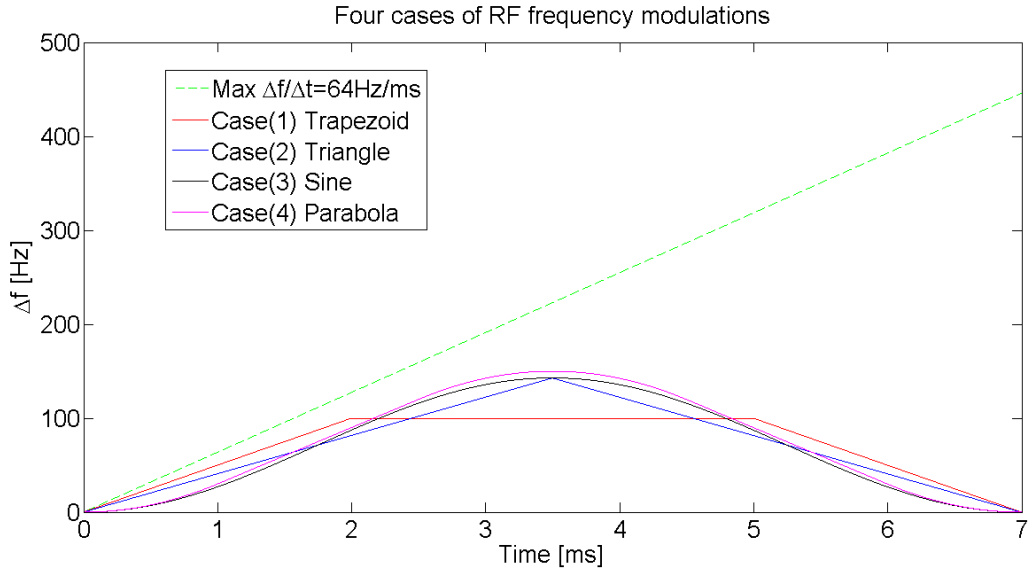


Figure 6.1: Examples of RF frequency modulation.

Fig. 6.2 shows the time derivation of four rf frequency modulations, which are smaller than the maximum time derivative of rf frequency during the acceleration ramp 64Hz/ms for the adiabaticity consideration. The acceleration ramp is an adiabatical process.

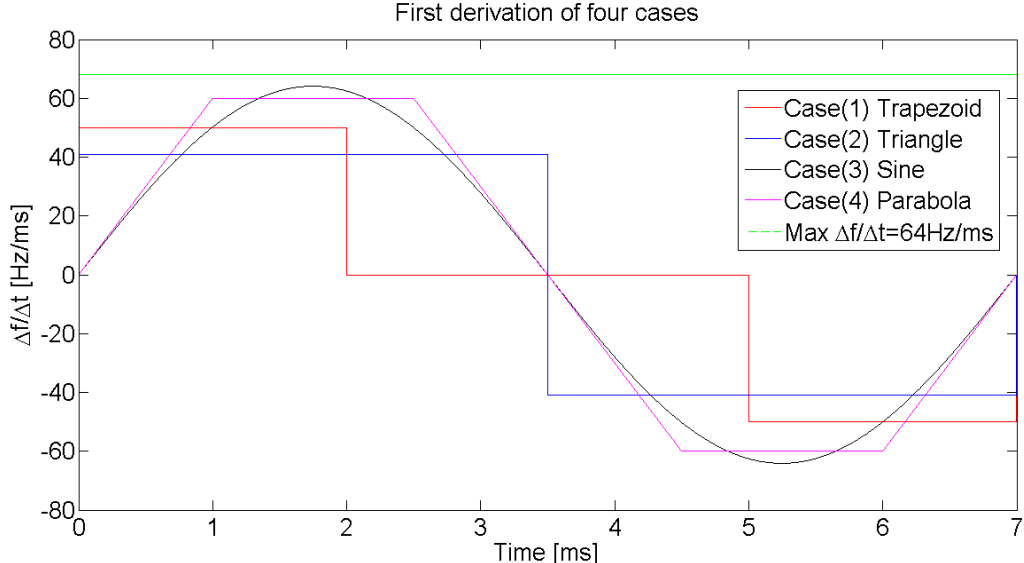


Figure 6.2: Time derivation of four modulations

Fig. 6.3 shows the corresponding phase shift modulation of four cases.

## 6.1. Investigation of two synchronization methods for $U^{28+}$ B2B transfer from SIS18 to SIS100 from the beam dynamics viewpoint

---

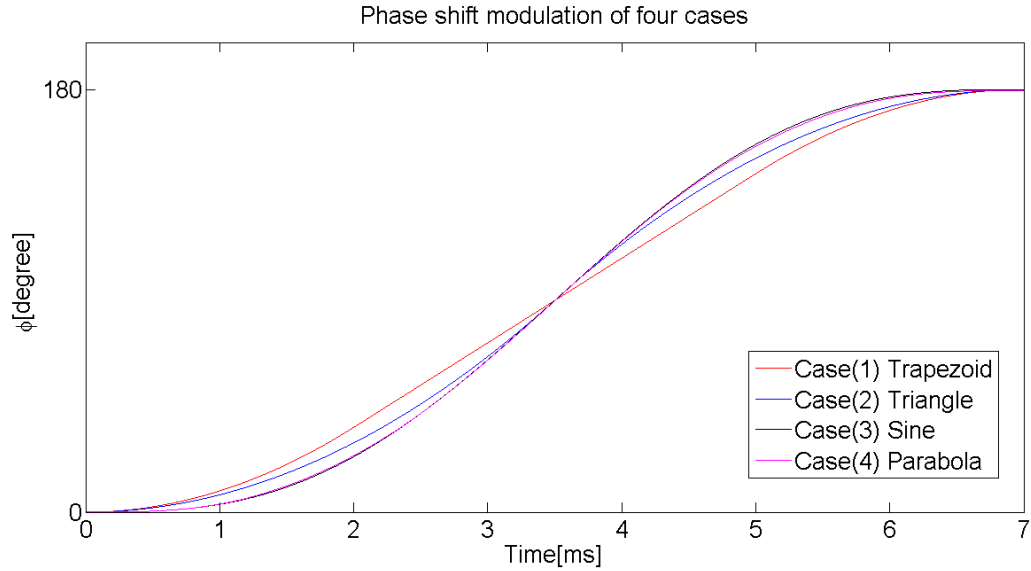


Figure 6.3: The phase shift modulation of four cases

### 6.1.1.1 Longitudinal dynamic analysis for the simulation

In this section, the average radial excursion, the relative momentum shift, synchronous phase, bucket size and adiabaticity of four rf frequency modulations are analyzed.

- Average radial excursion

The average radial excursion is calculated for the four cases of rf frequency modulations by eq. (2.15). Fig. 6.4 shows the calculation result [42].

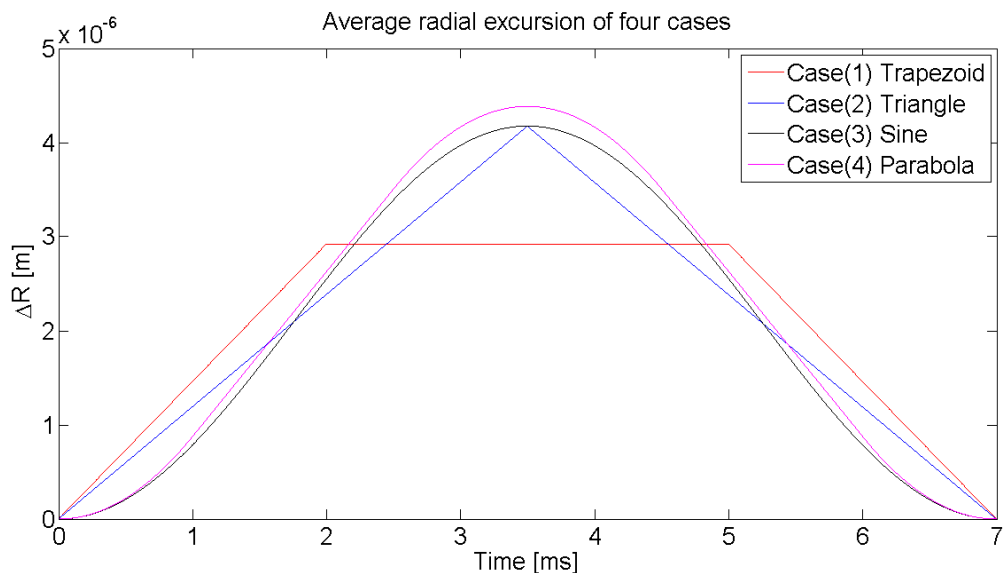


Figure 6.4: Average radial excursions of four cases.

## 6.1. Investigation of two synchronization methods for $U^{28+}$ B2B transfer from SIS18 to SIS100 from the beam dynamics viewpoint

---

Table 6.1: The maximum average radial excursion of four cases

	Case (1)	Case (2)	Case (3)	Case (4)
Max avg radial excursion	$2.93 \times 10^{-6}$	$4.17 \times 10^{-6}$	$4.18 \times 10^{-6}$	$4.38 \times 10^{-6}$
Time	flat	3.5 ms	3.5 ms	3.5 ms

Tab. 6.1 shows the maximum average radial excursion and the time for four cases. The maximum tolerable radial excursion of SIS18 is  $\pm 2.4 \times 10^{-4}$ . For all cases, the average radial excursion is within the acceptable range. Hence, all cases are applicable.

- Relative momentum shift

The relative momentum shift is calculated for the four cases of rf frequency modulations by eq. (2.16). Fig. 6.5 shows the calculation result.

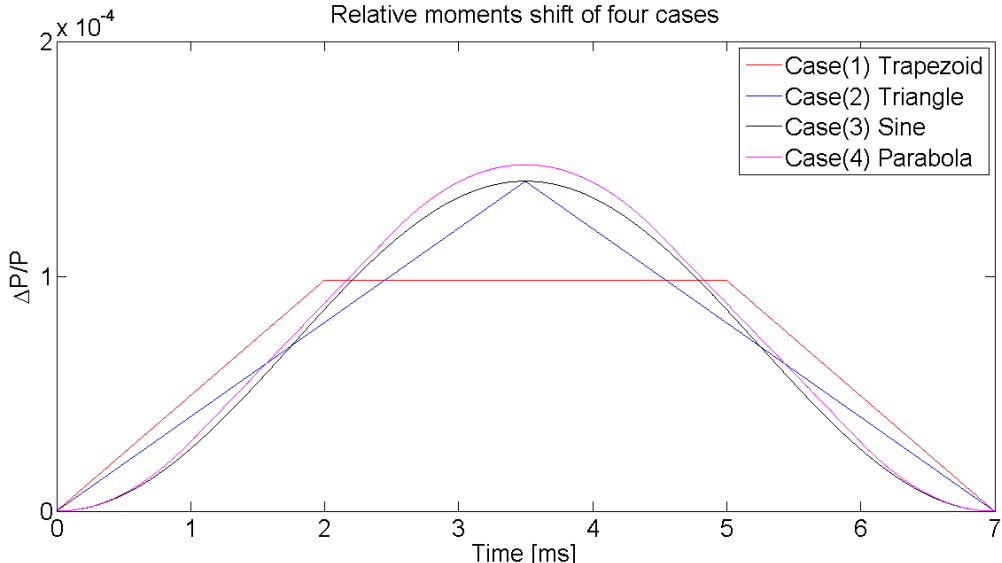


Figure 6.5: Relative momentum shift of four cases.

Table 6.2: The maximum relative momentum shift of four cases

	Case (1)	Case (2)	Case (3)	Case (4)
Max relative momentum shift	$9.83 \times 10^{-5}$	$1.38 \times 10^{-4}$	$1.40 \times 10^{-4}$	$1.48 \times 10^{-4}$
Time	flat	3.5 ms	3.5 ms	3.5 ms

Tab. 6.2 shows the maximum relative momentum shift and the time for four cases. The maximum tolerable relative momentum shift of SIS18 is  $\pm 0.008$ .

## 6.1. Investigation of two synchronization methods for $U^{28+}$ B2B transfer from SIS18 to SIS100 from the beam dynamics viewpoint

---

For all cases, the maximum relative momentum shift is within the acceptable range. Hence, all cases are applicable.

- Synchronous phase

The rf frequency modulations make the synchronous phase deviate from the nominal value  $0^\circ$ . Fig. 6.6 shows the changes in the synchronous phase,  $\Delta\phi_s(t)$ . It is calculated by substituting values into eq. 2.23. For case (1), the phase jumps in  $\Delta\phi_s(t)$  appear at the start and end of the frequency modulation, and at two points where the slope of modulation changes from upward to flat and from flat to downward. For case (2), the phase jumps in  $\Delta\phi_s(t)$  appear at the start and end of the frequency modulation, and at the midpoint where the slope of modulation changes from upward to downward. For case (3) and (4), the synchronous phase  $\Delta\phi_s(t)$  during the modulations are continuous. The phase jumps endanger the beam stability. Hence, only case (3) and (4) are applicable.

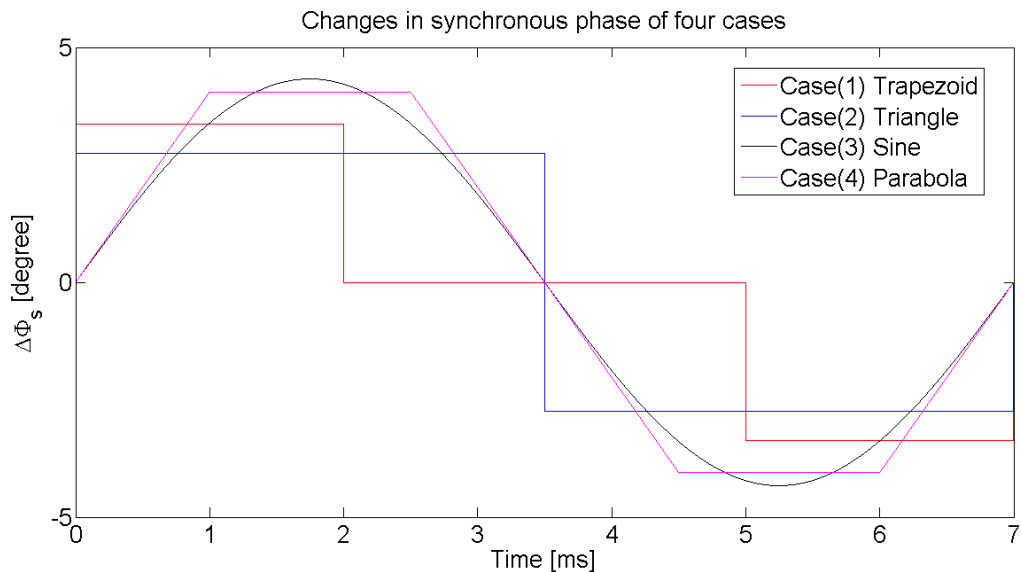


Figure 6.6: Changes in synchronous phase of four cases

- Bucket size

The bucket area factor  $\alpha_b(\phi_s)$  varies during rf frequency modulations. Before the modulations, the synchronous phase  $\phi_s=0^\circ$  and  $\alpha_b(0^\circ) = 1$ . By substituting the changes in synchronous phase into eq. (6.6), we get the ratio of bucket areas of a running bucket to the stationary bucket for four cases, see Fig. (6.7).

$$\alpha_b(\phi_s) \approx \frac{1 - \sin\phi_s}{1 + \sin\phi_s} \quad (6.6)$$

## 6.1. Investigation of two synchronization methods for $U^{28+}$ B2B transfer from SIS18 to SIS100 from the beam dynamics viewpoint

---

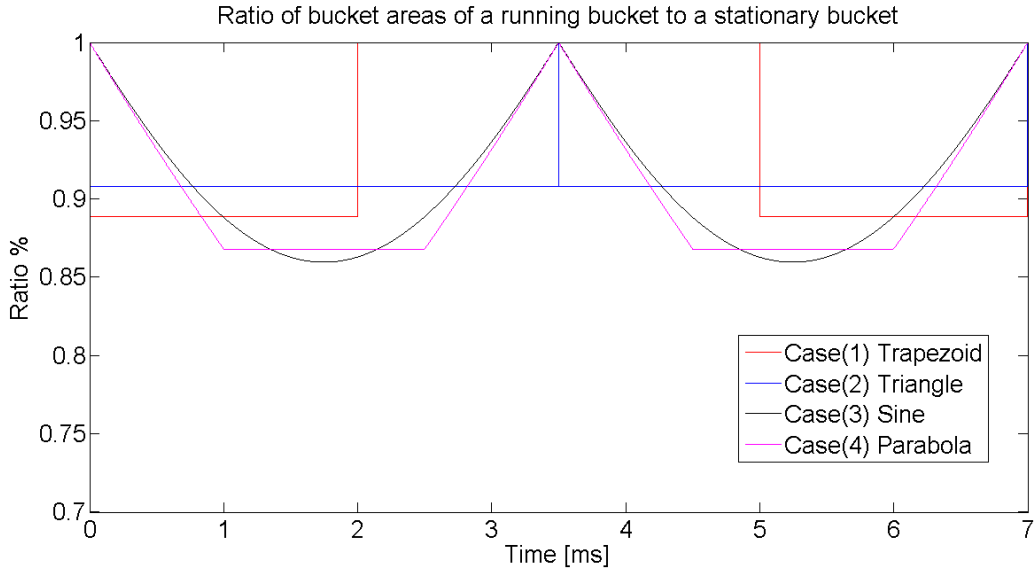


Figure 6.7: Ratio of bucket areas of a running bucket to the stationary bucket of four cases

Tab. 6.3 shows the bucket area factor for four cases. For all cases, the running bucket area factor is larger than 85%. Hence, all cases are applicable.

Table 6.3: The minimum bucket area factor of four cases

	Case (1)	Case (2)	Case (3)	Case (4)
Min bucket area factor	88%	90%	86%	86%

- Adiabaticity

By substituting the values of  $d\Delta\phi_s(t)/dt$  obtained from Fig. 6.6 and the other appropriate values into eq. 2.27, we can calculate the adiabaticity parameter,  $\varepsilon$ , for the case (3) and (4), see Fig. 6.8. Because  $d\Delta\phi_s(t)$  changes discontinuously for case (1) and (2), this abrupt change gives rise to a coherent bunch oscillation at a synchrotron frequency, resulting in emittance dilution. So the rf frequency modulations of case (1) and (2) are not applicable.

For case (4), the maximum of  $\varepsilon$ , 0.000059, occurs at 1ms, 2.5ms, 4.5ms and 6ms. From Fig. 6.6, we could see the change of the synchronous phase  $d\Delta\phi_s(t)/dt$  at these time points is big but smoothly. For case (3), the maximum of  $\varepsilon$  is 0.000030. So the frequency modulation is adiabatical for case (3) and (4).

## 6.1. Investigation of two synchronization methods for $U^{28+}$ B2B transfer from SIS18 to SIS100 from the beam dynamics viewpoint

---

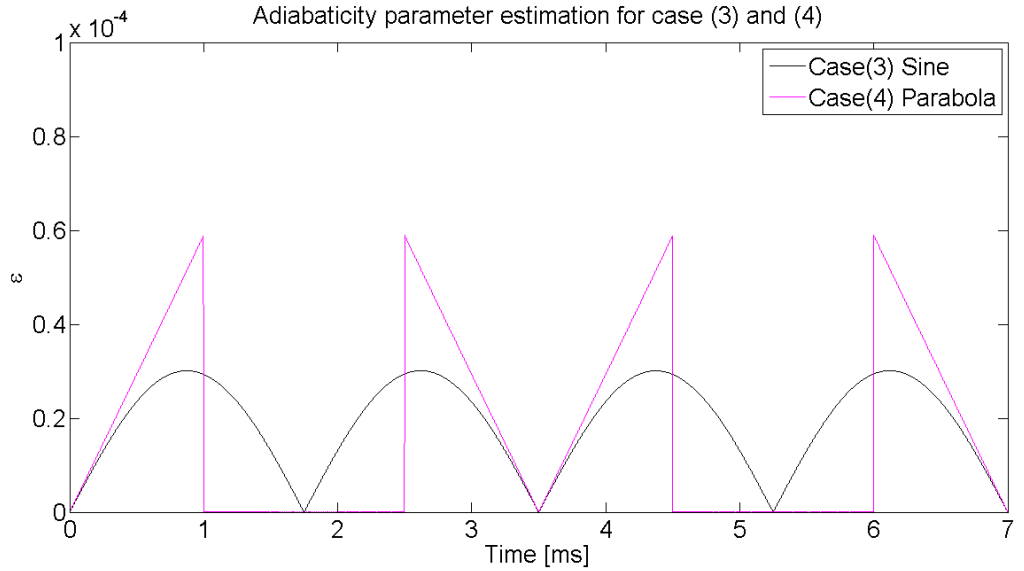


Figure 6.8: Adiabaticity parameter estimation of case (3) and (4)

### 6.1.1.2 Transverse dynamics analysis for the simulation

For SIS18, the chromaticity  $Q_x$  and  $Q_y$  is 4.17 and 3.4. Substituting chromaticity and maximum momentum shift (see. Tab. 6.2) into eq. 2.17. The chromatic tune shift  $\Delta Q_x$  and  $\Delta Q_y$  during rf modulations for four cases can be calculated.

Case (1)

$$\Delta Q_x = 4.17 \times 9.83 \times 10^{-5} = 4.10 \times 10^{-4} \quad (6.7)$$

$$\Delta Q_y = 3.4 \times 9.83 \times 10^{-5} = 3.34 \times 10^{-4} \quad (6.8)$$

Case (2)

$$\Delta Q_x = 4.17 \times 1.38 \times 10^{-4} = 5.75 \times 10^{-4} \quad (6.9)$$

$$\Delta Q_y = 3.4 \times 1.38 \times 10^{-4} = 4.69 \times 10^{-4} \quad (6.10)$$

Case (3)

$$\Delta Q_x = 4.17 \times 1.40 \times 10^{-4} = 5.84 \times 10^{-4} \quad (6.11)$$

$$\Delta Q_y = 3.4 \times 1.40 \times 10^{-4} = 4.76 \times 10^{-4} \quad (6.12)$$

Case (4)

$$\Delta Q_x = 4.17 \times 1.48 \times 10^{-4} = 6.17 \times 10^{-4} \quad (6.13)$$

$$\Delta Q_y = 3.4 \times 1.48 \times 10^{-4} = 5.03 \times 10^{-4} \quad (6.14)$$

The chromatic tune shift for four cases are significantly small, which could be negligible.

### 6.1.2 Frequency beating method

In the case of the frequency beating method, we guarantee the extraction and injection energy always match, which means that the momentum is not affected by the frequency detune, namely  $\Delta p = 0$ , So the frequency beating method has no influence on the transverse dynamics.

## 6.2. GMT systematic investigation for the B2B transfer system

---

### 6.1.2.1 Longitudinal dynamics analysis of the frequency beating for SIS18

For the frequency beating method, the rf frequency de-tune is done accompanying with the RF ramp. Accepting to decentre the orbit by 8mm [35] for the SIS18

$$\frac{\Delta R}{R} = \pm 2.4 \times 10^{-4} \quad (6.15)$$

From eq. 2.32 and eq. 2.33, the RF frequency and the magnetic field change at the  $U^{28+}$  extraction energy 200MeV/u  $\gamma_t = 5.8$  are

$$\frac{\Delta f}{f} = \pm 2.4 \times 10^{-4} \quad (6.16)$$

$$\frac{\Delta B}{B} = \frac{\Delta f}{f} \gamma_t^2 = \pm 8.1 \times 10^{-3} \quad (6.17)$$

where the maximum RF frequency de-tune is approximate to 370 Hz at 1.57 MHz for the  $U^{28+}$ . Fig. 6.9 shows the rf frequency derivation during the rf ramp. In the simulation, it is assumed that the rf frequency is detuned at 0.2756s with  $6.08 \times 10^6$ Hz/s, see blue rectangle in Fig. 6.9. For the sake of simplicity, 200 Hz is used as the rf frequency detune. SIS18 needs approximate 33us to reach 200 Hz with  $6.08 \times 10^6$ Hz/s.

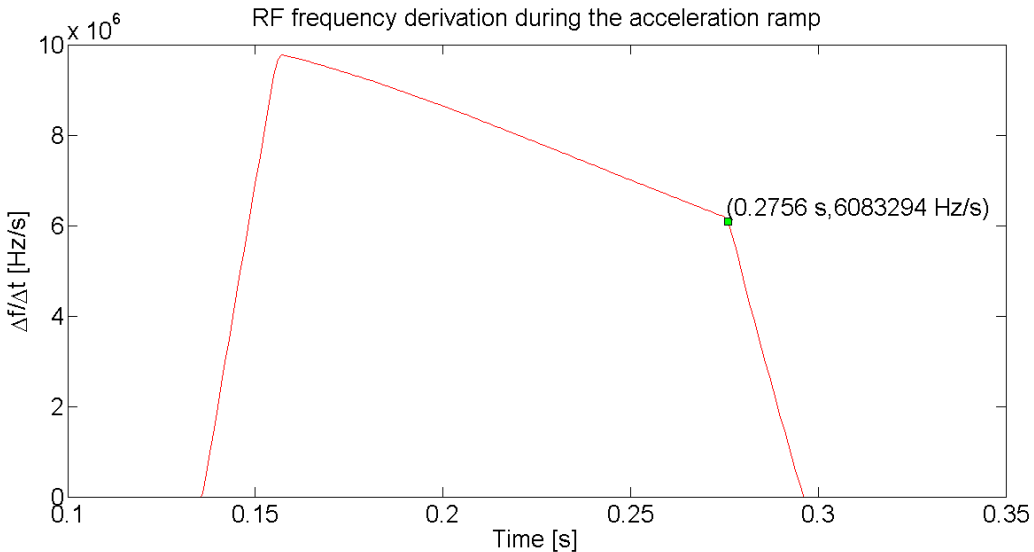


Figure 6.9: RF frequency derivation of the  $U^{28+}$  rf ramp

From eq. 2.32 and eq. 2.33, we could get the corresponding radial excursion and the magnetic field change during the detune process. The maximum radial excursion is  $-1.27 \times 10^{-4}$  at 33us of the rf detune process. The maximum magnetic field change is  $4.3 \times 10^{-3}$  at 33us of the rf detune process.

## 6.2 GMT systematic investigation for the B2B transfer system

GMT system plays a very important role for the B2B transfer system. It is responsible for the data collection, merging and redistribution. The main task of the data

## 6.2. GMT systematic investigation for the B2B transfer system

---

merging is the calculation of the synchronization window, within which the bunch could be injected into the correct bucket with the bunch to bucket center mismatch smaller than the upper bound. The data collection and redistribution make use of the WR network, so the measurement of the WR network latency is necessary.

### 6.2.1 Calculation of the synchronization window

According to the phase difference between two synchrotrons, the fine time for the alignment of two RF Reference Signals for both the phase shift and frequency beating methods can be calculated. This time is called “best estimate of alignment” and denoted by  $t_{best}$ , see Fig. 6.10. Because of the uncertainty [43] of the phase advance prediction and rf frequency modulation, the fine alignment lies between  $t_{best} - \delta t_{best}$  and  $t_{best} + \delta t_{best}$ , where  $\delta t_{best}$  is the uncertainty of the alignment.  $[t_{best} - \delta t_{best}, t_{best} + \delta t_{best}]$  is called “probable range of alignment”. In Sec.6.2.1.1 and Sec.6.2.1.2, the calculation of the best estimation of alignment and the probable range of alignment for the phase shift and frequency beating method will be explained. The probable range of alignment is within the synchronization window. For the correct selection of the same revolution frequency marker at different SCUs, the start of the synchronization window must be properly calculated. In Sec. 6.2.1.3, the calculation of the synchronization window will be explained.

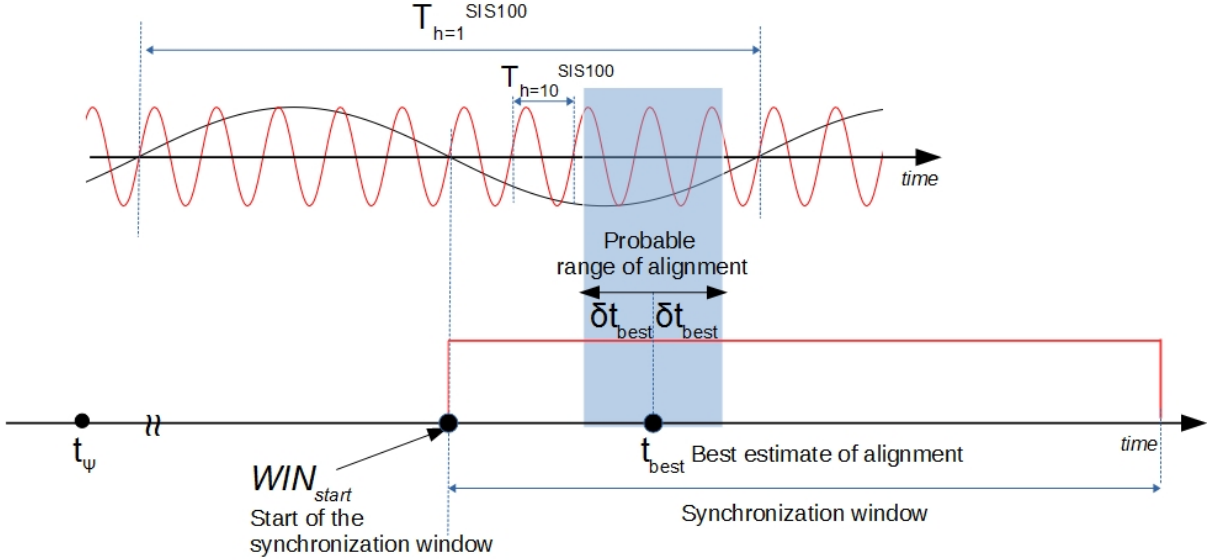


Figure 6.10: The illustration of the best estimate of alignment, the probable range of alignment and the synchronization window

For both the phase shift and frequency beating method, the calculation is based on the predicted phase of the rf signal locally. For example of the  $U^{28+}$  B2B transfer from SIS18 to SIS100, the PAP module extrapolates the rf phase  $\psi_{h=1}^{SIS100}$  for SIS100 rf  $h=1$  (157kHz) signal and  $\psi_{h=1/5}^{SIS18}$  for SIS18 rf  $h=1/5$  (157kHz) signal at  $t_\psi$  [32]. The more time is spent for the phase advance prediction, the better the predicted phase will be. Fig. 6.11 illustrates some basic definition of symbols for the calculation.

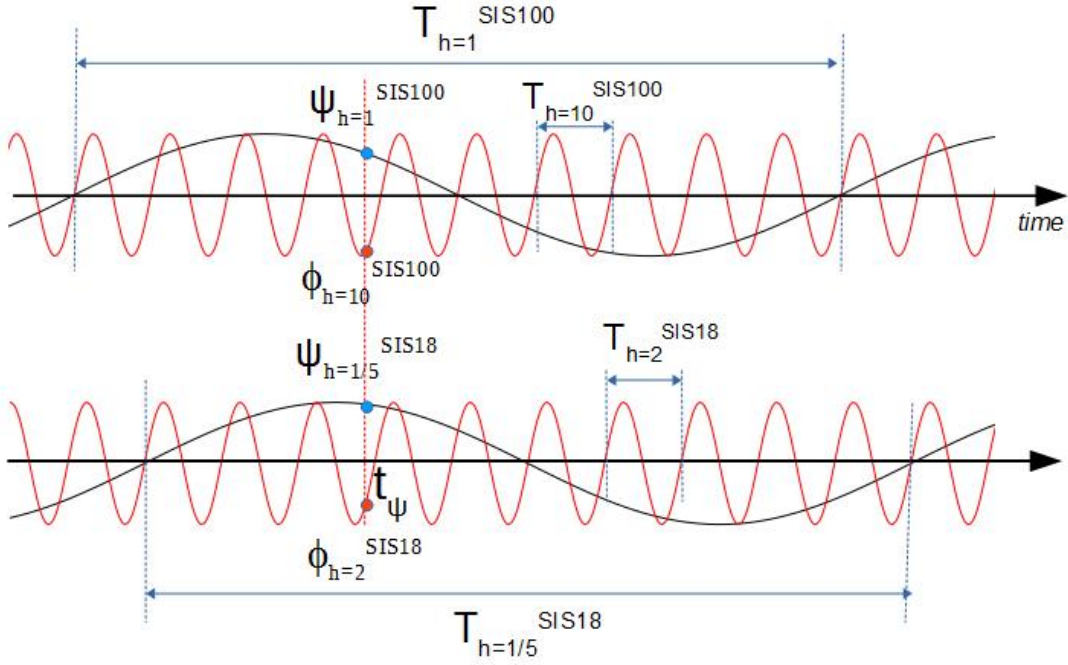


Figure 6.11: The illustration of symbols for the calculation

$\phi_{h=2}^{SIS18}$  and  $\phi_{h=10}^{SIS100}$  are individual rf phase of SIS18 and SIS100 Reference RF Signals at  $t_\psi$ . The relationship between  $\phi_{h=2}^{SIS18}$ ,  $\phi_{h=10}^{SIS100}$  and  $\psi_{h=1/5}^{SIS18}$ ,  $\psi_{h=1}^{SIS100}$  are given by eq. 6.18 and eq. 6.19.

$$\phi_{h=2}^{SIS18} = \frac{\frac{\psi_{h=1/5}^{SIS18}}{360^\circ} \times T_{h=1/5}^{SIS18} \bmod T_{h=2}^{SIS18}}{T_{h=2}^{SIS18}} \times 360^\circ \quad (6.18)$$

$$\phi_{h=10}^{SIS100} = \frac{\frac{\psi_{h=1}^{SIS100}}{360^\circ} \times T_{h=1}^{SIS100} \bmod T_{h=10}^{SIS100}}{T_{h=10}^{SIS100}} \times 360^\circ \quad (6.19)$$

substituting  $T_{h=2}^{SIS18} \times 10 = T_{h=1/5}^{SIS18}$ ,  $T_{h=10}^{SIS100} \times 10 = T_{h=1}^{SIS100}$  into eq.6.18 and eq.6.19 yields

$$\phi_{h=2}^{SIS18} = \frac{\frac{\psi_{h=1/5}^{SIS18} \times 10}{360^\circ} \times T_{h=2}^{SIS18} \bmod T_{h=2}^{SIS18}}{T_{h=2}^{SIS18}} \times 360^\circ \quad (6.20)$$

$$\phi_{h=10}^{SIS100} = \frac{\frac{\psi_{h=1}^{SIS100} \times 10}{360^\circ} \times T_{h=10}^{SIS100} \bmod T_{h=10}^{SIS100}}{T_{h=10}^{SIS100}} \times 360^\circ \quad (6.21)$$

Here we explain the inevitable uncertainty of the phase advance prediction and rf frequency modulation.

- Uncertainty of the predicted phase advance

If the phase prediction time is 500us, the uncertainty of the predicted phase advance  $\delta t_\psi$  is 100ps [44]. We calculate the uncertainty of the predicted phase

## 6.2. GMT systematic investigation for the B2B transfer system

---

advance,  $\delta\psi_{h=1}^{SIS100}$  and  $\delta\psi_{h=1/5}^{SIS18}$ , from the time to phase domain.

$$\delta t_\psi = 100ps \quad (6.22)$$

$$\delta\psi_{h=1/5}^{SIS18} = \delta\psi_{h=1}^{SIS100} = \frac{100ps}{1/157kHz} \times 360^\circ \approx 0.006^\circ \quad (6.23)$$

Based on the eq. 6.23, eq. 6.20 and eq. 6.21, the uncertainty of the phase at the Reference RF Signal of SIS18 and SIS100,  $\delta\phi_{h=10}^{SIS100}$  and  $\delta\phi_{h=2}^{SIS18}$ , is calculated.

$$\delta\phi_{h=2}^{SIS18} = \sqrt{\left(\frac{\partial\phi_{h=2}^{SIS18}}{\partial\psi_{h=2}^{SIS18}}\delta\psi_{h=2}^{SIS18}\right)^2} = \sqrt{(10 \times \delta\psi_{h=2}^{SIS18})^2} = 0.06^\circ \quad (6.24)$$

$$\delta\phi_{h=10}^{SIS100} = \sqrt{\left(\frac{\partial\phi_{h=10}^{SIS100}}{\partial\psi_{h=1}^{SIS100}}\delta\psi_{h=1}^{SIS100}\right)^2} = \sqrt{(10 \times \delta\psi_{h=1}^{SIS100})^2} = 0.06^\circ \quad (6.25)$$

- Uncertainty of the rf frequency modulation

For the rf frequency modulation, the uncertainty is  $0.2^\circ$  at 5.4MHz [45]. We calculate the uncertainty in time domain, see eq. 6.26.

$$\delta\Delta f_{(t)} = \frac{0.2^\circ}{360^\circ} \times \frac{1}{5.4MHz} = 100ps \quad (6.26)$$

### 6.2.1.1 The best estimate of alignment and the probable range of alignment for the phase shift method

Different relation between  $\phi_{h=2}^{SIS18}$  and  $\phi_{h=10}^{SIS100}$  requires different phase adjustment for SIS18. Fig. 6.12 illustrates all scenarios of their relation and the required phase adjustment for each scenario. We would like to introduce a phase shift of up to  $\pm 180^\circ$ . The blue and red line represents the phase of SIS100 and SIS18 RF Reference Signal. The clockwise arrow from the SIS18 to SIS100 rf phase represents the negative phase adjustment for SIS18 and the anticlockwise represents the positive phase adjustment. The required phase adjustment of SIS18 is denoted by  $\Delta\phi_{shift}$ .

- Scenario (a):  $\phi_{h=10}^{SIS100} \in [0, 90^\circ]$ , see Fig. 6.13 (a).
- $\phi_{h=10}^{SIS100} < \phi_{h=2}^{SIS18} < \phi_{h=10}^{SIS100} + 180^\circ$ , which denotes by the yellow semicircle in Fig. 6.13 (a). The phase adjustment is

$$\Delta\phi_{shift} = -(\phi_{h=2}^{SIS18} - \phi_{h=10}^{SIS100}) \quad (6.27)$$

- $\phi_{h=2}^{SIS18} < \phi_{h=10}^{SIS100}$  or  $\phi_{h=2}^{SIS18} > \phi_{h=10}^{SIS100} + 180^\circ$ , which denotes by the white semicircle in Fig. 6.13 (a). The phase adjustment is

$$\Delta\phi_{shift} = 360^\circ - \phi_{h=2}^{SIS18} + \phi_{h=10}^{SIS100} \quad (6.28)$$

## 6.2. GMT systematic investigation for the B2B transfer system

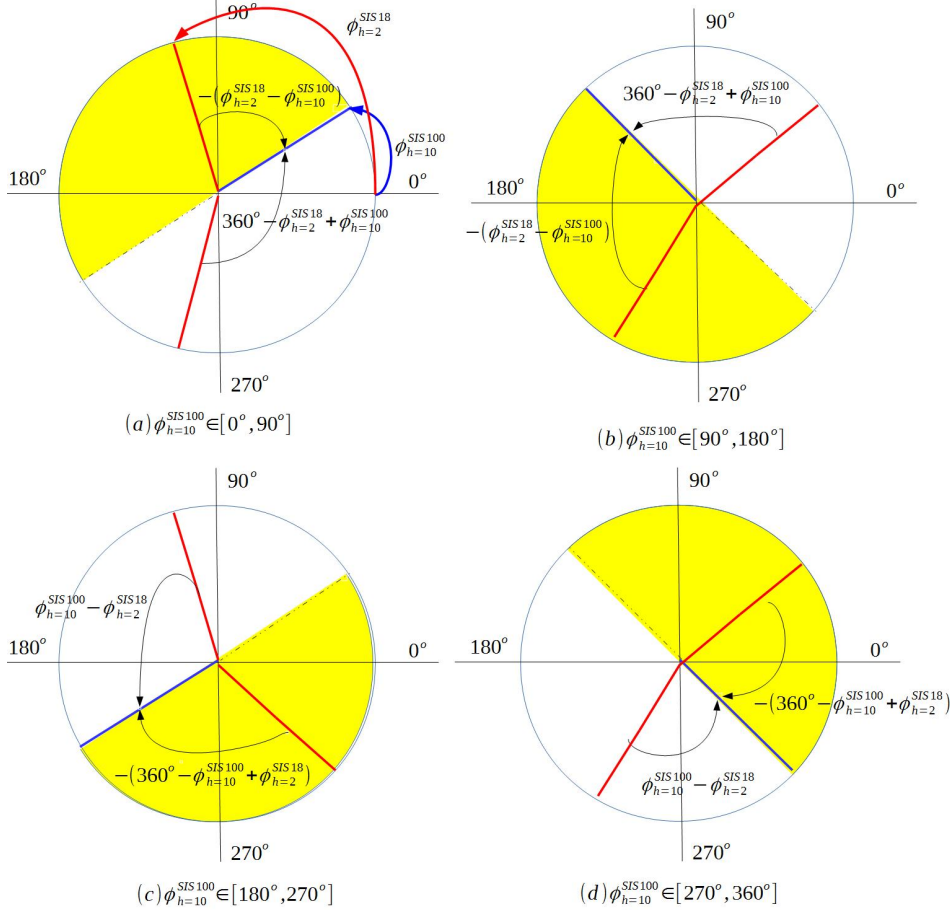


Figure 6.12: Scenarios for the phase shift method

- Scenario (b):  $\phi_{h=10}^{SIS100} \in [90^\circ, 180^\circ]$ , see Fig. 6.13 (b).
  - $\phi_{h=10}^{SIS100} < \phi_{h=2}^{SIS18} < \phi_{h=10}^{SIS100} + 180^\circ$ , which denotes by the yellow semicircle in Fig. 6.13 (b). The phase adjustment is

$$\Delta\phi_{shift} = -(\phi_{h=2}^{SIS18} - \phi_{h=10}^{SIS100}) \quad (6.29)$$

- $\phi_{h=2}^{SIS18} < \phi_{h=10}^{SIS100}$  or  $\phi_{h=2}^{SIS18} > \phi_{h=10}^{SIS100} + 180^\circ$ , which denotes by the white semicircle in Fig. 6.13 (b). The phase adjustment is

$$\Delta\phi_{shift} = 360^\circ - \phi_{h=2}^{SIS18} + \phi_{h=10}^{SIS100} \quad (6.30)$$

- Scenario (c):  $\phi_{h=10}^{SIS100} \in [180^\circ, 270^\circ]$ , see Fig. 6.13 (c). The phase adjustment is
  - $\phi_{h=2}^{SIS18} > \phi_{h=10}^{SIS100}$  or  $\phi_{h=2}^{SIS18} < \phi_{h=10}^{SIS100} + 180^\circ - 360^\circ$ , which denotes by the yellow semicircle in Fig. 6.13 (c). The phase adjustment is

$$\Delta\phi_{shift} = -(360^\circ - \phi_{h=10}^{SIS100} + \phi_{h=2}^{SIS18}) \quad (6.31)$$

- $\phi_{h=10}^{SIS100} - 180^\circ < \phi_{h=2}^{SIS18} < \phi_{h=10}^{SIS100}$ , which denotes by the white semicircle in Fig. 6.13 (c). The phase adjustment is

$$\Delta\phi_{shift} = \phi_{h=10}^{SIS100} - \phi_{h=2}^{SIS18} \quad (6.32)$$

## 6.2. GMT systematic investigation for the B2B transfer system

---

- Scenario (d):  $\phi_{h=10}^{SIS100} \in [270, 360^\circ]$ , see Fig. 6.13 (d).
- $\phi_{h=10}^{SIS100} - 180^\circ < \phi_{h=2}^{SIS18} < \phi_{h=10}^{SIS100}$ , which denotes by the yellow semicircle in Fig. 6.13 (d). The phase adjustment is
$$\Delta\phi_{shift} = \phi_{h=10}^{SIS100} - \phi_{h=2}^{SIS18} \quad (6.33)$$
- $\phi_{h=2}^{SIS18} > \phi_{h=10}^{SIS100}$  or  $\phi_{h=2}^{SIS18} < \phi_{h=10}^{SIS100} + 180^\circ - 360^\circ$ , which denotes by the white semicircle in Fig. 6.13 (d).
$$\Delta\phi_{shift} = -(360^\circ - \phi_{h=10}^{SIS100} + \phi_{h=2}^{SIS18}) \quad (6.34)$$

The phase adjustment is achieved by the phase shift method within the upper bound time,  $T_{phase\_shift}^{upper\_bound}$ . For the  $U^{28+}$  B2B transfer from SIS18 to SIS100, we assume that  $T_{phase\_shift}^{upper\_bound}$  equals to 7ms, which means that the phase shift  $\Delta\phi_{shift}$  is achieved within 7ms. So the best estimate of alignment is expressed by

$$t_{best} = t_\psi + T_{phase\_shift}^{upper\_bound} \quad (6.35)$$

The uncertainty in the phase prediction  $\delta t_\psi$  is 100ps, see eq. 6.22. The phase shift uncertainty  $\delta\Delta\phi_{phase}$  is caused by the rf frequency modulation, whose jitter is 100ps, see eq. 6.26. The phase shift uncertainty equals to the uncertainty in the phase shift upper bound time,  $\delta T_{phase\_shift}^{upper\_bound} = 100$ ps. Both cause an uncertainty in the best estimate of alignment  $t_{best}$ .

$$\begin{aligned} \delta t_{best} &= \sqrt{\left(\frac{\partial t_{best}}{\partial t_\psi} \delta t_\psi\right)^2 + \left(\frac{\partial t_{best}}{\partial T_{phase\_shift}^{upper\_bound}} \delta T_{phase\_shift}^{upper\_bound}\right)^2} \\ &= \sqrt{(\delta t_\psi)^2 + (T_{phase\_shift}^{upper\_bound})^2} = \sqrt{100ps^2 + 100ps^2} \approx 140ps \end{aligned} \quad (6.36)$$

The uncertainty of the alignment for the phase shift method is about 140ps. So the proper range of alignment is  $[t_{best}-140ps, t_{best}+140ps]$  for  $U^{28+}$  B2B transfer from SIS18 to SIS100.

### 6.2.1.2 The best estimate of alignment and the probable range of alignment for the frequency beating method

Fig. 6.13 illustrates two scenarios for the frequency beating method. With the frequency beating method, SIS18 can only achieve positive phase adjustment, which is denoted by  $\Delta\phi_{adjustment}$ . Eq. 6.37 shows the best estimate of alignment for the phase adjustment of  $\Delta\phi_{adjustment}$ .

$$t_{best} = t_\psi + \frac{\Delta\phi_{adjustment}}{360^\circ \times \Delta f} \quad (6.37)$$

where  $\Delta f$  is the beating frequency.

According to the relation between  $\phi_{h=2}^{SIS18}$  and  $\phi_{h=10}^{SIS100}$ , there are two scenarios, see Fig. 6.13.

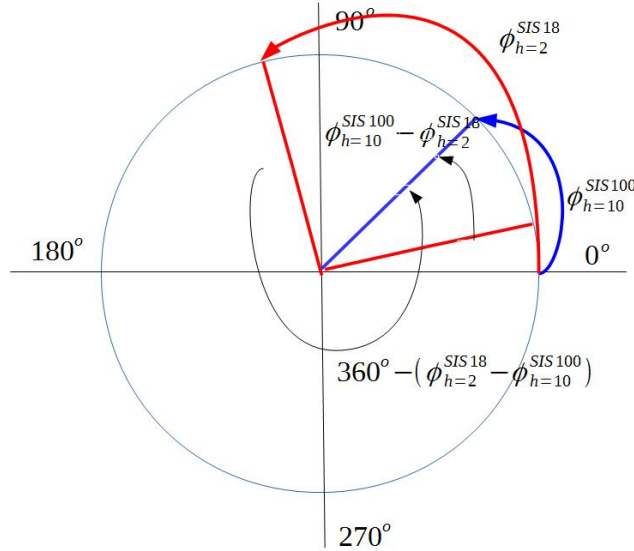


Figure 6.13: Two scenarios for the frequency beating method

- Scenario (a):  $\phi_{h=2}^{SIS18} < \phi_{h=10}^{SIS100}$

$$\Delta\phi_{adjustment} = \phi_{h=10}^{SIS100} - \phi_{h=2}^{SIS18} \quad (6.38)$$

Replacing  $\Delta\phi_{adjustment}$  in eq. 6.37 with eq. 6.38, we have

$$t_{best} = t_\psi + \frac{\phi_{h=10}^{SIS100} - \phi_{h=2}^{SIS18}}{360^\circ \times \Delta f} \quad (6.39)$$

- Scenario (b):  $\phi_{h=2}^{SIS18} \geq \phi_{h=10}^{SIS100}$

$$\Delta\phi_{adjustment} = 360^\circ - (\phi_{h=2}^{SIS18} - \phi_{h=10}^{SIS100}) \quad (6.40)$$

Replacing  $\Delta\phi_{adjustment}$  in eq. 6.37 with eq. 6.40, we have

$$t_{best} = t_\psi + \frac{360^\circ - (\phi_{h=2}^{SIS18} - \phi_{h=10}^{SIS100})}{360^\circ \times \Delta f} \quad (6.41)$$

Based on these two scenarios, we could deduce the formula for the best estimate of alignment.

$$t_{best} = t_\psi + \frac{\Delta n \times 360^\circ - (\phi_{h=2}^{SIS18} - \phi_{h=10}^{SIS100})}{360^\circ \times \Delta f} \quad (6.42)$$

where  $\Delta n$  equals 0 when  $\phi_{h=2}^{SIS18} < \phi_{h=10}^{SIS100}$  and equals 1 when  $\phi_{h=2}^{SIS18} \geq \phi_{h=10}^{SIS100}$ .

The uncertainty of the alignment is the result of the error propagation of uncertainties of the phase prediction and rf frequency detune, see eq. 6.43. Because the rf frequency detune has the long term stability,  $\int \delta\Delta f = 0$ , the uncertainty caused by rf frequency detune is 0. The uncertainty of the phase prediction  $\phi_{h=2}^{SIS18}$  and  $\phi_{h=10}^{SIS100}$  is  $0.06^\circ$ , see eq. 6.24 and eq. 6.25.  $\Delta f$  is 200Hz. The maximum

## 6.2. GMT systematic investigation for the B2B transfer system

---

$\Delta n \times 2\pi - (\phi_{h=2}^{SIS18} - \phi_{h=10}^{SIS100})$  is  $2\pi$ .

$$\begin{aligned}
 \delta t_{best} &= \sqrt{\left(\frac{\partial t_{best}}{\partial \phi_{h=2}^{SIS18}} \delta \phi_{h=2}^{SIS18}\right)^2 + \left(\frac{\partial t_{best}}{\partial \phi_{h=10}^{SIS100}} \delta \phi_{h=10}^{SIS100}\right)^2 + \left(\frac{\partial t_{best}}{\partial \Delta f} \delta \Delta f\right)^2} \\
 &= \sqrt{\left(\frac{-1}{2\pi \times \Delta f} \delta \phi_{h=2}^{SIS18}\right)^2 + \left(\frac{1}{2\pi \times \Delta f} \delta \phi_{h=10}^{SIS100}\right)^2 + \left(-\frac{\Delta n \times 2\pi - (\phi_{h=2}^{SIS18} - \phi_{h=10}^{SIS100})}{2\pi \times \Delta f^2} \delta \Delta f\right)^2} \\
 &\leq \sqrt{\left(\frac{-1}{2\pi \times 200} 0.06^\circ\right)^2 + \left(\frac{1}{2\pi \times 200} 0.06^\circ\right)^2 + 0} \\
 &\approx 1.178\text{us}
 \end{aligned} \tag{6.43}$$

From eq. 6.43 we could get the uncertainty of the alignment is 1.178us, so the probable range of alignment is  $[t_{best} - 1.178\text{us}, t_{best} + 1.178\text{us}]$ .

### 6.2.1.3 Calculation the synchronization window and its accuracy

In the last section, we get the probable range of alignment, within which the two Reference Rf Signals could be aligned with each other. The synchronization window is used to select the revolution frequency marker for the extraction and injection kicker firing, which is closest to the probable range of alignment, See Fig. 6.14. For the selection, the length of the synchronization window must be a least one SIS100 revolution period. The best estimate of the start of the synchronization window is exactly half revolution period before the selected revolution frequency marker. The blue and orange rectangles represent two scenarios of the probable range of alignment. In Fig. 6.14, the 2nd revolution frequency marker is the closest one to the probable range of alignment. The best estimate of the start of the synchronization window aligns with the negative zero crossing point of the revolution marker signal.

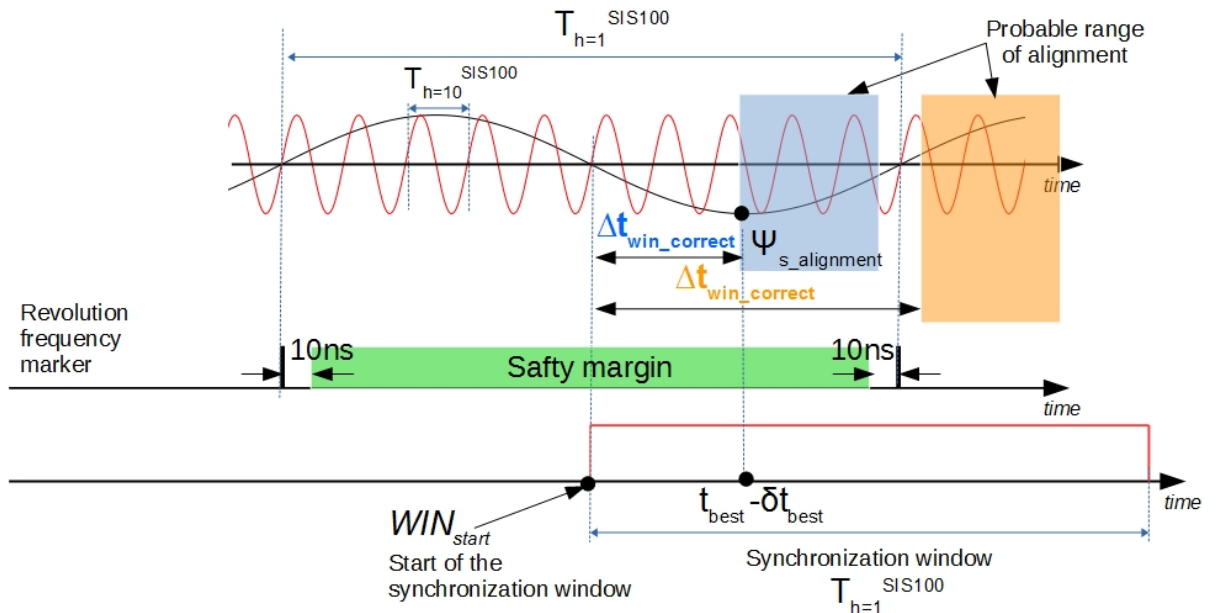


Figure 6.14: The illustration of the synchronization window and its accuracy

## 6.2. GMT systematic investigation for the B2B transfer system

---

For SIS100, the rf phase of the revolution frequency is  $\psi_{h=1}^{SIS100}$  at  $t_\psi$ . We could calculate the rf phase  $\psi_{s\_alignment}$  of the revolution frequency at the start of the probable range of alignment,  $t_{best}-\delta t_{best}$ .

$$\psi_{s\_alignment} = \frac{(t_{best} - \delta t_{best} - t_\psi - \frac{360^\circ - \psi_{h=1}^{SIS100}}{360^\circ} \times T_{h=1}^{SIS100}) \bmod T_{h=1}^{SIS100}}{T_{h=1}^{SIS100}} \times 360^\circ \quad (6.44)$$

For the calculation of the best estimate of the start of the synchronization window, there are two scenarios.  $\Delta t_{win\_correct}$  is the time correction for the start of the probable range of alignment to the best estimate of the start of the synchronization window, see Fig. 6.14.

- $\psi_{s\_alignment} \in [0^\circ, 180^\circ]$ , the orange rectangle in Fig. 6.14

$$\Delta t_{win\_correct} = \frac{\psi_{s\_alignment}}{360^\circ} \times T_{h=1}^{SIS100} + \frac{T_{h=1}^{SIS100}}{2} \quad (6.45)$$

$$WIN_{start} = t_{best} - \delta t_{best} - \Delta t_{win\_correct} \quad (6.46)$$

- $\psi_{s\_alignment} \in [180^\circ, 360^\circ]$ , the blue rectangle in Fig. 6.14

$$\Delta t_{win\_correct} = \frac{\psi_{s\_alignment} - 180^\circ}{360^\circ} \times T_{h=1}^{SIS100} \quad (6.47)$$

$$WIN_{start} = t_{best} - \delta t_{best} - \Delta t_{win\_correct} \quad (6.48)$$

The actual start of the synchronization window is impossible to be exactly at the best estimate of the start of the synchronization window because of the precision and trueness [46]. The precision is defined as the closeness of agreement between the actual start of the synchronization window of different SCUs and the trueness as the closeness of agreement between the average actual start of the synchronization window of different SCUs and the best estimation start of the synchronization window. The precision comes from the random error, e.g. IO port TTL signal rising oscillation. The trueness is the systematic error, e.g. FPGA process time. The accuracy is defined as the closeness of agreement between the observed start and the best estimate of the start of the synchronization window, which is the sum of the precision and trueness. The B2B transfer system will be used for many transfers for FAIR. Therefore, we have to find the most stringent accuracy requirement. The shortest revolution period of the target machine is 433 ns, which comes from RIB transfer from CR to HESR. We keep 10ns as a forbidden range, which means that the actual start is not allowed 10 ns before and after the revolution frequency marker. The green region in Fig. 6.14 represents the safety margin for the start of the synchronization window. So the accuracy of the start of the synchronization window is

$$Accuracy = \pm \frac{433 - 10 \times 2}{2} \approx \pm 200 \text{ ns} \quad (6.49)$$

### 6.2.2 Measurement of the WR network for the B2B transfer

GMT system implements the tree WR network topology. The WR network measurement is achieved by the Xena traffic generator <sup>1</sup>, which offers a new class of

---

<sup>1</sup><http://xenanetworks.com/layer-2-3-platform/>

## **6.2. GMT systematic investigation for the B2B transfer system**

---

professional Layer 2-3 Gigabit Ethernet test platform. It is used to measure the frame loss rate<sup>2</sup>, latency<sup>3</sup> and jitter<sup>4</sup> for the WR network. For the measurement, Xena traffic generator sends the traffic streams with a unique stream ID for identifying latency, jitter and packet loss. The WR network for FAIR has the following traffic [47].

- DM Broadcast

DM forwards broadcast timing frames<sup>5</sup> with 110 bytes ethernet frame length downwards to all FECs. The average bandwidth for the DM broadcast is 100 Mbit/s. The burst<sup>6</sup> speed is 12 packets per 100 µs.

- DM Unicast

DM sends 10Mbit/s unicast timing frames with 110 bytes ethernet frame length to some specified FECs at the burst speed of 3 packets per 300 µs.

- B2B Unicast

The source B2B SCU sends the timing frame with 110 bytes ethernet frame length upwards to the DM. For the B2B transfer upper bound time 10 ms of each supercycle, 2 unicast timing frames are sent to the DM. The maximum repetition frequency is of the  $U^{28+}$  supercycle, 2.82 Hz. For the estimation of the upper bound bandwidth, we use 3Hz/s as the maximum repetition frequency. So the bandwidth is  $3 \text{ Hz/s} \times 2 \text{ packets/supercycle} \times 110 \text{ byte} \times 8 \text{ bit} \approx 5.5 \text{ kbit/s}$ .

- B2B Broadcast

Maximum 10 B2B broadcast timing frames with 110 ethernet frame length are sent within 10 ms. So the bandwidth is  $3 \text{ Hz/s} \times 10 \text{ packets/supercycle} \times 110 \text{ byte} \times 8 \text{ bit} \approx 26.5 \text{ kbit/s}$ .

- Management Traffic

The average bandwidth for the management traffic is 10 Mbit/s. It broadcasts packets with random ethernet frame length from 64 bytes to 1518 bytes.

The requirements for the B2B Broadcast and Unicast traffic are summarized in Tab. A.1 [47].

For the WR network for FAIR, three VLANs with different priorities are applied according to the importance of the traffic.

---

<sup>2</sup>The ratio of the number of the lost frames to the number of the theoretic received frames of a tested port.

<sup>3</sup>The time interval between the time of Xena port receiving frame and the time of another Xena port sending frame.

<sup>4</sup>The absolute value of the difference between the latency of two consecutive received frames belonging to the same stream from one Xena port to another Xena port.

[http://www.xenatenetworks.com/wp-content/uploads/Measuring\\_Frame\\_latency\\_Variation.pdf](http://www.xenatenetworks.com/wp-content/uploads/Measuring_Frame_latency_Variation.pdf)

<sup>5</sup><https://www-acc.gsi.de/wiki/Timing/TimingSystemEvent>

<sup>6</sup>A group of consecutive frames with shorter interframe gaps than frames arriving before or after the burst of frames.

## 6.2. GMT systematic investigation for the B2B transfer system

---

Table 6.4: The B2B transfer requirements for the WR network

	Frame Loss Rate	Upper bound latency of WR network	Upper bound latency per WR switch layer
B2B Broadcast	$10^{-12}$	500 $\mu$ s	30 $\mu$ s
B2B Unicast	$10^{-12}$	500 $\mu$ s	30 $\mu$ s

### 6.2.2.1 WR network test setup

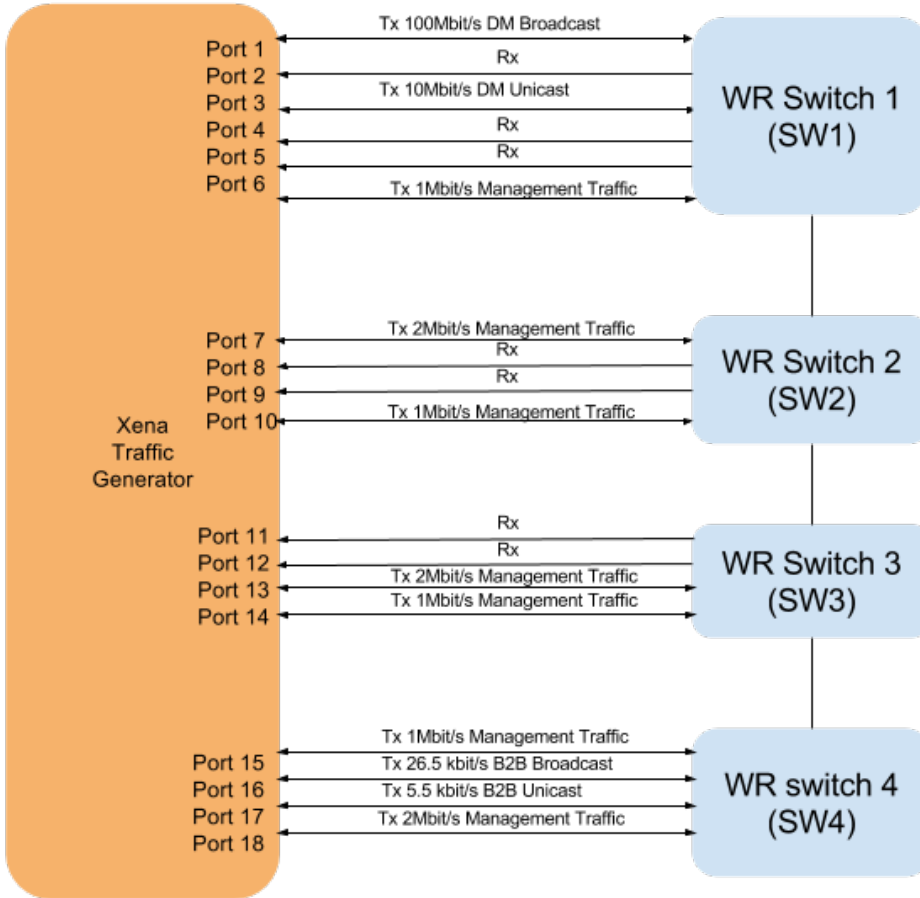


Figure 6.15: The WR network test setup

Based on the mentioned traffic, the measurement setup is built, see Fig. 6.15 [47]. Four WR switches are connected to the port 1 to 18 of the Xena traffic generator. All ports of four WR switches are assigned to three VLANs, VLAN 5, VLAN 6 and VLAN 7. Tab. 6.5 shows the bandwidth, VLAN, VLAN priority and usage of the traffic of each Xena port in details. The test is running for 14 hours.

## 6.2. GMT systematic investigation for the B2B transfer system

---

Table 6.5: The connection between Xena ports and WR switches

Switch	Xena Port	Traffic	VLAN	Priority	Usage
WR switch 1	Port 1	100 Mbit/s 110bytes	7	7	DM Broadcast
	Port 2	Rx traffic			
	Port 3	10 Mbit/s 110bytes	7	7	DM Unicast
	Port 4	Rx traffic			
	Port 5	Rx traffic			
	Port 6	1 Mbit/s 64 - 1518 bytes	5	5	Management Broadcast
WR switch 2	Port 7	2 Mbit/s 64 - 1518 bytes	5	5	Management Broadcast
	Port 8	Rx traffic			
	Port 9	Rx traffic			
	Port 10	1 Mbit/s 64 - 1518 bytes	5	5	Management Broadcast
WR switch 3	Port 11	Rx traffic			
	Port 12	Rx traffic			
	Port 13	2 Mbit/s 64 - 1518 bytes	5	5	Management Broadcast
	Port 14	1 Mbit/s 64 - 1518 bytes	5	5	Management Broadcast
WR switch 4	Port 15	1 Mbit/s 64 - 1518 bytes	5	5	Management Broadcast
	Port 16	26.5 kbit/s 110bytes	6	6	B2B Broadcast
	Port 17	5.5 kbit/s 110bytes	7	7	B2B Unicast
	Port 18	2 Mbit/s 64 - 1518 bytes	5	5	Management Broadcast

### 6.2.2.2 Frame loss rate test result for B2B frames

The frame loss rate of the stream from port 17 to port 1 is measured for the B2B Unicast frames. The frame loss rate of the stream from port 16 to other ports is measured for the B2B Broadcast frame. Fig. 6.16 [47] shows the test result for both traffics. For the B2B Broadcast frames, the frame loss rate of each port is 0 %. For the B2B Unicast frames, the frame loss rate of port 1 is 0 %. So there is no B2B frame loss of the test WR network.

## 6.2. GMT systematic investigation for the B2B transfer system

---

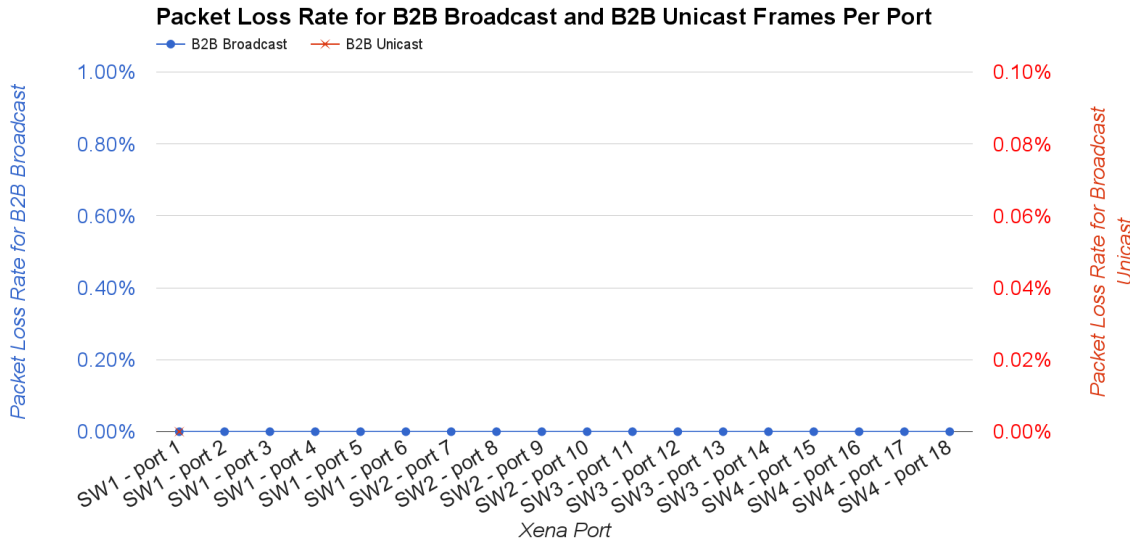


Figure 6.16: The frame loss rate for B2B Broadcast and B2B Unicast frames

### 6.2.2.3 Latency and jitter test result for B2B frames

The latency and jitter of the stream from port 16 to other ports are measured.

- Latency and jitter for B2B Broadcast frames

- Average Latency and jitter

Fig. 6.17 [47] shows the test result for the average latency and jitter for the B2B Broadcast frames. Tab. 6.6 shows the average latency and jitter of different WR switch layers. They meet the requirements of the B2B transfer.

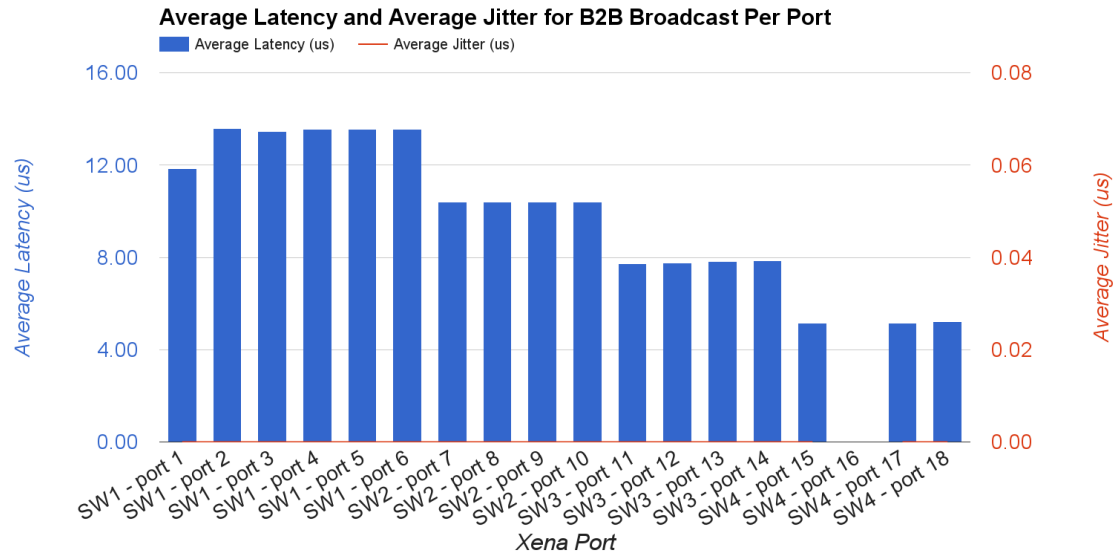


Figure 6.17: The average latency and jitter for B2B Broadcast frames

## 6.2. GMT systematic investigation for the B2B transfer system

---

Table 6.6: The average latency and jitter of the B2B Broadcast frames

	WR switch 4	WR switch 4, 3	WR switch 4, 3, 2	WR switch 4, 3, 2, 1
Avg latency	6 $\mu$ s	8 $\mu$ s	11 $\mu$ s	14 $\mu$ s
Avg jitter	0 ns	0 ns	0 ns	0 ns

- Maximum Latency and jitter

Fig. 6.18 [47] shows the test result for the maximum latency and jitter for the B2B Broadcast frames. Tab. 6.7 shows the maximum latency and jitter of different WR switch layers. They meet the requirements of the B2B transfer.

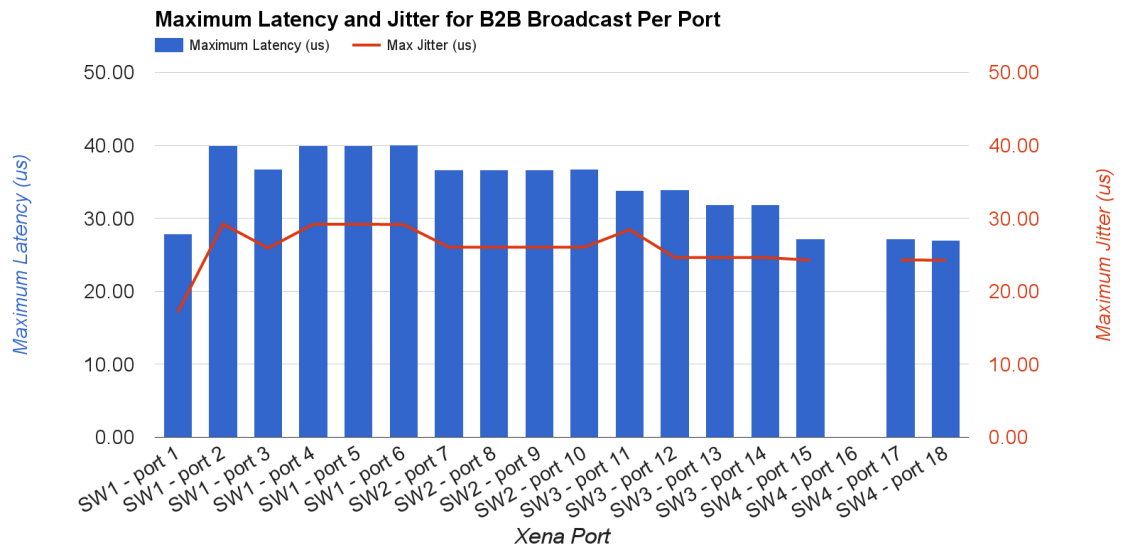


Figure 6.18: The maximum latency and jitter for B2B Broadcast frames

Table 6.7: The maximum latency and jitter of the B2B Broadcast frames

	WR switch 4	WR switch 4, 3	WR switch 4, 3, 2	WR switch 4, 3, 2, 1
Max latency	28 $\mu$ s	34 $\mu$ s	37 $\mu$ s	41 $\mu$ s
Max jitter	25 $\mu$ s	25 $\mu$ s	27 $\mu$ s	30 $\mu$ s

- Latency and jitter for B2B Unicast frames

For the B2B unicast frames, the latency and jitter of the stream from port 16 to port 1 are measured.

## 6.2. GMT systematic investigation for the B2B transfer system

---

- Average Latency and jitter

For the B2B Unicast frames, 4 WR switch network has approximate 11  $\mu$ s average latency and 0  $\mu$ s average jitter.

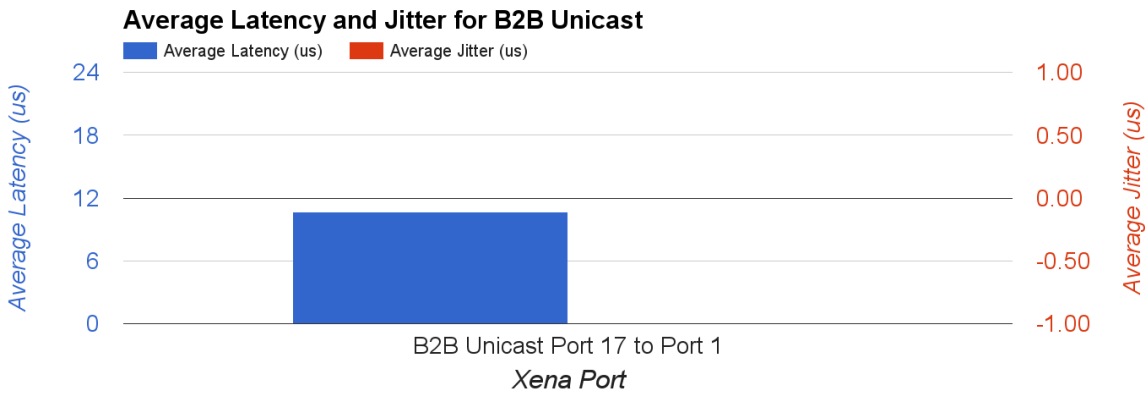


Figure 6.19: The average latency and jitter for B2B Unicast frames

- Maximum Latency and jitter

For the B2B unicast frames, 4 WR switch network has approximate 23  $\mu$ s maximum latency and 13  $\mu$ s maximum jitter.

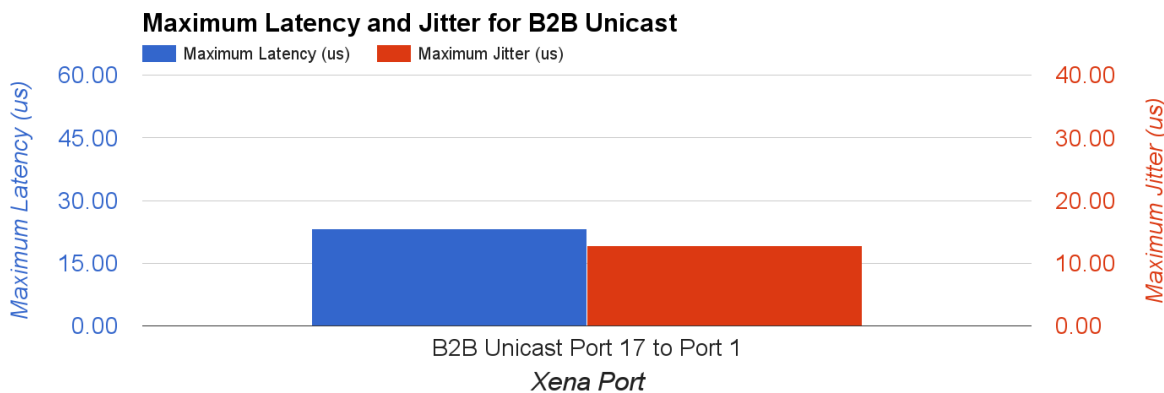


Figure 6.20: The maximum latency and jitter for B2B Unicast frames

More test configuration and results, please see “Testing the WR Network of the FAIR General Machine Timing System“.

### 6.2.2.4 Result and conclusion

Tab. 6.8 shows the result of the test. The frame loss rate and latency meet the requirements of the B2B Broadcast and B2B Unicast traffic.

### 6.3. Kicker systematic investigation for the B2B transfer system

---

Table 6.8: The result of the WR network test for the B2B transfer

	Frame Loss Rate	Average Latency	Maximum Latency	Average Jitter	Maximum Jitter
B2B Broadcast	0 %	6 $\mu$ s/switch	28 $\mu$ s/switch	0 $\mu$ s/switch	25 $\mu$ s/switch
B2B Unicast	0 %	11 $\mu$ s/4switch 3 $\mu$ s/switch	23 $\mu$ s/4switch 6 $\mu$ s/switch	0 $\mu$ s/4switch 0 $\mu$ s/switch	13 $\mu$ s/4switch 4 $\mu$ s/switch

For the B2B transfer system, the upper bound latency of the frames in the B2B Broadcast and B2B Unicast traffic is 500  $\mu$ s, see Tab.6.4. The latency of the WR network is decided by the layers of WR switches and the length of the optical fiber. The latency of the optical fiber is about 204 m/ $\mu$ s [48] and the longest distance in the FAIR campus is around 2 km, so the latency of a 2 km optical fiber is about 10  $\mu$ s. The layers of WR switches play a more important role in the latency.

- B2B Broadcast

Here we calculate the layer of the WR switch between the B2B source SCU and B2B target SCU, between B2B source SCU and source trigger SCU and between B2B source SCU and target trigger SCU.

$$\frac{500 \mu\text{s} - 10 \mu\text{s}}{28 \mu\text{s}/\text{switch}} \approx 17 \quad (6.50)$$

- B2B Unicast

Here we calculate the layer of the WR switch between the B2B source SCU and DM.

$$\frac{500 \mu\text{s} - 10 \mu\text{s}}{6 \mu\text{s}/\text{switch}} \approx 81 \quad (6.51)$$

## 6.3 Kicker systematic investigation for the B2B transfer system

The SIS18 extraction kicker consists of 9 kicker units. In the existing topology, 5 kicker units are installed in the 1st crate and the other 4 units are in the 2nd crate. The width of each kicker unit is 0.25m and the distance between two kicker units is 0.09m. The distance between two crates is 19.167m. SIS100 injection kicker consists of 6 kicker units, which are equally located. The width of each kicker unit is 0.22m and the distance between two units is 0.23m. For the B2B transfer, the rise time of SIS18 extraction kicker and SIS100 injection kicker unit are 90ns and 1/20 of the revolution period. The rise time of these kickers must fit within the bunch gap, 25% of rf reference period [17, 36]. The bunch gap is denoted by G. All the analysis in this section dose not consider the jitter of the kicker trigger signal. Here we are discussing about the following possibilities.

### 6.3. Kicker systematic investigation for the B2B transfer system

- For SIS18, whether the kicker units in the 2nd crate could be fired a fixed delay after the firing of the kicker units in the 1st crate for ion beams over the whole range of stable isotopes.
- For SIS100, whether the kicker units could be fired instantaneously.

#### 6.3.1 SIS18 extraction kicker units

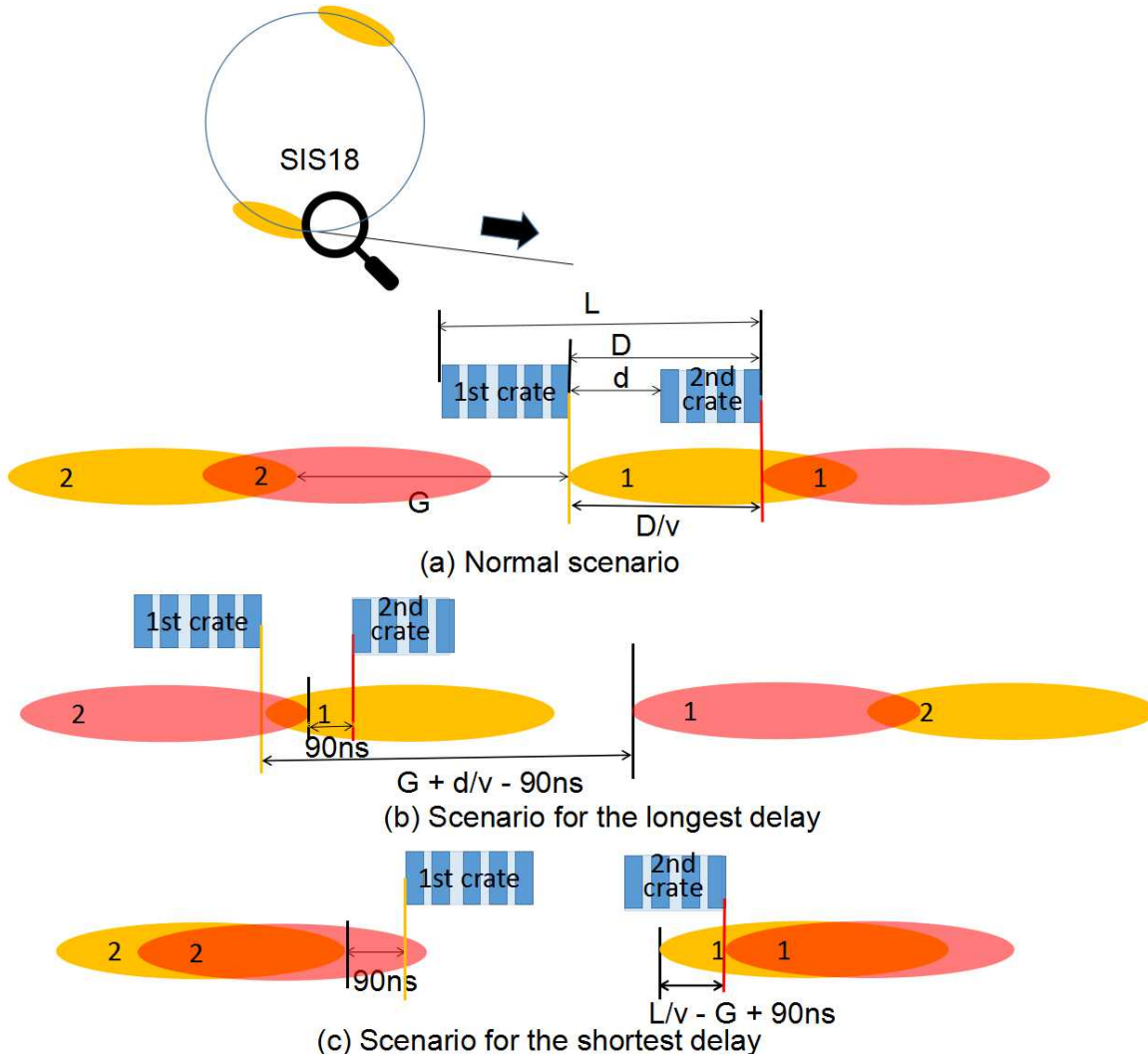


Figure 6.21: Three scenarios for the delay of SIS18 extraction kicker

Here we take three ion beams,  $H^+$ ,  $U^{28}$  and  $U^{73+}$ , to check the possibility, because the boundary ion species have the most stringent requirements. Fig. 6.21 shows three scenarios of the firing delay between two crates. Beam is firstly kicked by kicker units in the 1st crate and than kicked by the units in the 2nd crate to the transfer line. The yellow and red ellipse represents the position of the bunches, when the kicker units in the 1st and 2nd crate are fired. The number in the ellipse is used to tell different bunches. The head of the bunch is at the right side. The bunch 2 is firstly kicked. Here we assume that the kicker units in the same crate are triggered

### 6.3. Kicker systematic investigation for the B2B transfer system

---

instantaneous.  $d$  denotes the distance between two crates.  $L$  denotes the distance from the leftmost to the rightmost kicker unit.  $D$  denotes the sum distance of  $d$  and the 2nd crate.  $d$  equals to 19.167 meter.  $L$  equals to  $22.047\text{m} = d + 9 \times 0.25\text{m} + 7 \times 0.09\text{m}$ .  $D$  equals to  $20.437\text{m} = d + 4 \times 0.25\text{m} + 3 \times 0.09\text{m}$ .

Fig. 6.21 (a) is the easiest scenario. The kicker units in the 1st crate are fired when the tail of the bunch 1 passes by the 1st crate completely. The kicker units in the 2nd crate are fired when the tail of the bunch 1 passes by the 2nd crate completely. The delay for the firing two crates in this scenario is  $D/\beta c$ .

Fig. 6.21 (b) shows the scenario of the maximum delay between the firing of two crates. The kicker units in the 1st crate are fired when the tail of the bunch 1 passes by the 1st crate completely. The kicker units in the 2nd crate are fired 90ns before the head of the bunch 2 passes by it. The delay equals to  $G+d/\beta c-90\text{ns}$ .

Fig. 6.21 (c) shows the scenario of the minimum delay. The kicker units in the 1st crate are fired 90ns before the head of the bunch 2 passes by it. The kicker units in the 2nd crate are fired when the bunch 1 passes by the 2nd crate. The delay is  $L/\beta c-G+90\text{ns}$ .

Tab. 6.9 shows delay for three scenarios and related parameters. The fixed delay is determined primarily by the boundary delay range from  $H^+$ ,  $U^{28}$  and  $U^{73+}$  beams, the delay range for other heavy ion species beams must be contained in these boundary range. According to the result, a fixed delay is available for firing kicker units in two crate for different beams. e.g. 80ns.

Table 6.9: The delay for firing two crates of SIS18 extraction kicker

Beam	$\beta$	time $L/\beta c$	bunch gap $G$	minimum delay $L/\beta c-G+90\text{ns}$	delay $D/\beta c$	maximum delay $G+d/\beta c-90\text{ns}$
$H^+$	0.982	75ns	184ns	0ns	69ns	163ns
$U^{28}$	0.568	130ns	159ns	61ns	120ns	189ns
$U^{73+}$	0.872	84ns	104ns	70ns	78ns	92ns

### 6.3.2 SIS100 injection kicker units

Two bunches from SIS18 will be continuously injected into two RF buckets after the other in SIS100. See Fig. 6.10. The yellow ellipse represents the circulating bunch in SIS100 and the red one represents the bunch to be injected. The head of the bunch is at the left side. The preparation of the SIS100 injection kicker must be done during the bunch gap and it must be established for at least one SIS18 revolution period. For the instantaneous firing, all kicker units are fired only if the tail of the circulating bunch passes the leftmost kicker unit. The kicker pass time is the time needed for the tail of a bunch to pass from the rightmost unit to the leftmost kicker unit. The rise time of the kicker unit is 1/20 of the revolution period [17]. Therefor the preparation time is the sum of the kicker pass time and rise time. The distance from the rightmost to the leftmost kicker unit is 3.79m,  $6 \times 0.22\text{m} + 5 \times 0.23\text{m}$ . If the preparation time is shorter than bunch gap, all kicker units could be fired instantaneous. Tab. 6.10 shows the preparation time for  $H^+$ ,  $U^{28}$  and  $U^{73+}$  beams and their bunch gap. The preparation time is much shorter than the bunch gap. So the kicker units could be fired instantaneous.

## 6.4. Test setup for the data collection, merging and redistribution of the B2B transfer system

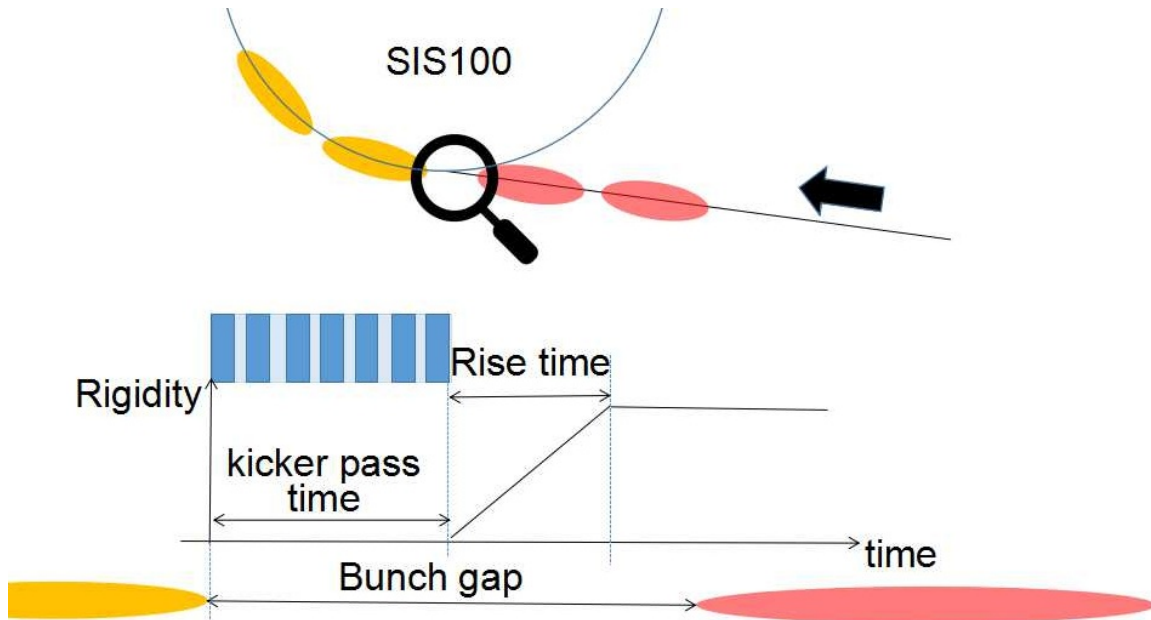


Figure 6.22: SIS100 injection kicker

Table 6.10: The delay for firing SIS00 injection kicker

Beam	$\beta$	kicker pass time $L/\beta c$	Rise time $1/20 \times T_{rev}^{SIS100}$	Preparation time $L/\beta c + 1/20 \times T_{rev}^{SIS100}$	bunch gap $2.25 \times T_{rev}^{SIS100}$
$H^+$	0.982	3ns	184ns	187ns	828ns
$U^{28}$	0.568	22ns	318ns	333ns	1431ns
$U^{73+}$	0.872	15ns	207ns	222ns	932ns

## 6.4 Test setup for the data collection, merging and redistribution of the B2B transfer system

In this section, the test setup for the B2B transfer system is described, focusing only on the timing aspects.

### 6.4.1 Test functional requirement

The test setup achieves the following functional requirement.

- After receiving the B2B beginning frames, both the B2B source and target SCUs collect predicted phase equivalent data locally. The equivalence is a timestamp for the zero crossing point of the simulated RF Reference Signal of SIS18 and SIS100.

## 6.4. Test setup for the data collection, merging and redistribution of the B2B transfer system

- The B2B target SCU transfers the frame containing the timestamp to the B2B source SCU.
- After receiving the data, the B2B source SCU calculates the synchronization window.
- The B2B source SCU sends the frame containing the beginning of the synchronization window to the WR network.
- After receiving the frame, the trigger SCU produces TTL output indicating the start of the synchronization window.

### 6.4.2 Test setup

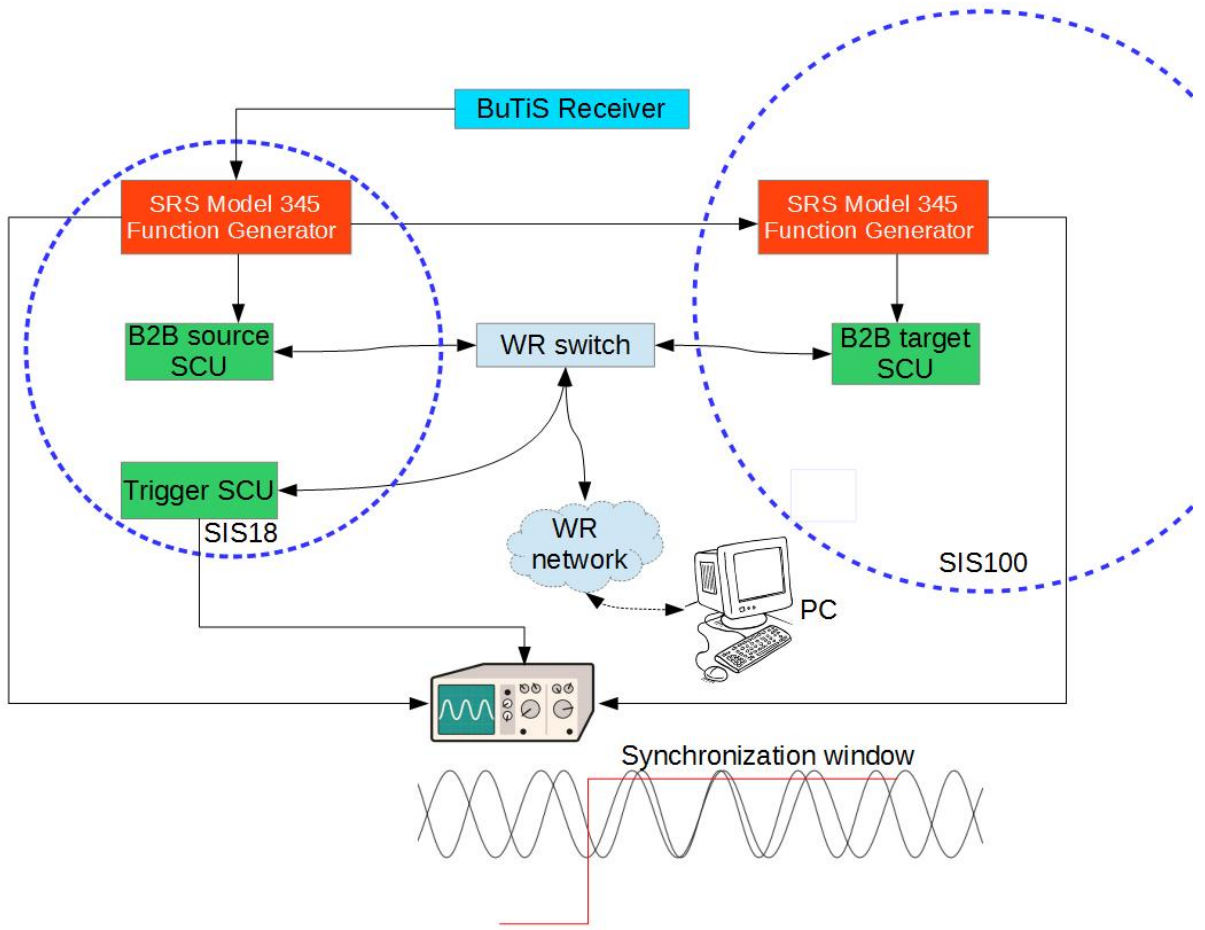


Figure 6.23: Schematic of the test setup

Fig. 6.23 shows the schematic of the test setup. In this test setup, two MODEL DS345 Synthesized Function Generators<sup>7</sup> are used, which are with the frequency accuracy of  $\pm 5$  ppm of the selected frequency to simulate RF Reference Signals of SIS18 and SIS100. DS345 of SIS18 is directly triggered by the 10 MHz of BuTiS

<sup>7</sup><http://www.thinksrs.com/downloads/PDFs/Manuals/DS345m.pdf>

#### **6.4. Test setup for the data collection, merging and redistribution of the B2B transfer system**

receiver and DS345 of SIS100 is triggered by DS345 of SIS18. So both DS345s are synchronized to BuTiS. The B2B source SCU, B2B target SCU and trigger SCU are connected to the same WR switch, which connects to the timing network. PC<sup>8</sup> is used as a DM to produce the B2B start timing frame. Besides, it monitors the status of the B2B transfer programs in all SCUs. The oscilloscope is used to monitor the alignment of the two simulated RF Reference Signals within the synchronization window provided by the trigger SCU.

Fig. 6.24 shows the front and back view of the test setup. DS345 of SIS18 produces the sine wave of 1.572 200 MHz frequency for the B2B source SCU. DS345 of SIS100 produces the sine wave of 1.572 000 MHz for the B2B target SCU. So the beating frequency is 200 Hz and the synchronization period is 5 ms.

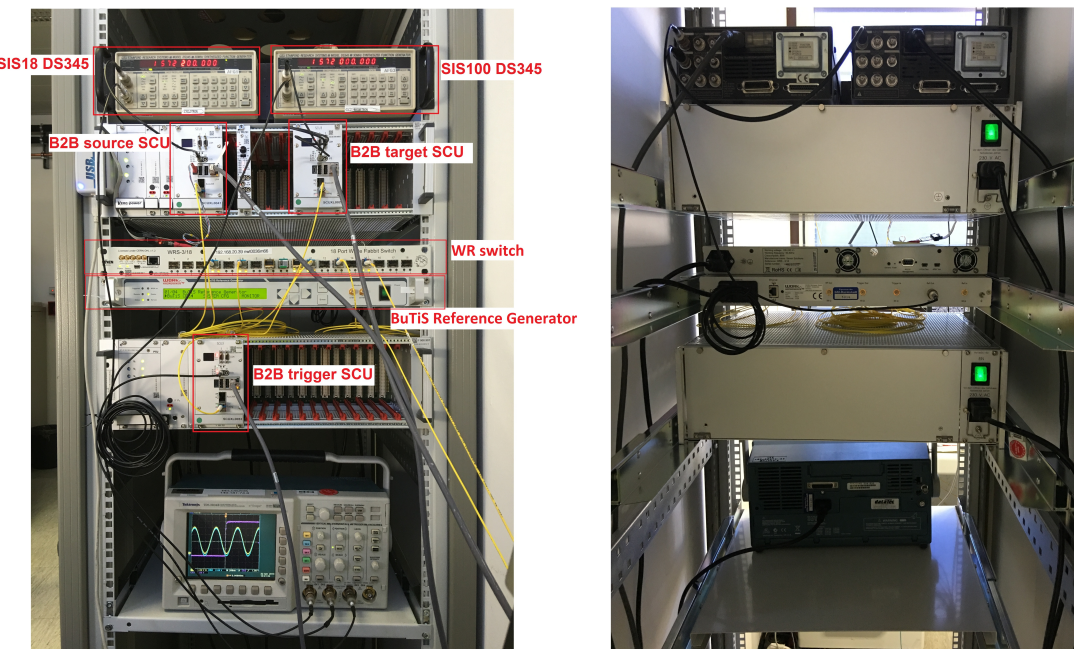


Figure 6.24: The front and back view of the test setup

### 6.4.3 The firmware of the B2B transfer system

The B2B source, B2B target and trigger SCUs have different firmware running on their soft CPU, LM32<sup>9</sup>. The firmware are activated by the B2B start timing frame, *CMD\_START\_B2B*, which indicates the source and target synchrotrons of the B2B transfer.

- Firmware for the B2B source SCU

The firmware for the B2B source SCU is the core program of the B2B transfer system. See Fig. 6.25.

<sup>8</sup>A Linux personal computer is installed with the standard TR tools and library.  
<https://www-acc.gsi.de/wiki/Timing/TimingSystemNodesCurrentRelease>

<sup>9</sup>LatticeMico32 is a 32-bit microprocessor soft core from Lattice Semiconductor optimized for field-programmable gate arrays (FPGAs).

## 6.4. Test setup for the data collection, merging and redistribution of the B2B transfer system

---

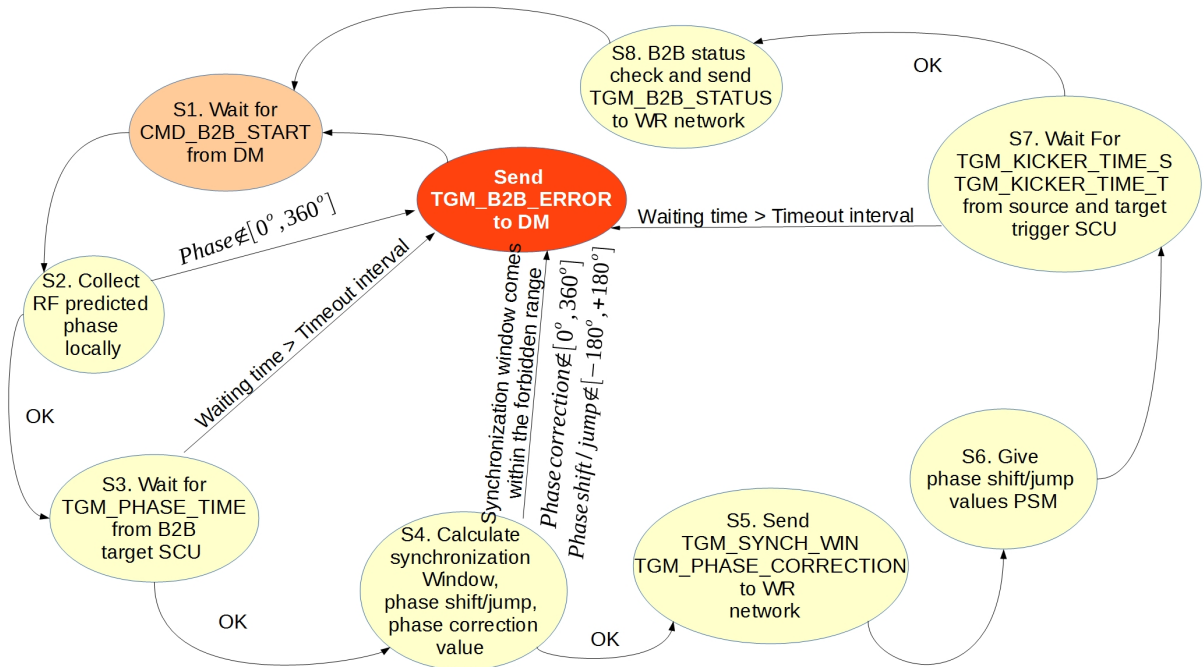


Figure 6.25: Flow chart of the firmware for B2B source SCU.

Flow chart of the firmware for B2B source SCU. Step is represented as ‘S’ in the figure.

- Step 1. The program waits for the CMD\_START\_B2B timing frame.
- Step 2. When it receives the timing frame CMD\_START\_B2B, it collects the predicted phase and checks whether it is within a proper range of  $0^\circ$  to  $360^\circ$ . If not, it sends a timing frame TGM\_B2B\_ERROR to the WR network and goes back to the step 1, which indicates the data error.
- Step 3. It waits for the TGM\_PHASE\_TIME timing frame from the B2B target SCU, which contains the predicted phase and the slop of the target synchrotron.
- Step 4. When it receives the timing frame TGM\_PHASE\_TIME within a specified timeout interval, it calculates the synchronization window, the phase shift/jump value and the phase correction value. Or it sends a timing frame TGM\_B2B\_ERROR to the WR network and goes back to the step 1, which indicates the timeout error of the frame. Besides, it checks whether the phase correction is in the range of  $0^\circ$  to  $360^\circ$ , the required phase shift in the range of  $-180^\circ$  to  $180^\circ$  and the start of the synchronization window not in the forbidden range. If at least one of them is not correct, it sends a timing frame TGM\_B2B\_ERROR to the WR network and goes back to the step 1, which indicates the calculation error.
- Step 5. It sends the timing frame TGM\_SYNCH\_WIN and TGM\_PHASE\_CORRECTION to the WR network. TGM\_SYNCH\_WIN indicates the start of the synchronization window and TGM\_PHASE\_CORRECTION is used for the trigger SCUs for the reproduction of the bucket label

## 6.4. Test setup for the data collection, merging and redistribution of the B2B transfer system

- signal.
- Step 6. It gives the phase correction and phase shift/jump values to corresponding modules.
  - Step 7. It waits for the timing frame TGM\_KICKER\_TIME\_S from the source trigger SCU and TGM\_KICKER\_TIME\_T from the target trigger SCU, which contains the extraction/injection kicker trigger and firing timestamp. When it does not receive the timing frames within a specified timeout interval, it sends a timing frame TGM\_B2B\_ERROR to the WR network and goes back to the step 1, which indicates the timeout error of the frame.
  - Step 8. When it receives the timing frames mentioned in the step 7 within a specified timeout interval, it checks the B2B transfer status and sends TGM\_B2B\_STATUS to the WR network and goes to the step 1. The B2B transfer is successful, if all of the following checks are correct. Or the B2B transfer is failure.
    - \* Trigger time < firing time of the extraction kicker of the source synchrotron
    - \* Trigger time < firing time of the injection kicker of the target synchrotron
    - \* Firing time of the extraction kicker < firing time of the injection kicker
- Firmware for the B2B target SCU

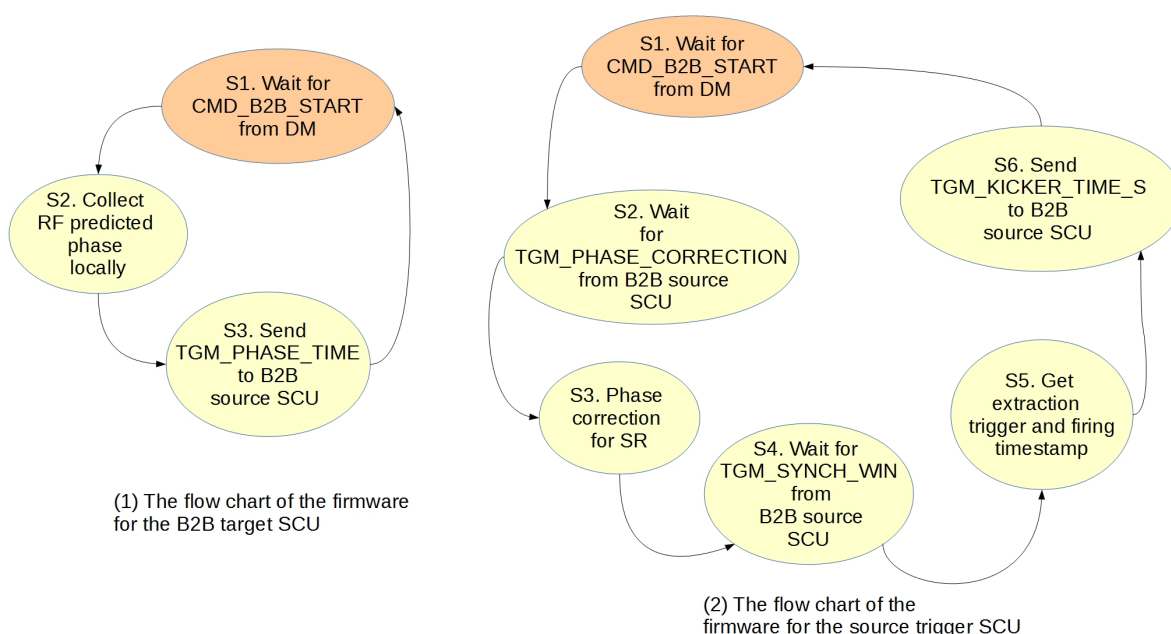


Figure 6.26: Flow chart of the firmware for B2B target SCU.  
Flow chart of the firmware for B2B target SCU. Step is represented as S in the figure.

## 6.4. Test setup for the data collection, merging and redistribution of the B2B transfer system

---

Fig. 6.26 (a) shows the flow chart of the program of the B2B target SCU.

- Step 1. The program waits for the CMD\_START\_B2B timing frame.
- Step 2. When it receives the timing frame CMD\_START\_B2B, it collects the predicted phase.
- Step 3. It sends the TGM\_PHASE\_TIME timing frame to the B2B source SCU and goes back to the step 1.

- Firmware for the trigger SCU

Fig. 6.26 (b) shows the flow chart of the program of the source trigger SCU. For the target trigger SCU, the flow chat is same only with the different name of the timing frame TGM\_KICKER\_TIME\_T.

- Step 1. The program waits for the CMD\_START\_B2B timing frame.
- Step 2. The program waits for the TGM\_PHASE\_CORRECTION timing frame.
- Step 3. The program gives the phase correction value to the corresponding module for the bucket label signal reproduction.
- Step 4. When it receives the timing frame CMD\_START\_B2B, it waits for the timing frame TGM\_SYNCH\_WIN to indicate the synchronization window for the kicker trigger.
- Step 5. After the beam extraction, it collects the trigger and firing timestamp.
- Step 6. It sends the TGM\_KICKER\_TIME\_S timing frame to the B2B source SCU and goes back to the step 1.

### 6.4.4 The time constraints of the B2B transfer system

For the B2B transfer system, the time constraints are very important and strict. Fig. 6.27 shows the time constraint of the system. The *CMD\_START\_B2B* is executed at  $t_{B2B}$ . The RF phase prediction needs 500  $\mu$ s, so the B2B source and target SCUs collect the phase data at  $t_{B2B} + 500 \mu\text{s}$  and need about 450 ns for the data collection. The B2B source SCU receives the timing frame TGM\_PHASE\_TIME at around  $t_{B2B} + 500 \mu\text{s} + 450 \text{ ns} + 500 \mu\text{s} \approx t_{B2B} + 1 \text{ ms}$ . The second 500  $\mu$ s is the worst latency of the WR network. After that, the B2B source SCU needs about 100  $\mu$ s for the calculation, the sending of the timing frame TGM\_SYNCH\_WIN and TGM\_PHASE\_CORRECTION and data transferring to the corresponding module. TGM\_SYNCH\_WIN is sent at around  $t_{B2B} + 1 \text{ ms} + 100 \mu\text{s} \approx t_{B2B} + 1.1 \text{ ms}$ . The trigger SCU receives TGM\_PHASE\_CORRECTION and TGM\_SYNCH\_WIN at around  $t_{B2B} + 1.1 \text{ ms} + 500 \mu\text{s} \approx t_{B2B} + 1.6 \text{ ms}$ . The 500  $\mu$ s is the latency of the WR network. The start of the synchronization window must be later than  $t_{B2B} + 1.1 \text{ ms} + 2 \times 500 \mu\text{s} \approx t_{B2B} + 2.1 \text{ ms}$ , because the TGM\_SYNCH\_WIN must be transferred back to the DM and the DM transfers it further to the beam instrumentation devices via WR network. The upward to DM transfer needs maximum 500  $\mu$ s and the transfer from the DM to BI needs another 500  $\mu$ s. Because the upper bound B2B transfer time is 10 ms and there is no hard real time for the collection of the trigger and firing timestamps and timing frame TGM\_KICKER\_TIME\_S sending, we give

#### **6.4. Test setup for the data collection, merging and redistribution of the B2B transfer system**

---

1 ms for the source trigger SCU to do this task and the source trigger SCU sends TGM\_KICKER\_TIME\_S at around  $t_{B2B} + 10\text{ ms} + 1\text{ ms} \approx t_{B2B} + 11\text{ ms}$ . The same time constraints is also for the target trigger SCU. The B2B source SCU receives TGM\_KICKER\_TIME\_S and TGM\_KICKER\_TIME\_T at around  $t_{B2B} + 11\text{ ms} + 500\text{ }\mu\text{s} \approx t_{B2B} + 11.5\text{ ms}$ . The  $500\text{ }\mu\text{s}$  is the latency of the WR network. The B2B source SCU sends TGM\_B2B\_STATUS at around  $t_{B2B} + 11.5\text{ ms} + 100\text{ }\mu\text{s} \approx t_{B2B} + 11.6\text{ ms}$ . The BI devices receives the timing frame TGM\_B2B\_STATUS at around  $t_{B2B} + 11.6\text{ ms} + 2 \times 500\text{ }\mu\text{s} \approx t_{B2B} + 12.6\text{ ms}$ .

## 6.4. Test setup for the data collection, merging and redistribution of the B2B transfer system

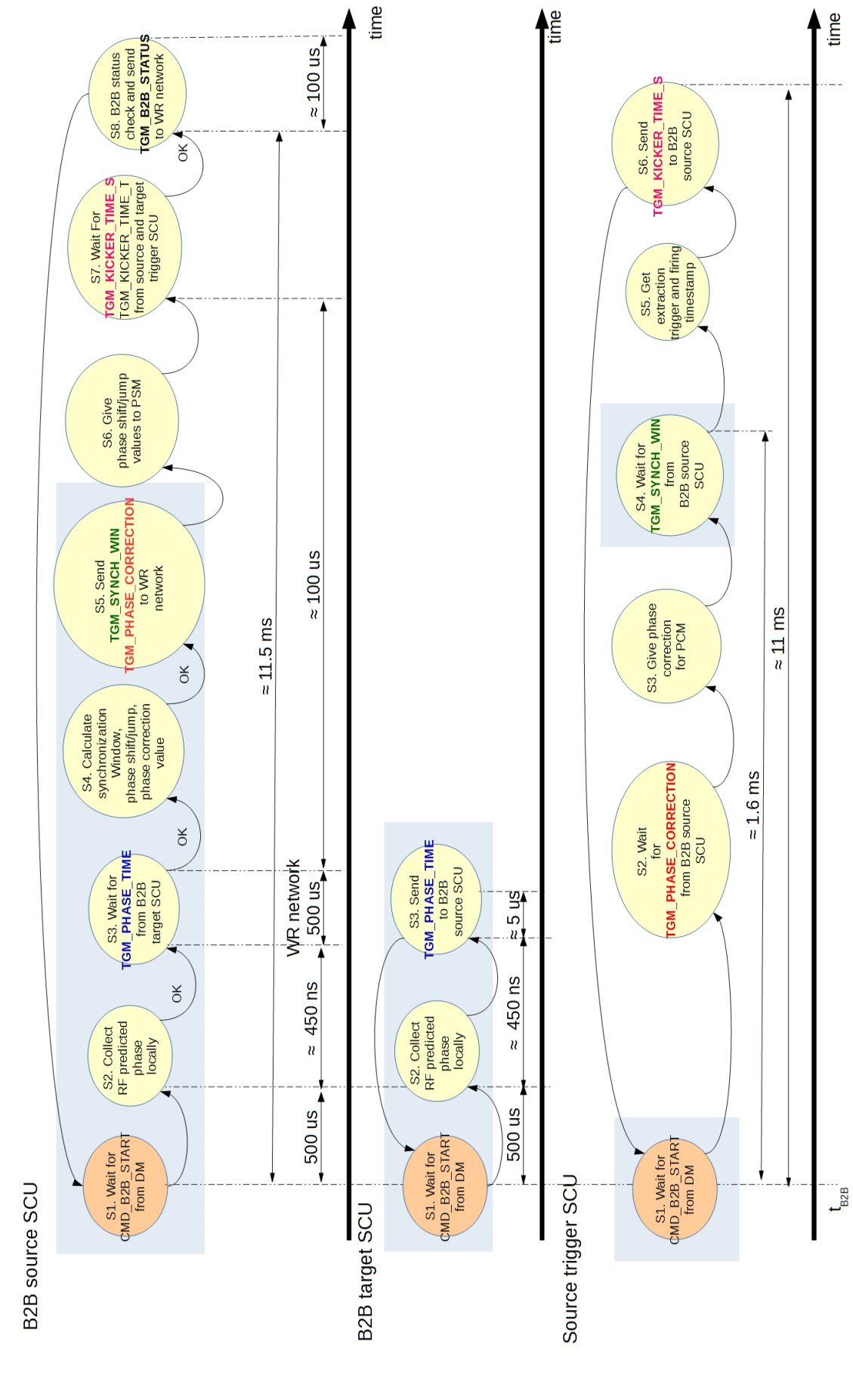


Figure 6.27: The time constraints of the B2B transfer system.

The time constraints of the B2B transfer system. The sent and received timing frame pairs have the same color. The test setup realizes

#### **6.4. Test setup for the data collection, merging and redistribution of the B2B transfer system**

#### 6.4.5 Test result

Because some modules of the B2B transfer system are still under the development, the test setup realizes parts of the whole function, mainly concentrated on the data collection from two simulated RF reference signals, the calculation of the synchronization window and the distribution of the start of the synchronization window. The steps with the blue rectangle in Fig. 6.27 are realized in this test setup. The test result of the B2B programs on B2B source, B2B target and trigger SCUs are shown as follows.

## 6.4. Test setup for the data collection, merging and redistribution of the B2B transfer system

---

WR network  
6 Event execution timestamp: GMT 1970-01-08 21:07:27.450028674

After both B2B source and target programs receive the *CMD\_START\_B2B* frame, they trigger another unit connected to the System-on-Chip<sup>10</sup> (SoC) bus to get the timestamp of the next zero crossing point of the DS345 sine waves, which is simulated as an equivalent to the predicted phase. The triggers of the B2B source and target SCUs are not simultaneous, namely the B2B source and target SCU do not get the timestamp of the adjacent zero crossing points of two RF simulated sine signals, see Line 10 and 14 of the test result of the B2B source SCU. All timestamp are shown in the format of Greenwich Mean Time (GMT). The timestamp got by the B2B source SCU is Thu, Jan 8, 1970, 21:07:27 0.445405856 second and the timestamp got by the B2B target SCU is Thu, Jan 8, 1970, 21:07:27 0.445364560 second. The time difference between two timestamps is 41.296  $\mu$ s. There are two reasons for the asynchronous triggers.

- The SoC bus might be granted to other program and B2B program must wait until it is free.
- The printout of the user friendly messages of the LM32 programs causes the non real time of the programs.

The difference between timestamps of the adjacent zero crossing points, 592ns, is the remainder resulting from 41.296us dividing SIS18 revolution period 636 051 ps. Based on eq. 6.52 and eq. 6.53,

$$\frac{T_{h=2}^{SIS18}}{5ms} = \frac{592ns}{\Delta t} \quad (6.52)$$

$$\frac{\Delta t}{T_{h=1}^{SIS18}} = 3634 \quad (6.53)$$

we could get that the beating time  $\Delta t$  is 4.622 818 ms and the number of the SIS18 revolution period is 3634 for the test.

For the real application of the B2B transfer system, in order to guarantee the time constraints of the B2B programs, see Fig. 6.27, the B2B source, target and trigger SCUs run only their corresponding B2B program. The SoC bus is occupied only by the B2B program. Besides, the programs running on LM32 are forbidden to print out any user friendly messages.

---

<sup>10</sup>A system-on-chip is an integrated circuit that integrates all components of a computer or other electronic system into a single chip.

# Chapter 7

## Conclusion and outlook

For many large scale accelerator facilities, it is inevitable to transfer bunched beam from one ring accelerator to another to gain higher energy or to accumulate beam for some research experiments. Without the proper transfer, the beam will be subject to various disturbances and even beam loss, e.g. dipole oscillation caused by the injection energy or phase error, quadrupole oscillation caused by the cavity voltage error. Hence, the proper bunch-to-bucket transfer between two accelerators is of great importance.

Facility for Antiproton and Ion Research (FAIR) aims at providing high-energy beam with high intensities. SIS100/300 of FAIR is under construction at GSI Helmholtz Centre for Heavy Ion Research GmbH at current stage. The B2B transfer has never been practiced between the existing machines, e.g. SIS18, ESR and CRYRING. The new developed Bunch-to-Bucket transfer system for FAIR in the dissertation is designed for all complex B2B transfer between FAIR accelerators. It is capable to transfer different species beam from one machine cycle to another. It is capable to parallel transfer beam through FAIR accelerators. It is also able to transfer the beam between two synchrotrons via FRS or Super FRS. It focuses first of all on the transfer from SIS18 to SIS100, but it will be firstly tested for the transfer from SIS18 to ESR and further to CRYRING.

The B2B transfer system for FAIR is introduced in the dissertation at hand from the functional point of view. The basic principles for B2B transfer are realized based on the existing FAIR technical basis (e.g. LLRF and FAIR control systems) and unique FAIR demands (e.g. Machine Protection System, MPS). The phase difference between two RF systems of two ring accelerators is obtained with the help of a shared reference signal at two ring accelerators. The source synchrotron works as the “B2B transfer master” for the rf phase collection, data (e.g. synchronization window, phase correction, phase shift and so on) calculation, synchronization window redistribution and B2B status check. In addition, the dissertation presents how FAIR accelerators apply the B2B transfer system and how precise the bunch-to-bucket transfer is achieved with the system. The rules for the application of the system is explained, which is determined by the relation between the circumference ratio/energy ratio and the cavity harmonic number of two synchrotron.

In addition, the beam dynamic of the  $U^{28+}$  B2B transfer from SIS18 to SIS100 is simulated for two synchronization methods, the phase shift and frequency beating method. The dissertation explains the timing constraints of the system, the calculation of the synchronization window and presents the usage of the WR network for

## CHAPTER 7. CONCLUSION AND OUTLOOK

---

the B2B transfer system. Further, the SIS18 extraction and SIS100 injection kickers are analyzed for the different triggering possibilities.

The dissertation presents a test setup for the system, achieving the phase collection of two synchrotrons locally, phase transfer from the target to source synchrotron, synchronization window calculation at the source synchrotron, synchronization window redistribution to the WR network, synchronization window reproduced at the source/target synchrotron.

Although the B2B transfer system for FAIR is flexible and with high compatibility, there still exists several improvement.

In order to reduce the synchronization time, the synchronization process could be started during the acceleration. The phase difference between two Reference RF Signals of the source and target synchrotrons at the flattop could be predicted by comparison the phases of these two signals at any time during the acceleration. Once the phase difference at the flattop is predicted, the synchronization process can be carried out.

- Phase shift method

First, the radial loop must be turned off. At some time during the acceleration, the phases difference between the source and target synchrotrons are obtained with the help of the Synchronization Reference Signal, and the phase difference at the flattop is picked up from the look-up table. Then, a rf frequency modulation is superposed on the initial frequency pattern. The integration of the rf frequency modulation equals to the required phase difference. With this new frequency pattern, the phase difference at the flattop will be the required phase difference when the cavity rf frequency of the source and target synchrotrons reach the flattop.

- Frequency beating method

The radial loop keeps on. At some time during the acceleration, the phases difference between the source and target synchrotrons are obtained. Then, a frequency detune is superposed on the initial frequency pattern. With this new frequency pattern, the synchronization window will be calculated.

# **Appendix A**

## **B2B timing frames**

## APPENDIX A. B2B TIMING FRAMES

---

Table A.1: B2B timing frames

No	Fram Name	Event ID	Priority	Source	Destination
1	CMD_START_B2B		7	DM	Source and B2B target SCU
2	TGM_PHASE_TIME		6	B2B target SCU	B2B source SCU
3	TGM_SYNCH_WIN		6	B2B source SCU	DM, source and target Trigger SCUs
4	CMD_SYNCH_WIN		7	DM	Beam Instrumentation (BI)
5	TGM_PHASE_JUMP		6	B2B source SCU	B2B target SCU
6	TGM_PHASE_CORRECTION		6	B2B source SCU	Source Trigger SCU
7	TGM_KICKER_TRIGGER_TIME_S		6	Source Trigger SCU	B2B source SCU
8	TGM_KICKER_TRIGGER_TIME_T		6	Target Trigger SCU	B2B source SCU
9	TGM_B2B_STATUS		6	B2B source SCU	DM
10	CMD_B2B_STATUS		7	DM	BI
No	Content				Description
1	64 bits timestamp				Begin of the B2B transfer process
2	16 bits phase advance and 64 bits slop				Transfer of the phase advance and the slop
3	64 bits timestamp				Indication the start of the synchronization window
4	64 bits timestamp				Indication the start of the synchronization window
5	16 bits the expected jumped phase				Indication the jumped phase for the empty target machine
6	16 bits phase correction				Target revolution frequency reproduction
7	$2 \times 64$ bits timestamp				Timestamps of trigger and firing of extraction kicker
8	$2 \times 64$ bits timestamp				Timestamps of trigger and firing of injection kicker
9	64 bits timestamp + 1 bit				The actual beam extraction time and the status of the B2B system
10	64 bits timestamp + 1 bit				The actual beam extraction time and the status of the B2B system

# Appendix B

## Parameters of B2B transfer for FAIR accelerator pairs

### B.1 Parameters for the B2B transfer from SIS18 to SIS100

		Proton		Heavy Ion	
	Unit	SIS18 Ext <sup>1</sup>	SIS100 Inj <sup>2</sup>	SIS18 Ext	SIS100 Inj
Design orbit	m	216.72	1083.6	216.72	1083.6
Inj orbit	m	216.72	1083.6	216.72	1083.6
$C_{SIS18} : C_{SIS100}$		5		5	
Ext kinetic energy	MeV/u	4000		200	
Inj kinetic energy	MeV/u		4000		200
Cavity h		1	10(1×4)	2	10(2×4)
$f_{rf}$	MHz	1.359	2.718	1.572	1.572
$T_{rf}$	μs	0.736	0.368	0.636	0.636
$f_{rev}$	MHz	1.359	0.272	0.786	0.157
$T_{rev}$	μs	0.736	3.678	1.272	6.359
Max $\Delta p/p$		±0.008	±0.01	±0.008	±0.01
$\Delta R/R$		$\pm 0.8 \times 10^{-4}$		$\pm 2.4 \times 10^{-4}$	
Slip factor <sup>3</sup>		-0.026		-0.647	
Transition Energy $\gamma_t$		10		5.8	
Compaction factor $\alpha_p$		0.010		0.030	
$\beta$		0.982	0.982	0.568	0.568
$\gamma$		5.294	5.294	1.215	1.215
		Injection four times		Injection four times	
		Frequency beating method			

### B.1. Parameters for the B2B transfer from SIS18 to SIS100

---

	MHz	$f_{rf} + \Delta f =$ 1.359 + 200Hz	$f_{rf} =$ 1.359	$f_{rf} + \Delta f =$ 1.572 +200Hz	$f_{rf} =$ 1.572
Beating frequency	Hz	200 Hz		200 Hz	
Synchronization period	ms	5		5	
Synchronization window	$\mu$ s	7.356		12.718	
Mismatch	degree	$\pm 0.31^\circ$		$\pm 0.50^\circ$	
Phase shift method					

Table B.1: Parameters for the B2B transfer from SIS18 to SIS100

## B.2 Parameters for the B2B transfer from SIS18 to ESR

		Proton/Heavy Ion		Heavy Ion	
	Unit	SIS18 Ext	ESR Inj	SIS18 Ext	ESR Inj
Design orbit	m	216.72	108.36	216.72	108.36
Inj orbit	m	216.72	108.36 +0.15	216.72	108.36 +0.15
$C_{SIS18} : C_{ESR}$		1.997		1.997	
Ext kinetic energy	MeV/u	550		30	
Inj kinetic energy	MeV/u		400		30
Cavity h		1	1	4	1
$f_{rf}$	MHz	0.989756	1.976777	1.373201	0.685651
$T_{rf}$	μs	1.010350	0.505874	0.728226	1.458468
$f_{rev}$	MHz	0.989756	1.976777	0.343300	0.685651
$T_{rev}$	μs	1.010350	0.505874	2.912903	1.458468
$\Delta p/p$ compared with design orbit			1%		1%
$\Delta R/R$			0.138%		0.138%
Slip factor		-0.480	-0.310	-0.909	-0.759
Transition Energy $\gamma_t$		10	2.357	5.8	2.357
Compaction factor $\alpha_p$		0.010	0.18	0.030	0.18
$\beta$		0.715	0.715	0.248	0.248
$\gamma$		1.429	1.429	1.032	1.032
		Accumulation beam in injection orbit		Accumulation beam in injection orbit	
Frequency beating method					
	kHz	$f_{rf}/1 =$ 988.388 + 1368Hz	$f_{rf}/2 =$ 988.388	$f_{rf}/2 =$ 685.652 + 948Hz	$f_{rf}/1 =$ 685.65250
Beating frequency	Hz	1368 Hz		948 Hz	
Synchronization period	ms	0.731		1.055	
Synchronization window	μs	2.034		2.917	
Mismatch	degree	$\pm 0.50^\circ$		$\pm 0.51^\circ$	
Phase shift method					
$\Delta R/R$ for RF frequency match		0.2%		0.1%	

## B.2. Parameters for the B2B transfer from SIS18 to ESR

---

For SIS18, it is impossible to change the orbit to match the RF frequency within the radius excursion range. So the phase shift method could not be implemented

Table B.2: Parameters for the B2B transfer from SIS18 to ESR

## B.3 Parameters for the B2B transfer from SIS18 to ESR via FRS

		Heavy Ion Beam	Rare Isotope Beam
	Unit	SIS18 Ext	ESR Inj
Design orbit	m	216.72	108.36
Inj orbit	m	216.72	108.36 +0.15
$C_{SIS18} : C_{ESR}$		1.997	
Ext kinetic energy	MeV/u	400	
Inj kinetic energy	MeV/u		400
Cavity h		1	1
$f_{rf}$	MHz	1.076965	1.976777
$T_{rf}$	μs	0.928535	0.505874
$f_{rev}$	MHz	1.076965	1.976777
$T_{rev}$	μs	0.928535	0.505874
$\Delta p/p$ compared with design orbit			1%
$\Delta R/R$			0.138%
Slip factor		-0.366	-0.310
Transition Energy $\gamma_t$		5.8	2.357
Compaction factor $\alpha_p$		0.030	0.18
$\beta$		0.778	0.715
$\gamma$		1.590	1.429
		Accumulation beam in injection orbit	
Frequency beating method			
	kHz	$f_{rf}/5 =$ 219.642 + 4249Hz	$f_{rf}/9 =$ 219.642
Beating frequency	Hz	4249 Hz	
Synchronization period	ms	0.235349	
Synchronization window	μs	9.106	
Mismatch	degree	$\pm 6.92^\circ$	
Phase shift method			
$\Delta R/R$ for RF frequency match		2%	

### B.3. Parameters for the B2B transfer from SIS18 to ESR via FRS

---

For SIS18, it is impossible to change the orbit to match the RF frequency within the radius excursion range. So the phase shift method could not be implemented

Table B.3: Parameters for the B2B transfer from SIS18 to ESR via FRS

## B.4 Parameters for the B2B transfer from ESR to CRYRING

		Proton/Antiproton		Heavy Ion					
	Unit	ESR Ext	CRYRING Inj	ESR Ext	CRYRING Inj				
Design orbit	m	108.36	54.17	108.36	54.17				
Ext orbit	m	108.36 +0.15		108.36 +0.15					
$C_{ESR} : C_{CRYRING}$		2		2					
Ext kinetic energy	MeV/u	30		4-10					
Inj kinetic energy	MeV/u		30		4-10				
Cavity h		1	1	1	1				
$f_{rf}$	MHz	0.686	1.372	0.254-0.401	0.508-0.802				
$T_{rf}$	μs	1.458	0.729	3.932-2.494	1.966-1.247				
$f_{rev}$	MHz	0.686	1.372	0.254-0.401	0.508-0.802				
$T_{rev}$	μs	1.458	0.729	3.932-2.494	1.966-1.247				
Slip factor		-0.759							
Transition Energy $\gamma_t$		2.357		2.357					
Compaction factor $\alpha_p$		0.18		0.18					
$\beta$		0.248	0.248	0.092-0.145	0.092-0.145				
$\gamma$		1.032	1.032	1.004-1.011	1.004-1.011				
		One time injection		One time injection					
Phase shift method									
There is no beam in CRYRING, so the phase jump of CRYRING is preferred.									

Table B.4: Parameters for the B2B transfer from ESR to CRYRING

## B.5 Parameters for the B2B transfer from CR to HESR

		Antiproton		Rare Isotope Beam	
	Unit	CR Ext	HESR Inj	CR Ext	HESR Inj
Design orbit	m	221.45	575	221.45	575
$C_{ESR} : C_{CRYRING}$		2.6		2.6	
Ext kinetic energy	GeV/u	3		0.74	
Inj kinetic energy	GeV/u		3		0.74
Cavity h		1	1	1	1
$f_{rf}$	MHz	1.317	0.507	1.125	0.433
$T_{rf}$	μs	0.759	1.972	0.889	2.309
$f_{rev}$	MHz	1.317	0.507	1.125	0.433
$T_{rev}$	μs	0.759	1.972	0.889	2.309
Max $\Delta p/p$		±3%		±1.5%	
Slip factor		-0.011		0.178	
Transition Energy $\gamma_t$		3.85		2.711	
Compaction factor $\alpha_p$		0.067			
$\beta$		0.972	0.972	0.830	0.830
$\gamma$		4.221	4.221	1.794	1.794
		100 times Injection per 10 seconds		100 times Injection per 10 seconds	
Frequency beating method					
	kHz	$f_{rf}/13 =$ 101.290 + 136Hz	$f_{rf}/5 =$ 101.426	$f_{rf}/13 =$ 86.493 + 113Hz	$f_{rf}/5 =$ 86.608
Beating frequency	Hz	136 Hz		113 Hz	
Synchronization period	ms	7.353		8.850	
Synchronization window	μs	19.719		23.090	
Mismatch	degree	±0.48°		±0.47°	
Phase shift method					
$\Delta R/R$ for RF frequency match		0.2%		0.1%	
The beam in CR is stochastic cooling and electrons exist during the B2B process. The phase shift method doesn't work. The remove of electrodes is about 100 ms.					

Table B.5: Parameters for the B2B transfer from CR to HESR

## B.6 Parameters for the B2B transfer from SIS100 to CR

		Proton→ Antiproton		Heavy Ion→ RIB					
	Unit	SIS100 Ext	CR Inj	SIS100 Ext	CR Inj				
Design orbit	m	1083.6	221.45	1083.6	221.45				
$C_{ESR} : C_{CRYRING}$		4.893		4.893					
Ext kinetic energy	GeV/u	28.8		1.5					
Inj kinetic energy	GeV/u		3		0.74				
Cavity h		5(1 bunch)	1	2(1 bunch)	1				
$f_{rf}$	MHz	1.345	1.318	0.460	1.125				
$T_{rf}$	μs	0.743	0.759	2.176	0.889				
$f_{rev}$	MHz	0.269	1.318	0.230	1.125				
$T_{rev}$	μs	3.716	0.759	4.352	0.889				
$\beta$		0.999	0.972	0.924	0.830				
$\gamma$		31.918	4.221	2.610	1.794				
		One time injection		One time injection					
Phase shift method									
There is no beam in CR, so the phase jump of CR is preferred.									

Table B.6: Parameters for the B2B transfer from SIS100 to CR

# Bibliography

- [1] Helmut Wiedemann. Particle Accelerator Physics. Springer, July 2015. ISBN 978-3-319-18317-6. Google-Books-ID: oR0\_CgAAQBAJ.
- [2] Accelerators for Society. URL <http://www.accelerators-for-society.org/about-accelerators/index.php?id=21#linac>.
- [3] Oscar Barbalat. Applications of particle accelerators. Technical report, CERN, 1994. URL <http://cds.cern.ch/record/260280/files/P00021907.pdf>.
- [4] Jürgen Eschke. International Facility for Antiproton and Ion Research (FAIR) at GSI, Darmstadt. Journal of Physics G: Nuclear and Particle Physics, 31(6):S967, 2005. URL <http://iopscience.iop.org/article/10.1088/0954-3899/31/6/041/meta>.
- [5] FAIR - Facility for Antiproton and Ion Research, May 2011. URL <https://www.gsi.de//forschungbeschleuniger/fair.htm>.
- [6] P. Spiller and G. Franchetti. The FAIR accelerator project at GSI. Nuclear Instruments and Methods in Physics Research Section A, 561(2):305–309, 2006. URL <http://www.sciencedirect.com/science/article/pii/S0168900206000507>.
- [7] M. Steck, R. Bär, U. Blell, C. Dimopoulou, A. Dolinskii, P. Forck, B. Franzke, O. Gorda, V. Gostishchev, U. Jandewerth, and others. Advanced Design of the FAIR Storage Ring Complex. In In Proc. of EPAC, 2008. URL <https://accelconf.web.cern.ch/AccelConf/PAC2009/papers/fr1gri03.pdf>.
- [8] P. Baudrenghien. Low-level RF. 13(14):15, 2010. URL <https://cas.web.cern.ch/cas/Denmark-2010/Writeups/Baudrenghien.docx>.
- [9] R Garoby. Timing aspect of bunch transfer between circular machines. State of the art in the PS complex, PS/RF. Technical report, Note 84-6, 17 December 84, 1984.
- [10] Harms Barletta. Overview on Magnetic fields. URL [http://uspas.fnal.gov/materials/12MSU/xverse\\_dynamics.pdf](http://uspas.fnal.gov/materials/12MSU/xverse_dynamics.pdf).
- [11] Jochen Michael Grieser. Beam phase feedback in a heavy-ion synchrotron with dual-harmonic cavity system. PhD thesis, Technical University Darmstadt, 2015. URL <http://tuprints.ulb.tu-darmstadt.de/4634/>.

## BIBLIOGRAPHY

---

- [12] K. Gross, U. Hartel, U. Laier, D. Lens, K. P. Ningel, S. Schäfer, B. Zipfel, and H. Klingbeil. Bunch-by-Bunch Longitudinal RF Feedback for Beam Stabilization at FAIR. In Proc. of IPAC, 2015. URL <http://accelconf.web.cern.ch/AccelConf/IPAC2015/papers/mopha021.pdf>.
- [13] Eizi Ezura, Masahito YOSHII, Fumihiko TAMURA, and Alexander SCHNASE. Beam-Dynamics View of RF Phase Adjustment for Synchronizing J-PARC RCS with MR or MLF, 2008. URL <http://ccdb5fs.kek.jp/tiff/2008/0826/0826001.pdf>.
- [14] Claude Bovet, Robert Gouiran, Karl Helmut Reich, and Igor Gumowski. A selection of formulae and data useful for the design of AG synchrotrons. Technical report, CERN, 1970. URL <http://cds.cern.ch/record/280305>.
- [15] B. J. Holzer. Introduction to transverse beam dynamics. CERN Yellow Report, 2013. URL <http://arxiv.org/abs/1404.0923>.
- [16] S Y Lee. Accelerator Physics. WORLD SCIENTIFIC, Singapore, 3 edition, November 2011. ISBN 978-981-4374-94-1 978-981-4374-95-8. URL <http://www.worldscientific.com/worldscibooks/10.1142/8335>.
- [17] Blell Udo. Injection and Extraction Components of SIS 100 / 300, 2014.
- [18] Peter Forck. Lecture Notes on Beam Instrumentation and Diagnostics, 2011. URL [https://scholar.google.de/scholar?q=Lecture+Notes+on+Beam+Instrumentation+and+Diagnostics&btnG=&hl=de&as\\_sdt=0%2C5](https://scholar.google.de/scholar?q=Lecture+Notes+on+Beam+Instrumentation+and+Diagnostics&btnG=&hl=de&as_sdt=0%2C5).
- [19] T. Hoffmann. FESA—The front-End Software architecture at FAIR. PCaPAC08, 2008. URL <http://accelconf.web.cern.ch/AccelConf/pc08/papers/wep007.pdf>.
- [20] Ralf Huhmann, Ralph C. Bär, Dietrich Hans Beck, Jutta Fitzek, Günther Fröhlich, Ludwig Hechler, Udo Krause, and Matthias Thieme. The FAIR control system—System architecture and first implementations. ICALEPS, 2013. URL <http://epaper.kek.jp/ICALEPS2013/papers/moppc097.pdf>.
- [21] Dietrich Beck, R. Bar, Mathias Kreider, Cesar Prados, Stefan Rauch, Wesley Terpstra, and Marcus Zweig. The new White Rabbit based timing system for the FAIR facility. PCaPAC, 2012. URL <http://accelconf.web.cern.ch/Accelconf/pcapac2012/papers/fria01.pdf>.
- [22] Peter Moritz. BuTiS—Development of a Bunchphase Timing System. GSI Scientific Report, 2006. URL <http://citeseerx.ist.psu.edu/viewdoc/download?doi=10.1.1.162.1765&rep=rep1&type=pdf>.
- [23] B. Zipfel, P. Moritz, and others. Recent Progress on the Technical Realization of the Bunch Phase Timing System BuTiS. Proc. IPAC, pages 418–420, 2011. URL <http://accelconf.web.cern.ch/accelconf/ipac2011/papers/mopc145.pdf>.
- [24] Dietrich Beck, Mathias Kreider, Cesar Prados, Wesley Terpstra, Stefan Rauch, and Marcus Zweig. The General Machine Timing System

## BIBLIOGRAPHY

---

- for FAIR and GSI. URL [https://www-acc.gsi.de/wiki/pub/Timing/TimingSystemDocuments/GMT\\_Description\\_v3-1.pdf](https://www-acc.gsi.de/wiki/pub/Timing/TimingSystemDocuments/GMT_Description_v3-1.pdf).
- [25] Dietrich Beck. Timing Messages of GMT system for FAIR, 2015. URL <https://www-acc.gsi.de/wiki/Timing/TimingSystemEvent>.
  - [26] Harald Klingbeil, Ulrich Laier, Klaus-Peter Ningel, Stefan Schäfer, Christof Thielmann, and Bernhard Zipfel. New digital low-level rf system for heavy-ion synchrotrons. *Physical Review Special Topics - Accelerators and Beams*, 14(10), October 2011. ISSN 1098-4402. doi: 10.1103/PhysRevSTAB.14.102802. URL <http://link.aps.org/doi/10.1103/PhysRevSTAB.14.102802>.
  - [27] Marko Mandakovic. FAIR Fast Beam Abort System. URL [https://fair-wiki.gsi.de/foswiki/pub/FC2WG/FairC2WGMinutes/20151021\\_Fast\\_Beam\\_Abort\\_System\\_Mandakovic.pdf](https://fair-wiki.gsi.de/foswiki/pub/FC2WG/FairC2WGMinutes/20151021_Fast_Beam_Abort_System_Mandakovic.pdf).
  - [28] Thibault Ferrand, Harald Klingbeil, and Heiko Damerau. Synchronization of Synchrotrons for bunch-to-bucket Transfers. Technical report, 2015. URL <http://cds.cern.ch/record/2053285>.
  - [29] J. Bai, T. Ferrand, D. Beck, R. Bär, O. Kester, D. Ondreka, C. Prados, and W. Terpstra. BUNCH TO BUCKET TRANSFER SYSTEM FOR FAIR. In ICALEPCS, 2015. URL <http://icalepcs.synchrotron.org.au/papers/wepgf119.pdf>.
  - [30] Jiaoni Bai and Thibault Ferrand. Concept of the FAIR Bunch To Bucket Transfer System, 2016.
  - [31] T. Ferrand and J. Bai. System Simulation of Bunch-to-Bucket Transfer Between Synchrotrons. GSI Scientific Report, 2014. URL <http://repository.gsi.de/record/184160/files/FG-GENERAL-28.pdf>.
  - [32] T. Ferrand and J. Bai. SYSTEM DESIGN FOR A DETERMINISTIC BUNCH-TO-BUCKET TRANSFER. In IPAC, 2015. URL <http://accelconf.web.cern.ch/AccelConf/IPAC2015/papers/wepma024.pdf>.
  - [33] Matthias Thieme, Wolfgang Panschow, and Stefan Rauch. SCU system goes productive. GSI Scientific Report, 2013. URL <http://repository.gsi.de/record/68061/files/FG-CS-07.pdf>.
  - [34] D. Beck, R. Bar, M. Kreider, C. Prados, S. Rauch, W. Terpstra, M. Zweig, and T. Fleck. White Rabbit Technology as Basis for the FAIR Timing System. GSI Scientific Report, 2011. URL <https://www-acc.gsi.de/wiki/pub/Timing/TimingSystemDocuments/PHN-ACC-RD-45.pdf>.
  - [35] H. Liebermann and D. Ondreka. FAIR and GSI Reference Cycles for SIS18, 2013.
  - [36] H. Liebermann and D. Ondreka. SIS100 Cycles, 2013.
  - [37] F. Herfurth, A. Brauning-Demian, W. Enders, H. Danared, and others. The low energy storage ring CRYRING@ ESR. Proc. of COOL2013 (Murren, Switzerland), 2013. URL <https://accelconf.web.cern.ch/accelconf/COOL2013/papers/thpm1ha01.pdf>.

- [38] M. Lestinsky, A. Bräuning-Demian, H\aa akan Danared, M. Engström, W. Enders, S. Fedotova, B. Franzke, A. Heinz, F. Herfurth, A. Källberg, and others. CRYRING@ ESR: present status and future research. *Physica Scripta*, 2015 (T166):014075, 2015. URL <http://iopscience.iop.org/article/10.1088/0031-8949/2015/T166/014075/meta>.
- [39] M. Steck, C. Dimopoulou, B. Franzke, O. Gorda, T. Katayama, F. Nolden, G. Schreiber, Germany D. Möhl, Switzerland R. Stassen, H. Stockhorst FZJ, and others. Demonstration of Longitudinal Stacking in the ESR with Barrier Buckets and Stochastic Cooling. page 140, Alushta, Ukraine, 2011. URL <http://accelconf.web.cern.ch/AccelConf/COOL2011/papers/proceed.pdf#page=150>.
- [40] A. V. Smirnov, D. A. Krestnikov, I. N. Meshkov, and others. Particle accumulation with a barrier bucket RF system. In COOL, 2009.
- [41] R. Toelle, K. Bongardt, J. Dietrich, F. Esser, O. Felden, R. Greven, G. Hansen, F. Klehr, A. Lehrach, B. Lorentz, and others. HESR at FAIR: Status of technical planning. In PAC07, 2007. URL <http://epaper.kek.jp/p07/PAPERS/TUPAN024.PDF>.
- [42] J. Bai12, R. Bär, D. Beck, T. Ferrand13, M. Kreider, D. Ondreka, C. Prados, S. Rauch, W. Terpstra, and M. Zweig. First Idea on Bunch to Bucket Transfer for FAIR. 2014. URL [http://epaper.kek.jp/PCaPAC2014/posters/fpo024\\_poster.pdf](http://epaper.kek.jp/PCaPAC2014/posters/fpo024_poster.pdf).
- [43] John R. Taylor. An introduction to error analysis: The study of uncertainty in physical measurements. Mill Valley, CA: Anonymous University Science Books, page 71ep, 1982.
- [44] Thibault Ferrand. Development of the LLRF system for a deterministic Bunch-to-Bucket transfer for FAIR. PhD thesis, Technical University Darmstadt.
- [45] U. Laier. Funktional-Spezifikation DDS, 2011.
- [46] Statistical and numerical tools in astrophysics I. Accuracy and precision. URL <http://www.astro.lu.se/Education/utb/ASTM11/lecture2.pdf>.
- [47] Cesar Prados and Jiaoni Bai. Testing the WR Network of the FAIR General Machine Timing System, 2016.
- [48] Calculating Optical Fiber Latency, 2012. URL <http://www.m2optics.com/blog/bid/70587/Calculating-Optical-Fiber-Latency>.

# Publications

- 2015 J. Bai, T. Ferrand, D. Beck, R. Br, O. Kester, D. Ondreka, C. Prados, and W. Terpstra. BUNCH TO BUCKET TRANSFER SYSTEM FOR FAIR. *In Proc. of ICAL EPICS*, 2015
- T. Ferrand and J. Bai. SYSTEM DESIGN FOR A DETERMINISTIC BUNCH-TO-BUCKET TRANSFER. *In Proc. of IPAC*, 2015
- 2014 J. Bai, D. Beck, R. Br, D. Ondreka, T. Ferrand, M. Kreider, C. Prados, S. Rauch, W. Terpstra, and M. Zweig. FIRST IDEA ON BUNCH TO BUCKET TRANSFER FOR FAIR. *In Proc. of PCaPAC*, 2014
- M. Kreider, J. Bai, R. Br, D. Beck, A. Hahn, C. Prados, S. Rauch, W. W. Terpstra, and M. Zweig. Launching the FAIR timing system with CRYRING. *In Proc. of PCaPAC*, 2014
- T. Ferrand and J. Bai. System Simulation of Bunch-to-Bucket Transfer Between Synchrotrons. *GSI Scientific Report*, 2014
- 2013 Bai Jiao-Ni, Zeng Lei, Wang Biao, Li Peng, Li Fang, Xu Tao-Guang, and Li Zi-Gao. Modified read-out system of the beam phase measurement system for CSNS. *Chinese physics C*, 37(10):107004, 2013
- D. Beck, J. Adamczewski-Musch, J. Bai, R. Br, J. Frhauf, J. Hoffmann, M. Kreider, N. Kurz, C. Prados, S. Rauch, and others. Paving the Way for the General Machine Timing System. *GSI Scientific Report*, 2013
- Mathias Kreider, Jiaoni Bai, Dietrich Beck, Cesar Prados, Wesley Terpstra, Stefan Rauch, and Marcus Zweig. Receiver Nodes of the General Machine Timing System for FAIR and GSI
- 2012 Jiaoni Bai, Shuai Xiao, Taoguang Xu, and Lei Zeng. The Development of Timing Control System for RFQ. *In Proc. of LINAC*, 2012

# Jiaoni Bai

---

## Curriculum Vitae

*"I am a slow walker, but I never stop walking." - Jiaoni Bai*

### Education

- 2013–Now **Doctoral Study**, Goethe University, Frankfurt am Main, Germany, .
- 2010–2013 **Master of Engineering Study in Computer Technology**, Institute of High Energy Physics, Chinese Academy of Sciences, China, GPA – 8.0.
- 2006–2010 **Bachelor of Engineering Study in Medical Informatics Engineering**, Southern Medical University, China, GPA – 9.0.

### PhD Thesis

- Title *Development of the timing system for the Bunch-to-Bucket transfer between the FAIR accelerators at GSI Helmholtz Centre for Heavy Ion Research GmbH*
- Professor Prof. Oliver Kester
- Supervisors Dr. Dietrich Beck and Dr. David Ondreka
- Description
  - Development of the Bunch-to-Bucket transfer system
  - Programming work on FPGA
  - Measurement of the White Rabbit network performance

### Master Thesis

- Title *The development of EPICS driver for customized VME hardwares*
- Supervisor Taoguang Xu
- Description
  - Development of the software interface between EPICS and VME hardware
  - Development of the operator controlling and monitoring interfaces by MEDM hardware
  - VxWorks program for Motorola VME board MVME5100

### Bachelor Thesis

- Title *The CCD performance test and analysis*
- Description
  - Investigation of the influence factors for CCD
  - Test how these factors influence CCD

## Awards

- 2012 Won "Scholarship of the head of the Institute of High Energy Physics, CAS" for master thesis
- 2007 Won second prize of "Mathematical Contest in Modeling in Southern Medical University"

## Key skills

- Intermediate Network engineering, Bash shell script and Visual Basic programming
- Advanced VHDL program for Altera FPGAs, C, Accelerator technology and beam dynamics, VxWorks programming and EPICS

## Computer literacy

- Basic Windows, Linux (Ubuntu/Debian), Microsoft Office and LaTeX applications
- Engineering Altera Quartus and Matlab applications
- Art design Photoshop and Corel VideoStudio application
- Web design Dreamweaver

## Languages

- Mandarin Mothertongue Chinese
- English Good written and spoken
- German Goethe-Zertifikat B2